Universidade de Aveiro
Ano 2017

Departamento de química

Diana Domingues Lopes

Bioreator de perfusão para a análise high-throughput de combinações de biomateriais/células estaminais

Perfusion bioreactor for the high-throughput analysis of combinations of biomaterials/stem cells

Universidade de Aveiro Departamento de química
Ano 2017

Diana Domingues Lopes

Bioreator de perfusão para a análise high-throughput de combinações de biomateriais/células estaminais

Tese apresentada à Universidade de Aveiro para cumprimento dos requisitos necessários à obtenção do grau de Mestre em Biotecnologia, ramo Industrial e Ambiental, realizada sob a orientação científica da Doutora Mariana de Braga Oliveira e do Professor Catedrático João Filipe Mano do Departamento de Química da Universidade de Aveiro

o júri

Presidente	**Doutora Mara Guadalupe Freire Martins** Equiparado a Investigador Coordenador, Universidade de Aveiro
Vogal	**Professora Doutora Odete Abreu Beirão da Cruz e Silva** Professora Auxiliar com Agregação, Universidade de Aveiro
Vogal	**Doutora Mariana Braga de Oliveira** Bolseira de Pós-Doutoramento, Departamento de Química da Universidade de Aveiro

agradecimentos

A realização desta dissertação de mestrado contou com importantes apoios e incentivos sem os quais não se teria tornado uma realidade e aos quais estarei eternamente grata.

À minha orientadora, Mariana de Braga de Oliveira expresso o meu profundo agradecimento, por toda a orientação cientifica, conhecimento transmitido, assim como pela paciência e persistência demonstradas na resolução de problemas inerentes a este estudo. Ao apoio incondicional demonstrado, que muito ajudou no crescimento do meu conhecimento cientifico e estimulação pela curiosidade de querer saber mais e fazer sempre melhor.

Ao meu co-orientador, professor João Filipe Mano, pela orientação cientifica e pela oportunidade de me integrar no seu grupo de investigação, Compass, assim como pela confiança demonstrada para a realização deste projeto.
A todos os meus colegas de investigação grupo do COMPASS, pela amizade, companheirismo e disponibilidade para esclarecimento de dúvidas.

À Doutora Sónia Patrício pela ajuda indispensável envolvida na preparação e aquisição de imagens de microscopia eletrónica de varrimento.

Agradeço ao CICECO, por todos os meios disponibilizados para a realização deste trabalho, assim como ao projeto ATLAS pelo apoio financeiro, pois sem estes a realização deste trabalho nunca teria sido possível.

À minha família e amigos, conforto nas alturas mais difíceis.
Findada esta etapa tão importante do meu percurso, espero retribuir todo o carinho, apoio e dedicação demonstrado.

palavras-chave

Células estaminais, bioreatores, análise high-throughput, tensão de corte, perfusão, matriz extracelular, proteínas, estímulos mecânicos, nicho do osso, osso, interações proteína-célula, interações célula-célula, regeneração do osso, engenharia de tecidos, microambiente do osso, biomateriais, alcalino fosfatase.

resumo

A engenharia de tecidos combina células humanos, materiais e engenharia de modo a induzir respostas biológicas com o objetivo de proporcionar uma regeneração rápida e correta do tecido danificado. O uso de matrizes tridimensionais (3D) para suportar o crescimento celular, ao contrário dos convencionais materiais 2D, é de grande importância para a simulação da organização estrutural de tecidos biológicos. Outros aspetos da matriz extracelular (ECM), para além da sua arquitetura são conhecidos por afetar a resposta celular. Fatores biomecânicos apresentados às células através das proteínas da ECM influenciam a adesão celular e fenómenos tais como manutenção do fenótipo, diferenciação celular e proliferação. Estudos in vitro muitas vezes falham na apresentação de fatores fisiológicos que incluem dinâmica de fluidos, o qual pode levar a uma correta oxigenação do biomaterial com células incorporadas, bem como a fenómenos de mecanotransdução. Neste trabalho, propomos um sistema que revela o efeito de 32 combinações de proteínas da ECM na adesão e expressão da alcalina fosfatasse (ALP) em células estaminais derivadas da coluna óssea (MSCs), tanto em ambiente estático como dinâmico. Um bioreator foi desenhado de modo a permitir um estudo high-throughput, para que fossem analisadas 32 combinações biomaterial-célula simultaneamente. Este bioreactor foi construído a partir de material de laboratório comum e de baixo custo (incluindo tubos e seringas descartáveis). As MSCs foram semeadas em scaffolds de quitosano poroso, modificado covalentemente com proteínas da ECM do osso, assim como proteínas responsáveis por contacto célula-célula e componentes do esmalte. Uma análise fatorial permitiu correlacionar a presença das várias combinações proteicas com melhor adesão celular ao biomaterial, assim como uma expressão de ALP após 24 horas e 5 dias de cultura. Os dados foram analisados tanto para ambiente estático, como dinâmico na presença de um pequeno fluxo, previamente comprovado como potenciador da diferenciação osteogénica de MSCs. O sistema desenvolvido foi útil na interpretação da grande complexidade das interações célula-ECM, e poderá ter possível aplicação no desenvolvimento de biomateriais para regeneração óssea, bem como em futuras aplicações como modelos de doença. .

keywords

Stem cell, bioreactors, high-throughput analysis, shear stress, perfusion, extracellular matrix, proteins, mechanical stimuli, bone niche, bone, protein-cell interactions, cell-cell interactions, bone regeneration, tissue engineering, bone microenvironment, biomaterials, alkaline phosphatase.

abstract

Tissue engineering combines human cells, materials and engineering to induce biological responses seeking the rapid and accurate healing of damaged tissues. The use of three-dimensional (3D) matrices to support cellular growth, in opposition to traditionally used two dimensional (2D) materials, are of utmost importance to emulate the structural organization of biological tissues. Other aspects of the extracellular matrix (ECM) beyond its architecture are known to affect cell response. The biochemical cues presented to cells by ECM proteins influence cell adhesion and phenomena as cell phenotype maintenance, cell differentiation and proliferation. In vitro studies often lack physiological-like cues that include slow fluid dynamics, which may impair the correct oxygenation of the biomaterial-cells construct. Here, we engineered a system to disclose the effect of 32 different ECM protein combinations on the adhesion and alkaline phosphatase (ALP) expression of bone marrow-derived mesenchymal stem cells (MSCs), both under static and flow perfusion conditions. A novel bioreactor was designed to enable a high-throughput study, that allowed to withdraw data from 32 biomaterial-cell combinations in one single test. The bioreactor was assembled from widely available affordable labware (including plastic tubes and disposable syringes). MSCs were seeded on chitosan porous scaffolds covalently modified with bone ECM proteins, as well as cell-cell contact proteins and enamel components. A factorial analysis study allowed correlating the presence of single and combinations of proteins with improved cell adhesion to biomaterials, as well as improved ALP quantification after 24 hours and 5 days of culture. The data was analyzed both for static culture conditions, as well as in the presence of a slow perfusion rate, previously shown to potentiate MSCs osteogenic differentiation. The developed system has proven to be useful in the interpretation of the wide complexity of cells-ECM interactions, and may find application in the development of biomaterials for tissue regeneration or as disease model platforms.

List of Abbreviations

2D-two-dimensional
3D- three-dimensional
A- amelogenin
ALP- alkaline phosphatase
CBFβ- core-binding factor beta subunit
BMPs- bone morphogenic proteins
BMMSC- bone marrow mesenchymal cell
BMU- basic multicellular unit
C- Collagen type I
CX- connexin
Cxcl9- chemokine (C-X-C motif) ligand 9
CXCL12- chemokine stromal Cell-derived factor 1
DKK1- Dickkopf-related protein 1
Dlx5-Distal-less homeobox 5
DMP-1- dentin matrix protein 1
DOPA- polydopamine
E- e-cadherin
EC- endothelial cells
EDTA- Ethylenediaminetetraacetic acid
EDC- N-(3-Dimethylaminopropyl)-N′-ethylcarbodiimide hydrochloride
ECM- extracellular matrix
EGFP- Enhanced Green Fluorescent Protein
F- fibronectin
FGF- fibroblast growth factors
GAG- sulfated glycosaminoglycan
GDF- growth differentiation factors
HA- hydroxyapatite
HIF-1α -hypoxia-inducible factor-1
hiPSC- human induced pluripotent stem cells
HSCs- hemotopoietic
HSPGs- Heparan sulfate proteoglycan
IFN-γ- interferon gama
Ihh- Indian hedgehog homolog
IL- interleukin
Lepr- leptin receptor
LRP- Lipoprotein receptor-related protein
M-CSF- macrophage colony stimulating factor
MEPE- matrix extracellular phosphoglycoprotein
MOBL- mesenchymal osteoblast
MSCs- mesenchymal stem cells
MX1- Interferon-induced GTP-binding protein MX1
NaOH- sodium hydroxide
NHS- *N*-Hydroxysuccinimide
NO- nitric oxide
OPG- osteoprotegerin
ORP150- oxygen regulated protein
Osx- osterix
Panx- pannexin
PBS- phosphate buffered saline
PCL- polycaprotactone
PDGF- platelet derived growth factor
PDGFRα- platelet derived growth factor receptor alpha
PDMS- Polydimethylsiloxane
PEG- poly(ethylene glycol)
PELGA- poly(lactide-*co*-glycolide)-*b*-poly(ethylene glycol)-*b*-poly(lactide-*co*-glycolide
PGA- polyglycolic acid
PHEX- phosphate-regulating gene with homologies to endopeptidases on the X chromosome
PI- Propidium Iodide
PKA- protein kinase A
PLA- poly(lactic acid)
PLLA- poly(L-lactic acid
PLGA- poly (L-lactide-*co*-glycolide)
PRX- Periaxin
PTH- parathyroid hormone
PTHrP- parathyroid hormone-related peptide
RANK- Receptor Activator of Nuclear Factor κ B
RANKL- Receptor activator of nuclear factor kappa-β ligand
rhBMP2- recombinant human bone morphogenic protein-2
RUNX2- runt related transcription factor 2
SFRP1- secreted frizzled related protein
SOBL- surface osteoblast
TGF-β- transforming growth factor-β
TNF-α- tumor necrosis factor-alpha
UV- ultra-violet
V-vitronectin
VCAM- Vascular cell adhesion protein
VEGF - vascular endothelial growth factor

Index

Figures list

Table list

Chapter I- Introduction

1. Introduction

Bone physiology involves the coordinated regulation of a myriad of biological processes that lead to tissue development, homeostasis and repair upon trauma [1]. The regeneration process for bone, can thus be highly complicated to emulate, since several cues contribute to this niche. Some of these cues are: composition of bone's soluble microenvironment, extracellular matrix (ECM) insoluble proteins and glycoprotein composition and renewal, cell-cell and cell-ECM interactions, the role of mechanical stimulation, or recent trends as the role of microRNA. The understanding of these cues has inspired the design of a plethora of bone regeneration approaches [2]. It is estimated that by with increasing obesity and poor physical activity, bone related injuries are going to duplicate, so there is a growing need for effective and efficient regeneration methods [3].

The application of concepts learnt from nature for the emulation of the structure and physiology of healthy bone requires a careful approach: in general, the effect of (bio)chemical (e.g. presence of soluble cytokines, as bone morphogenic proteins – BMPs), structural and physical properties (e.g. different biomaterials chemistries), along with external mechanical stimuli (e.g. compressive stress or flow perfusion) on bone regeneration strategies have been explored in a unifactorial fashion. The same route has been taken for the design of biomaterials and tissue regeneration strategies. Nonetheless, one must not forget that bone is a complex, dynamic and intricate system, in which different biological processes and structural characteristics are proved to play complementary roles towards the successful regeneration and maintenance of bone's healthy behavior [1]. Additionally, the possible role of some components of bone – including the immune cells crosstalk or the role of hematopoietic stem cells [4] - are still in need of study. While the understanding of individual distinctive biological processes and structural features of bone biology are crucial to develop new proof-of-concept therapies based on tissue engineering approaches, bone must not be overlooked as a dynamic and complex system in which regulated crosstalk occurs involving, simultaneously, different processes.

The advent of stem cell biology, as well as the progressive know-how on the structural, biophysical and biochemical role of the extracellular matrix (ECM) components and the scrutiny of immune cells crosstalk supported recent advances in the design of biomaterials targeting bone regeneration [5]. The acknowledgement of such complexity may be an

effective manner to pave the way for the design of multifactorial strategies targeting bone regeneration and disease treatment. Some studies have approached aspects as crosstalk between different cell types (including mineral-forming cells, reabsorption cells, immune cells and vascular cells) [6,7], the combinatorial role of ECM proteins [8,9], the effect of physical factors as biomaterials stiffness and viscoelasticity [9], as well as the role of extrinsic mechanical forces actuating in the native bone (e.g., compression and shear stress) [10].

As a way to understand the current design of finely tuned biomaterials and regeneration strategies, developed to allow close-to-native regeneration, this Review focuses on (i) the description of the most well-known phenomena of bone biology and, in a second part, (ii) on the description of studies that used a multifactorial approach to design bioinspired tissue engineering strategies based on the integration of diverse aspects of bone biology.

2. A Macroscopic View of Bone

Bone is the anatomic structure responsible for the movement, protection, maintenance of mineral homeostasis and structure of the human body. In a fully-grown adult, this structure is composed of 206 individual bones (excluding the sesamoid bones), which are interconnected to compose the skeleton [11]. The bones of the human body are divided in five major categories, which include long (e.g. clavicles, raddi, metacarpals, tibiae, phalanges, femurs, humeri, metatarsals, fibulae and ulnae), short (e.g. patellae, tarsal and carpal), flat (skull, sternum, mandible, ribs and scapulae), irregular (e.g. vertebrae, coccyx, sacrum and hyoid) and sesamoid bones (patella) [12].

Bone tissue is constituted by both cortical/compact bone, which is dense and solid, and trabecular/cancellous bone, which contains a spongeus-like structure. They are both composed of osteons [13]. The ratio of these two bone types varies according to its anatomical site (e.g. femoral head as a ratio of 50:50 cortical to trabecular; vertebra has a 25:75; radial diaphysis is 95:5; and overall, the human skeleton is composed of the 80:20) [14].

3. Mechanisms of Bone Development and Repair

During mammals' fetal development and natural bone repair upon injury, bone formation is achieved through two processes: intramembranous and endochondral ossification. In

intramembranous ossification, mesenchymal stem cells recruited to the injury site differentiate into osteoblasts, forming the flat skull bones [1]. The primary structure for these two mechanisms to occur is the woven (or immature hollow) bone, that is readily replaced by the lamellar/secondary bone (parallel fibrils deposited in opposite directions) [15] This structure does not appear only in the fetal life, but every time a bone has a fracture, and this process continuously repeats itself (bone substitution) [15]. The formation of lamellar bone occurs at a much slower rate than that of woven bone [16].

3.1. Intramembranous bone formation

In intramembranous ossification, mesenchymal stem cells (MSCs) present in mesenchyme or in the medullary cavity (caused by a bone injury) develop into osteoblasts. In fetal development, this process is mainly responsible for the formation of the flat skull bones and in some parts of the clavicles [17]. Unlike in endochondral ossification, bone is formed without a cartilaginous intermediate. The formation of a nidus – a cluster of undifferentiated MSCs – is the starting point for the intramembranous ossification process. The cells in these clusters stop their proliferation and develop into osteoprogenitor cells which, eventually, develop into osteoblasts [17]. This differentiation occurs from a pre-osteoblast to osteoblast lineage [18]. Runx2 is the transcription factor responsible for the osteoblast differentiation [19,20]. After their differentiation, osteoblasts produce a non-mineralized type-I collagen-rich fibrillar extracellular matrix (ECM): the osteoid. While entrapped in this matrix, osteoblasts differentiate into mature osteocytes, and the matrix is further mineralized. The described mechanism is also the backbone for the bone formation of the subperiosteal bone, thus, being the process behind the woven and lamellar bone type formation in this region [21]. understanding schematic representation of the intramembranous ossification process can be found in Figure 1.

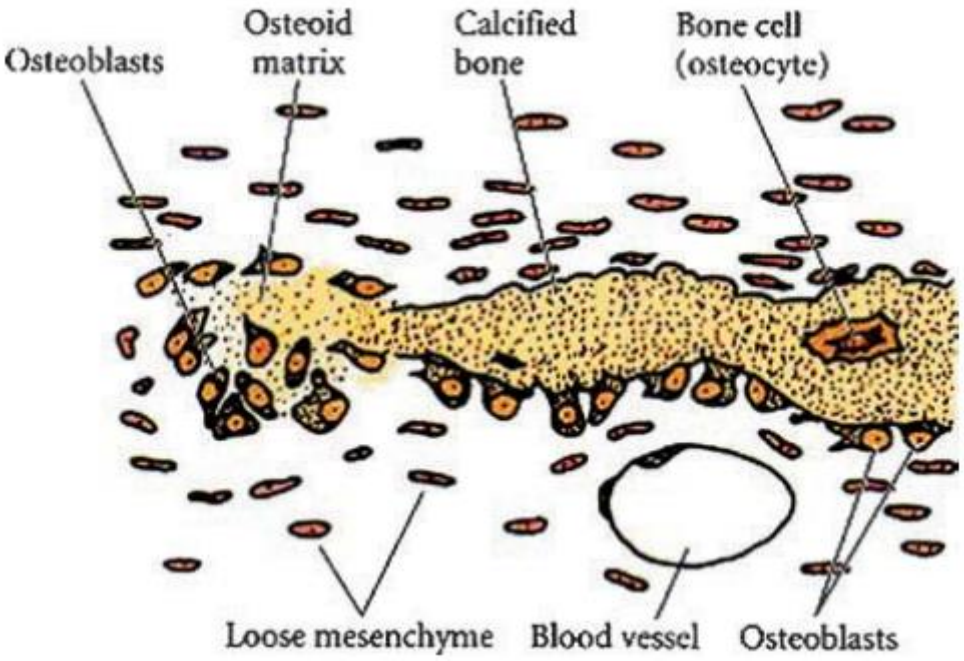

Figure 1-Schematic representation of the matrix base for intramembranous ossification to occur. The MSCs condense and produce osteoblasts, that mineralize the bone matrix. They line the surfaces of the bone that is growing and continuously produce the bone matrix by apposition. No cartilage proceeds the formation of this bone type. Taken from Gilbert, S. F. (2003) [22]

3.2. Endochondral ossification

In endochondral ossification chondrocytes from the surrounding cartilage form a matrix template, which is called the growth plane, and only then do they differentiate into the other bone structures [19]. When chondrocytes' morphology is round, they synthesize type II collagen [23] and then form a columnar layer and become pre-hypertrophic. They eventually differentiate in post-mitotic hypertrophic cells, which express type X collagen, mineralizing the surrounding matrix, and thus, forming the bone structure [24]. During the bone formation process, there are various cycles of death of the hypertrophic chondrocytes as well as invasion of the blood vessels, leading to the replacement of the matrix (collagen) by the trabecular bone, also known as primary spongiosa [25]. As the process continues, the trabecular bone is resorbed, and the center is split into different plates, and then this whole process is repeated (if chondrocytes are present in the plates) [25]. These cells act as a natural support for the formation of the primary bone structure [25]. The adequate

differentiation of chondrocytes into the hypertrophic phenotype is of extreme importance for the genesis and proliferation of bone tissue [25]. For a more visual comprehension of the whole process, please see figure 2.

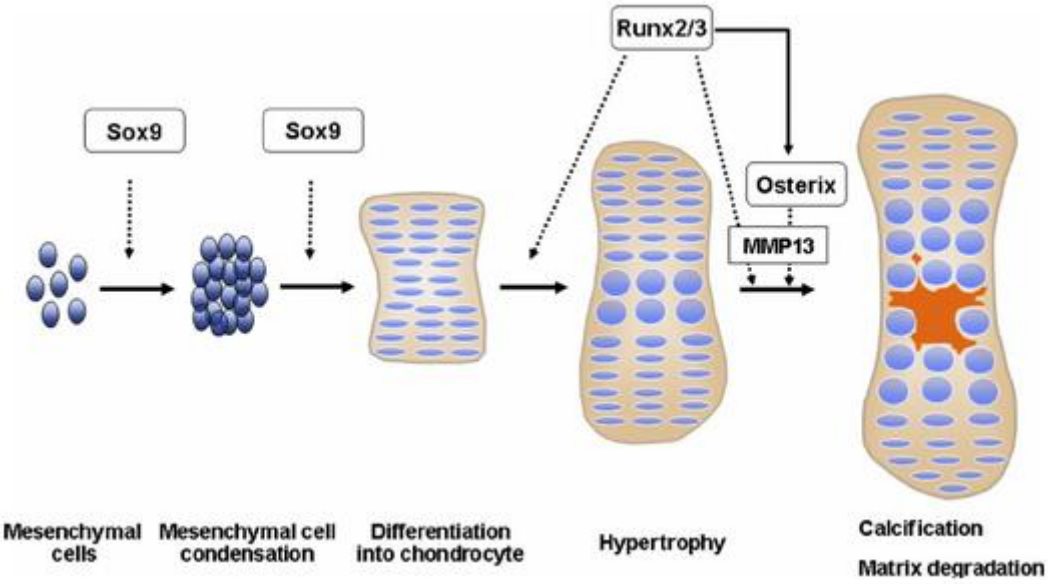

Figure 2 – Schematic representation of the chronological steps occurring during endochondral ossification. Taken from Nishimura et al. (2012) [26]

For the formation of bone during the endochondral ossification process, some conditions must be met, which include:

- The presence of the Sox Trio: Sox9/5/6. These molecules are responsible for the differentiation of MSCs into chondrogenic phenotype, as well as for the regulation of the expression of critical genes for the formation of the cartilaginous matrix [25,26];
- The fibroblast growth factors FGF receptor3, a membrane-spanning tyrosine kinase receptor expressed by chondrocytes, that has a domain to bind extracellular ligands, that binds (FGFs) and thus, initiates the receptor's autophosphorylation, as well as the stimulation of the tyrosine kinase activity, leading to the inhibition of proliferation and growth of chondrocytes [27,28];
- The bone morphogenic proteins (BMPs), which are responsible for the formation of mesenchymal condensations and formation of joints, in an initial stage of the endochondral ossification. After condensation, when long bones are already formed, BMP-2, -3, -4, -5 and -7 are expressed in the perichondrium, BMP-2 and -6 are expressed in the hypertrophic chondrocytes, and BMP7 on proliferative chondrocytes. BMPs positively regulate

chondrocyte proliferation and negatively modulate chondrocyte terminal differentiation [28,29];

- The parathyroid hormone-related peptide, which binds and activates the receptor PTH/PTHrP. This receptor is also activated by the parathyroid hormone (main regulator of calcium/phosphate metabolism and remodulation of the bone). This way, the PTH/PTHrP complex acts as a main regulator of bone development and mineral ion homeostasis. The PTH peptide acts by maturing the immature chondrocytes to a mature hypertrophic chondrocyte; when the chondrocytes express PTHrP or an activated form of the receptor, a decrease on the cartilage maturation and increase in bone formation is observed [30];
- Indian hedgehog homolog (Ihh), a protein present in the embryogenic patterning, controls the endochondral bone formation by inhibiting the differentiation of hypertrophic chondrocytes, therefore delaying the mineralization of the matrix. This leads to an increase of PTHrP in the growth plate, when the PTHrP pathway is present. Ihh also acts as a chondrocyte proliferation stimulator, in a PTHrP-independent pathway [31];
- Runt related transcription factor 2 (Runx2), Runx3 and core-binding factor beta subunit (CBFβ). These three transcription factors have been described in the literature as promoters of chondrocytic hypertrophy, complementing each other in the process [32,33];
- The proteins HIF-1α (hypoxia-inducible factor-1) and VEGF (vascular endothelial growth factor). These two factors are very important for bone vascularization, since HIF-1α acts by mediating hypoxic responses, allowing the survival of chondrocytes, and targets VEGF. VEGF is responsible for the stimulation of angiogenesis and vasculogenesis, and the restoration of the oxygen supply in hypoxic conditions. It is hypothesized that these two proteins act together in a pathway that regulates chondrocytes survival [34,35].

Stem cells osteogenic differentiation, that occurs in both ossification pathways, and are commonly targeted in tissue engineering, is divided in three main stages: (i) peak in cell number; (ii) cellular differentiation (with the first: step expression and transcription of alkaline phosphatase); (iii) and a terminal step: expression of osteocalcin and osteopontin [36]. In the human body, bone marrow MSCs reside in a specific niche composed of a large variety of support cells (hematopoietic progenitors; osteoclasts, immune cells and blood cells). This niche was first defined by Schofield, in 1908 [37]. The osteogenic differentiation of MSCs is influenced by factors secreted by osteoblasts and osteocytes

[38]. This phenomenon occurs through a communication network amongst two bone cells types - osteoblasts and osteocytes - that enhance a response in the MSCs, when these two bone cell types are in contact [38]. *In vitro*, the co-culture of MSCs with osteocytes showed greater osteodifferentation than the ones with osteoblasts, indicating that osteocytes induce MSCs' osteogenesis more effectively than osteoblasts [38]. On the other hand, osteoblasts helped the proliferation of the MSCs [38]. The *in vivo* interactions between both cell types, as well as other cells belonging to the bone, are reviewed in more detail in the **Section 5**. The know-how acquired from such studies shows the importance of the presence of different cell types for stem cell differentiation and growth.

4. Adult bone physiology

In adult humans, bone is formed in two ways: longitudinal and radial growth [1]. These phenomena happen during the childhood and adolescence period. Modeling occurs during the first years of life of the individual, by response to physiological or mechanical factors. This is achieved by the action of the bone osteoprogenitor-derived cells: osteoblasts and osteoclasts (see s**ection 5**) [38]. Bone morphogenesis regulated by exposure to mechanical challenges is reviewed in more detail in **Section 7**, where the Frost's "Mechanostat Theory" is explored, as well as its related biochemical signaling. Also, the role of cell types and their crosstalk during bone healthy state maintenance and upon trauma are reviewed in **Section 5** and further ahead on this section.

To form and maintain the complex and functional skeleton structure, bone tissues undergoes continuous remodeling during the whole life of adult individuals [1]. This process is related to the increasing fragility of bone throughout life, which leads to the necessity of the creation of new functional bone, allowing for the maintenance of the structural stability of the human body [11,12]. Bone remodeling is increased during adults' middle age and happens in four stages: activation (activation and recruitment of osteoprogenitor cells), resorption (resorption of the osteoprogenitor cells by osteoclasts), reversal (transitional phase from bone resorption to bone formation) and formation (matrix synthesis by osteoblasts) [1,39]. A detailed explanation of the previously mentioned phases is provided in a review paper by Clarke *et al*. (1938) [1].

During bone resorption, osteoclasts act by removing the "old bone" packets; afterwards, new synthesized matrix is created, along with mineralized tissue [1]. Bone formation and

degradation are tightly kept in equilibrium throughout humans' life by the bone homeostasis and remodeling process [1]. Osteoclasts (the promotors of bone resorption) and osteoblasts (with a role of bone formations) are the main mediators of this process [1]. The bone unit responsible to maintain this equilibrium is the basic multicellular unit (BMU), composed by osteoclasts, osteoblasts, connective tissue, nerves and blood vessels [40].

4.1. Bone Healing: tissue response upon injury

Since bone is the main structure of our body, it is important to have a system that guaranties its maintenance and integrity [11]. Its healing upon fracture, avoiding the formation of scar tissues, is of utmost importance, so the function of bone is not compromised [12]. Fractures are the most common large-organ, traumatic injuries in humans. The repair of bone fractures is a postnatal regenerative process that recapitulates many of the ontological events of embryonic skeletal development [41]. Although fracture repair usually restores the damaged skeletal organ to its pre-injury cellular composition, structure and biomechanical function, about 10% of fractures will not heal normally [41]. A schematic representation of the process occurring after trauma is shown in Figure 3.

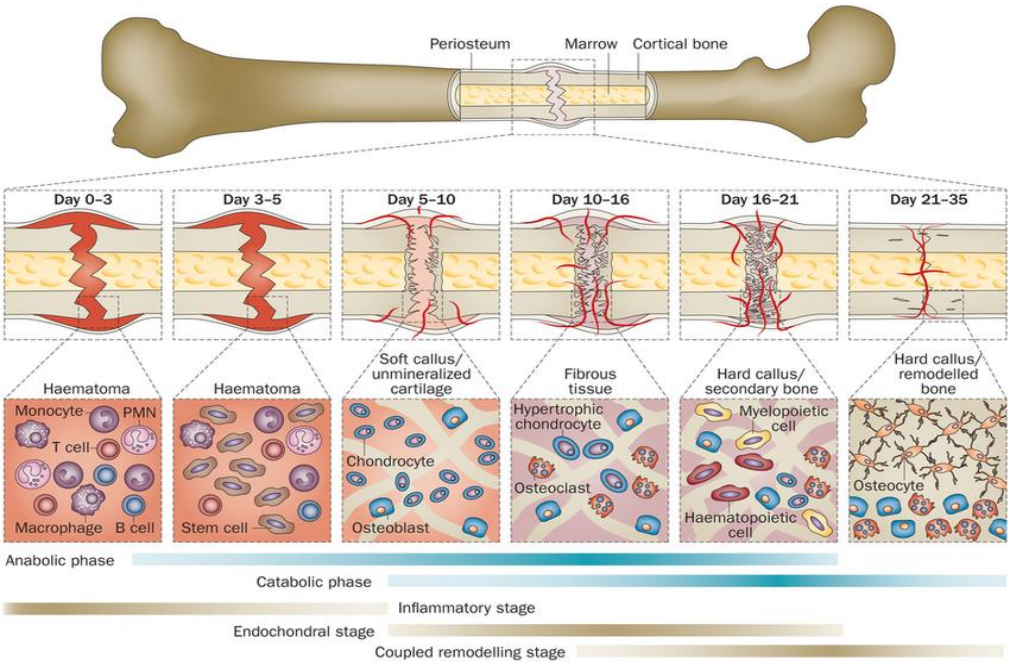

Figure 3-Bone healing chronological scheme: femur example. In blue are represented the major metabolic phases and in brown the biological ones. Taken from Einhorn, T. A., & Gerstenfeld, L. C. (2015) [43]

The bone healing phenomenon endows several stadia that occur in a sequential manner: inflammation, soft callus formation, hard callus formation and bone remodeling [41]. The different bone healing stadia are reviewed in the following topics:

- The **inflammatory phase**, which is characterized by the proliferation and migration of mesenchymal progenitor cells to the fracture site [42]. At this stage, blood also enters the defect, forming a hematoma [42]. There, several pro-inflammatory cytokines and growth factors (including tumor necrosis factor-alpha - TNF-α, interleukin-1 (IL-1), IL-6, IL-11 and IL-18) are expressed in a temporally and spatially controlled manner [43]. These signals recruit inflammatory cells and promote angiogenesis [43]. At this stage, platelets are recruited and activated in the defect site and produce transforming growth factor-β1 (TGF-β1) and platelet derived growth factor (PDGF) [43]. Simultaneously, recruited osteoprogenitor cells express BMPs which, in coordination with other factors, promote the recruitment and osteodifferentiation of MSCs [44,45].
- The **soft callus formation**. After the formation of a blood hematoma, blood cells, fibroblasts and immune cells are recruited to the injury site, forming the granulation tissue [43]. Bone is formed in the peripheric regions of the fractures sites via intramembranous ossification (Reviewed in **Section 3**) after 7 to 10 days after injury [46]. The inner parts of the fracture, which are mechanically less stable [47], are replaced by fibrovascular tissue (mainly composed of fibroblast cells). Cartilage is formed and, thus, a differentiation of the progenitor cells into chondrocytes takes place. These cells then proliferate until complete differentiation into a mature hypertrophic phenotype [43]. At this stage, TGF-β2 and -β3, as well as BMPs, mediate cell differentiation and proliferation at the injury site [48]. Upon the completion of this process, the soft callus if formed [43]. By the process of endochondral ossification (reviewed in **Section 3**), the soft callus is transformed in the **hard callus**, with a mineralized matrix, and the formation of primary bones and/or woven bone is started [43].
- The formed primary bone is gradually replaced by secondary (lamellar) bone, in the **bone remodeling process** [49]. At this stage, osteocytes undergo apoptosis in a reestablishment of the normal bone physiology. This stage can occur throughout several years [50].

Several immune system cells take part of the bone healing process. Macrophages are known to be highly influential of these processes; some studies point to their presence in the healing cascade [51-53], and their absence in the healing place can lead to a complete depletion on the regeneration of the tissue [54]. In bone healing, an optimal balance between M1 macrophages (with the role of initiating the inflammatory response [55] and secreting pro-inflammatory cytokines [56]) and M2 macrophages (responsible for tissue remodeling, with a phenotype induced by IL-4 and -13, and secreting IL-10 [56]) functions must be met, so an adequate regeneration of the tissue is achieved. These two macrophages types work together to start and finish the immune response, in an interlocked chain of events [57]. The initiation of the inflammatory response is carried out by the M1 macrophages, which are thought to be gradually substituted by pro-heling M2 macrophages [58]. An unbalance corresponding to a long M1 macrophages permanence at the defect site may lead excessive inflammation, which may compromise fracture healing [59].

A study by Schlundt *et al*. [60] showed that, although the reduction of macrophages did not appear to have any effect on bone regeneration in initial regeneration steps, the formation of the hard callus was delayed, and thus affecting endochondral ossification efficiency. The authors focused on determining in which specific time did M1 and M2 macrophages start to act. Since one of the most promising results they observed was the great presence of M2 on the ossification process, they induced this macrophage type (using IL-4 and 13 cytokines) and verified that bone formation was greatly enhanced.

Besides macrophages, other cell types are also present in the fracture location, which include monocytes, neutrophils and NK cells [61]. These cells produce cytokines that are responsible for the recruitment and activation of other cells with differentiation and proliferation potential to regenerate the tissue (e.g.: osteoprogenitor MSCs) [59]. When osteoprogenitor cells are recruited to the fracture place, their osteodifferentiation is partially induced immune cells present at the injury site [62].

Other immune cells known to participate in the healing process are T-lymphocytes: they act by inhibiting the healing process through the action of cytokines (IFN-γ (interferon gama) and TNF-α) [63-67]. Conversely, MSCs have been reported to affect the immune response in a plethora of ways, by suppressing or inhibiting it. This response is coordinated by the cellular microenvironment and the MSCs-to-T-lymphocytes ratio, with a high ratio

inhibiting the immune response, and a low ratio inducing it [66-69]. Nonetheless, the MSCs/T-cells interactions still require further studies, so their crosstalk is completely understood. The known interactions between MSCs and immune cells present at the period of bone fracture healing are depicted in Figure 4. The interactions between immune cells and bone cells are reviewed in **Section 5**.

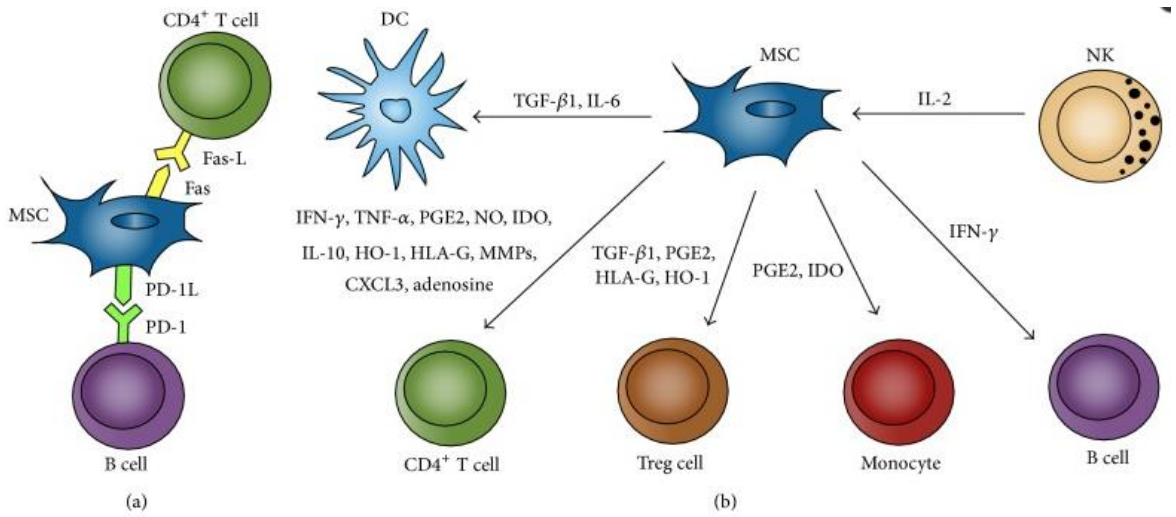

Figure 4- Scheme of the several mechanisms of MSCs modulation on immune cells. A) direct cell-cell contact, b) soluble factor interactions. Taken from Kovach T. K., et al. (2015) [70].

5. The adult bone cellular niche

5.1. Bone primary stem cell niche

The bone tissue comprises two primary niches: the osteoblastic and the vascular niche [4]. Two stem cells types - hematopoietic (HSCs) and mesenchymal (MSCs) – reside in the bone cavity, which is filled with bone marrow and blood vessels [71]. HSCs, which are surrounded by stromal cells in the bone marrow, are responsible for the formation of the immune and blood system, as well as osteoclasts [72]. MSCs also reside in the bone marrow and intervene in the formation of the mesenchymal lineage cells, which include osteoblasts, adipocytes, chondrocytes, fibroblast and other stromal cells [72]. Together, both stem cell types maintain the normal bone homeostasis and cellular generation [72]. Unlike what was thought until recent years, HSCs are not located on the inner surface of the bone [73]. Instead, HSCs were recently described to be on the perivascular niche where they are regulated by growth factors, chemokines and cytokines (ex: stem cell factor,

chemokine stromal cell-derived factor 1 (CXCL-12) and angiopoientin-I), through CXCL-12-abundant reticular cells, endothelial cells and MSCs [74,73].

MSCs, characterized by the expression of PDGFRα, CD51, nestin, CD139, interferon-induced GTP-binding protein MX1 (Mx1), leptin recptor (Lepr) and Prx, give rise to osteoprogenitor cells that form the osteoblastic niche. Thereafter, the factors referred previously are released to promote a correct HSC maintenance (reviewed by Yin, T., & Li, L. (1936) [76]). The maintenance of a functional microenvironment in the bone niche is dependent on the precise level of the hierarchical linages of the HSCs and MSCs, so that osteoblastogenesis and hematopoiesis can maintain a correct balance of osteoblast and osteoclast production. Importantly, only a subset of N-cadherin positive osteoblasts interacts with HSCs, since they help these cells in anchoring to the osteoblastic niche [77].

Cell signaling inside the bone niche, for example between osteoblasts and B lymphocyte precursors, is well known to determine features of the immune system [74]. Since in this Review immunogenesis will not be discussed, the interactions occurring in the bone niche will be described regarding the correct function of the bone tissue itself (see **Section 5**). However, it must be emphasized that the bone niche must maintain not only a proper functioning bone development, but also a continuous exportation of immune cells and tissue progenitor cells to the peripheral immune system, thus sustaining tissue repair and regeneration [78] (Figure 5).

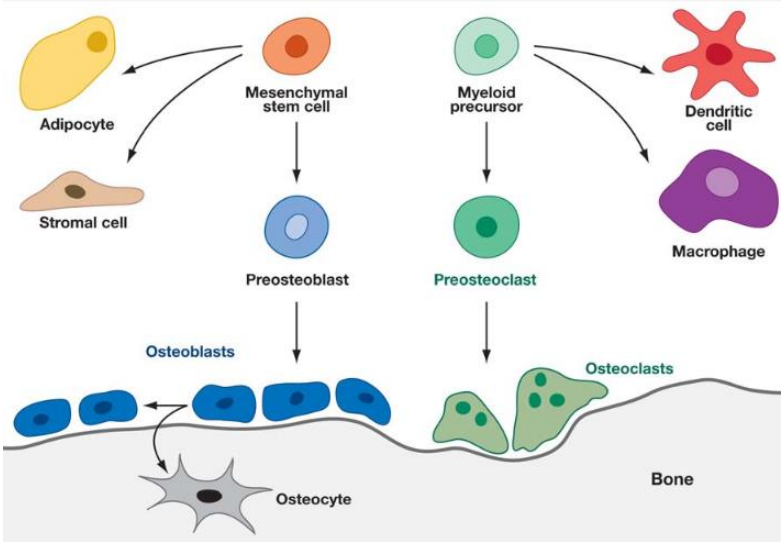

Figure 5 – Scheme of the bone cell differentiation process. The MSCs start by differentiate into prosteoblasts and then give rise to the osteoblasts, which then mature into osteocytes. Taken from Walsh, M. C. et al. (2016) [79].

5.2. Bone cells (resident)

5.2.1. Osteoblasts

Osteoblasts synthetize new bone matrix [1]. Different sub-populations of osteoblasts have shown to respond differently to several signals (mechanical, hormonal and from cytokines) [1]. Under physiological conditions, MSCs must undergo the Wnt/β-catenin pathway to differentiate into the osteoblastic phenotype. Osteoblasts have a cuboidal morphology while proliferating on the bone matrix surfaces, unlike their precursors cells (preosteoblasts), which have a spindle shape [1]. Mature osteoblasts secrete bone ECM proteins, such as collagen type I [80]. Typical gene indicators of osteoblast expression are Runx2, distal-less homeobox 5 (Dlx5), osterix (Osx) and ColIA1 [81, 82].

Osteoblasts can be divided in two types: mesenschymal (MOBL) or surface osteoblasts (SOBL) [83]. In the bone matrix, the undifferentiated MSCs start to differentiate into MOBL, which secrete collagen all thought the matrix, forming a woven structure, with random orientation of the collagen fibrils. After the creation of sufficient woven bone to form a platform-like structure, SOBL secrete collagen fibrils in a parallel way onto the previously made bone structure, creating the lamellar bone. Once this process finishes, osteoblasts are matured into osteocytes surrounded by collagen matrix [84] (Figure 6).

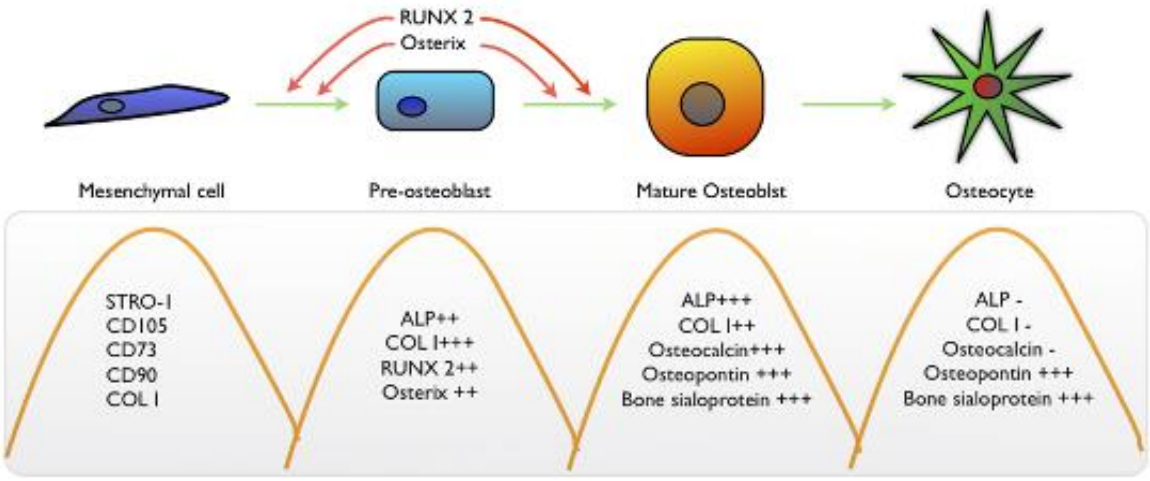

Figure 6 – Schematic representation of the differentiation of pre-osteoblast cells into osteoblasts, and into mature osteocytes. Figure taken from Miron, R. J. & Zhang, Y. F. (2012) [85].

5.2.2. Osteocytes

Osteocytes descend from the mesenchymal lineage, as they are differentiated osteoblasts (Figure 6) [85]. They compose 90% to 95% of the whole bone cells in adult bone, and may live up to decades in their mineralized environment, where they have a dendritic configuration. Their function is to support the skeleton and bone metabolism. As osteoblasts transition to osteocytesm the expression of alkaline phosphatase decreases, and casein kinase II and osteocalcin are elevated [1]. Other expressed markers include phosphate-regulating gene with homologies to endopeptidases on the X chromosome (PHEX), matrix extracellular phosphoglycoprotein (MEPE), dentin matrix protein 1 (DMP-1), fibroblast growth factor 23 (FGF-23), sclerostin, and oxygen regulated protein (ORP143), thought to protect against hypoxia [1]. These cells, located on the mineralized portion of the bone, were considered as "passive placeholders in bone" in the past. However, they were proved to have numerous functions, including bone remodeling, through the activation of both osteoclasts and osteoblasts, and also in endocrine cell functioning. [86]. The interactions between osteocytes and osteoblasts/osteoclasts is reviewed in **Section 5.3.1**. Osteoclasts are also responsible for the excretion of ECM proteins such as CD44, galectin 3 and osteocalcin. These proteins have the function to promote cell adhesion and the regulation of the mineral exchange in the bone. Osteocytes also express Cbfa1 and osterix, which are required for osteoblast differentiation, and are followed by alkaline phosphatase and collagen, necessary for the formation of the osteoid: the unmineralized collagenous matrix preceding bone [86]. Several soluble molecules produced by osteocytes interfere with biomineralization (e.g. PHEX, MEPE and DMP-1) [86]. The communication between osteocytes, occurring mainly by gaps composed of connexin 43 [87], are required for their survival, maturation and correct activity. The diverse roles of osteocytes also endow their phagocytic activity, during osteolysis, since they have lysosomes in their constitution. Also, one of the main functions of osteocytes is mechanosensing by translating stress factors into biologic signals [86]. The mechanotransduction phenomena occurring in bone through the action of osteocytes and other bone cells is reviewed in **Section 7**.

5.2.3. Osteoclasts

Osteoclasts, generated in the bone marrow from the mononuclear monocyte-macrophage precursors (derived from the hematopoietic lineage) [88], are the only cells capable of resorbing bone and, consequently, play an essential role in bone remodeling. Two cytokines – receptor activator of nuclear factor kappa-β ligand (RANKL) and macrophage colony stimulating factor (M-CSF) – drive osteoclasts' proliferation, differentiation and survival [88,89]. Bone resorption occurs in the presence of hydrogen ions (acidification of the resorption compartment, dissolving the mineral bone matrix) and cathepsin K (enzyme responsible for the digestion of the insoluble fraction of the matrix, manly type I collagen), both secreted by osteoclasts. These cells are bound by the bone matrix through integrins (β1 for collagen, laminin and fibronectin, and αvβ3 for osteopontin and bone sialoprotein) [88]. Such binding polarizes osteoclasts, creating an actin ring that seals the periphery of the ligation of the osteoclasts to the matrix, and a ruffled border in the resorbing surface, which leads to the secretion of H^+ ions, followed by the exocytosis of enzymes from the acidified vesicles [88].

5.3. Cell-cell interactions in bone

It is well established that bone cells interact in adult bone to regulate the homeostasis process, supporting the balance between bone resorption and formation that allows the maintenance of the tissue's integrity [90]. We review the interactions between the main cells constituting the healthy bone – osteoblasts, osteoblasts and osteocytes -, and the crosstalk occurring between such cells and the vascular system that irrigates bone. The main interactions between immune cells, present in bone fracture sites, with constituent bone cells is also reviewed.

5.3.1. Osteocytes – osteoblasts

Bone formation is regulated by several signaling pathways, from which the Wnt/β-catenin pathway is one of the most important [1]. The activation of canonical Wnt signaling in early osteoblasts promotes osteoblast differentiation and bone formation [91], with opposing effects observed when Wnt signaling is disrupted [92]. Osteocytes secrete Wnt antagonists, which include sclerostin and the LRP5/6 inhibitor DKK1 (Dickkopf-related protein 1). Both molecules were shown to inhibit osteoblast differentiation and bone formation [93-95]. Also, the *in vivo* loss of secreted frizzled-related protein 1 (SFRP1),

which is a competitive antagonist of Wnt ligand, resulted in increased bone mass and mineral density, and *in vitro* enhancing osteoblast proliferation and differentiation into osteocytes [96]. With their capacity to interfere in canonical Wnt signaling, therefore affecting osteoblasts differentiation, osteocytes show a regulating role in bone formation.

5.3.2. Osteoblasts-osteoclasts

Signaling between osteoblasts and osteoclasts is crucial for osteoclast maturation [1]. It is known that osteoblasts and stromal cells express RANKL, M-CSF, and osteoprotegerin (OPG), while early osteoclast precursors express c-Fms (M-CSF receptor) and receptor activator of nuclear factor κ B (RANK) (a receptor for RANKL) [97]. RANKL (the RANK ligand) and M-CSF stimulate osteoclast differentiation, while OPG is an inhibitor of RANKL, and competes with RANKL for RANK [98]. Low levels of OPG lead to accelerated osteoclast development, which culminates in osteoporosis, in which the bone resorption/formation balance is disrupted, and bone resorption exceeds bone growth [99]. In summary, the interactions between osteoblasts and osteoclasts are of extreme importance in the regulation of bone resorption and formation, and disruptions in this balance may trigger disease scenarios.

5.3.2. Osteocytes – osteoclasts

Osteocytes – both healthy and apoptotic at microdamage sites – have been reported to recruit osteoclasts to the bone remodeling sites [100], and were shown to send bone resorption cues to these cells [100-102]. The expression of the RANK ligand (RANKL) during the dendritic process associated with osteocytes maturation was associated with the osteocyte-led bone resorption [100]. Upon injury, right after damage, pro-apoptotic molecules are released by osteocytes; contrarily, anti-apoptotic molecules are expressed 1-2 mm from the cracks [100, 103]. The promotion of a defective performance of osteocytes in mice, through β-catenin deletion, led the increased osteoclasts activity, showing that osteocytes are necessary for a correct regulation of osteoclasts activity, and therefore, of the bone remodeling process [100]. Another indication of the close osteocyte/osteoclast interaction was the formation of osteocytes induced, *in vitro* and *in vivo*, by osteoclasts apoptotic bodies; the contact with osteoblast-derived apoptotic bodies did not have this effect [100,104]. Moreover, the induction of osteocytes formation by exposure to

osteoclasts' apoptotic bodies was not driven by RANKL, as it was shown to be a TNF-α-dependent process.

5.3.3. Vascular cells – osteoblasts

Bone-associated blood flow is responsible for the control of oxygen and nutrient delivery/exchange in the tissue. Also, bone formation and resorption are coupled with bone hemodynamics. During endochondral ossification, the vascularization of hypertrophic avascular cartilage is one of the determinant steps for bone elongation. During fracture healing, the generation of an efficient new tissue is also dependent on a successful vascularization. A tight connection between the growth of blood vessels in bone and the osteogenesis process has been reported [105]. Endothelial and osteoblastic cells have a molecular crosstalk in which angiogenesis and osteogenesis and synergistically promoted. Osteoblasts are known to secrete angiogenic factors, including vascular endothelial growth factor (VEGF) [106] and erythropoietin [107], which mediate their cross-talk with endothelial cells. Nonetheless, the mechanisms and molecules involved in this process have not yet been fully unraveled.

Recent findings have presented bone vasculature as a unique network, with substantial differences from other body vascular systems. Interestingly, vascular growth in bone was proved to be obtained by a tissue specific angiogenesis, in which the Notch pathway is responsible for the endothelial cell proliferation and the blood vessel growth in post-natal long bone. In a study conducted by Ramasamy *et al.* , the authors verified a deficiency on the bone vessel growth and morphology by knocking out the gene responsible for the Notch signaling. In turn, this led to reduced osteogenesis, resulting in the irregularity of bone structure in mice [108]. Recently, Huang *et al.* [109] identified chemokine (C-X-C motif) ligand 9 (Cxcl9) as a angiostatic factor secreted by osteoblasts in the bone marrow environment. Mice with constitutive mTORC1 (an Cxcl9 activator) in osteoblasts demonstrated enhanced VEGF secretion; however, this was accompanied by an unexpected decrease in the phosphorylation of its receptor (VEGFR2), as well as downstream signaling in endothelial cells, and reduced vasculature formation in bone.

The structure of bone vasculature has also shown to be unique by Kasumbe *et al.*, who identified a new capillary subtype in the murine skeletal system, presenting distinct molecular, morphological and functional properties. These vessels were shown to be crucial for the correct bone development and maintenance, since they generate a distinct

molecular and metabolic microenvironment, linking angiogenesis and osteogenesis, and lastly maintaining perivascular osteoprogenitors [110].

5.3.4. Immune cells interactions with bone cells

Despite not being found in bone tissue in healthy conditions (with the exception of "osteomacs"), immune cells residing in the bone marrow are in a close anatomic location with bone. The crosstalk between bone cells and immune system cells has often being overlooked, and usually focus on the role of such cells in disease [111]. We here report some of the studied cell crosstalk facts involving bone cells, and bone-related or bone-constituent (osteomacs) immune cells, related to the regulation of bone's normal physiology.

The reduction of bone-related immune cells of B- and T- lymphocytes in mice have led to osteoporotic scenario [112]. Moreover, it is known that mature B-cells produce more than half of bone marrow-derived OPG, contributing to osteoclastogenesis restriction [112]. It is also thought that T-lymphocytes may interact with B-cells to enhance OPG production [113]. Hematopoietic stem cells-derived megakaryocytes, known to produce platelets, were shown to enhance the *in vitro* osteoblast proliferation and differentiation through the expression of RANKL, OPG and some unknown anti-osteoclastic factors [114]. Nonetheless, the role of megakaryocytes is still unclear in bone physiology.

Osteomacs are probably the most studied immune system cells in bone tissue. They reside on the endosteal and periosteal surfaces, and compose 10 to 15% of most tissues [115]. *In vivo*, osteomacs form a shell over mature matrix-producing osteoblasts at sites of bone modeling. Depletion of macrophages *in vivo* results in complete loss of endosteal osteomacs and their associated osteoblasts, suggesting that osteomacs are needed to maintain mature osteoblasts in the bone structure [113,116].

5.4. Cell-cell contact in bone– the role of cadherins, connexins and pannexins

Cells can communicate by two processes, involving indirect and direct contact. Most interactions occurring during bone formation, development and remodeling have been shown to occur via cellular direct contact. Cadherins are the main proteins responsible for cell-cell adhesion [117]. These proteins are glycoproteins located at the cell membrane, which promote cell-cell adhesion by a calcium-mediated mechanism. Cadherins (molecular weight around 120 kDa) are constituted by two domains: the extracellular and the

transmembrane domain. The calcium-binding site (five repeats; responsible for the ability of cells to bind the same cadherin) is located in the extracellular domain. Cadherins can be classified in the following way: type I and type II. In these two types, cadherins can be divided even more: type I: N-, E, M- and R-; type II: 5 to 12 [117]. Cadherins have a cytoplasmic C-terminal tail that is responsible for the stabilization of the adhesion. This structure is organized by the binding of cadherin to β-catenin and plakoglobin, which connect cadherins to the actin cytoskeleton, via N-catenin, actinin, ZO-1 and vinculin. This binding is a dynamic process. Adherent junctions are the junctional structures between two adjoining cells that allow communication and adhesion between cells [117].

In bone, there are three major cadherins: E-cadherin, N-cadherin and cadherin-11 [118-121]. Cell-cell adhesion mediated by cadherins is essential for the function of bone-forming cells during osteogenesis. The inhibition of these cadherins was shown to inhibit osteoblasts differentiation [122]. During osteoblast differentiation, cadherin-2 is downregulated over the process, and cadherin-11 becomes the main cadherin for osteoblast functions. For successful osteogenesis, cell-cell contact amongst cells of the ostoblastic lineage and the osteoclasts precursors is necessary. This interaction is mediated by RANK (receptor) and RANKL (ligand). RANK is present in osteoclasts precursors, while RANKL is present in the membrane of osteoblastic cells [1].

Connexins are proteins involved in cell-cell contact, allowing the rapid dissemination of molecules (smaller than 1 kDa) and ions by diffusion among cells. They link cells through gap junction channels, that facilitate electrical and chemical coupling [122]. The most widely reported connexin in bone - expressed by osteocytes, osteoblasts and osteoclasts - is Cx43; those cells were also shown to express Cx37 [123], and osteoblasts also express Cx45 and Cx46. When osteochondroprogenitors, as well as committed osteoblast progenitors, are deleted from Cx43, there is a decrease in bone mass and density [123]. Interestingly, the deletion of this connexin from mature osteoblasts and osteocytes did not lead to any effect on bone mineral density or bone length [123]. This suggests that Cx43 is essential for osteochondral progenitors, but not in committed osteoblasts [123]. Cx37 has recently been proved to regulate bone mass [124]. Deletion of this connexin led to increase in bone mass; however, this effect was shown to be gender dependent, with males being more affected than females [124]. The higher bone mass observed in individuals with

depleted Cx37 is related with a decrease in osteoclast differentiation, driving impaired bone resorption [125].

Pannexins are proteins with a very similar structural topology to connexins. However, their sequence is not homologous with connexis, and they only function as an unpaired channel [125-127]. One of the genes encoding pannexins - Panx1 - is present in murine osteoblastic cells [128], whereas Panx3 is expressed in various osteoblastic cell lines and primary calvaria cells and in hypertrophic chondrocytes [129-132]. Although some studies have studied the role of pannexins *in vitro* in osteoblast differentiation, *in vivo* studies are still missing [125].

5.5. Cells-extracellular matrix (ECM) interactions in bone

5.5.1. Cell signaling and adhesion

The ECM is a complex network comprising proteins (soluble and insoluble), growth factors and polysaccharides. It provides physical structure and a biochemical context to the cellular microenvironment [133]. In body tissues, the communication amongst cells and the surrounding ECM is mainly made through three types of proteins: integrins, selectins and immunoglobulin [134]. This adhesion contributes to cell biological process as: immune response, metastases, inflammatory process, division and death of cells, tumor progression and cell polarity. Figure 7 shows a schematic of the various interactions that occur in the ECM.

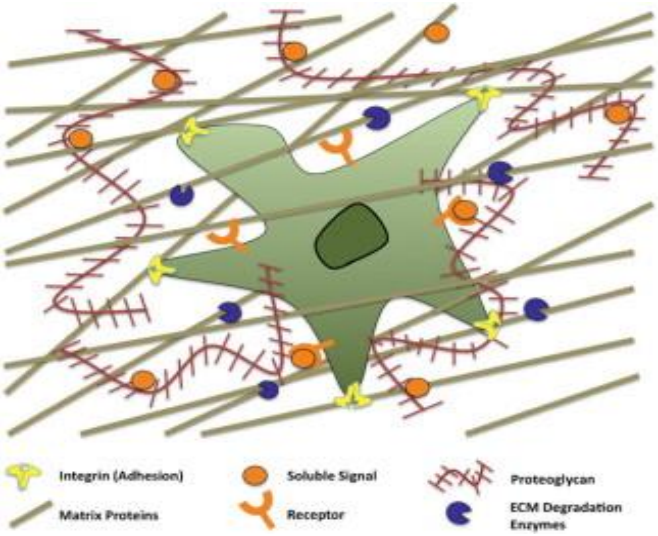

Figure 7 – Schematic representation of cell-ECM interactions. Figure taken from Wade, R. J., & Burdick, J. A. (2012)[135].

5.5.3. The adult bone extracellular matrix: the role of proteins and proteoglycans

The bone matrix is mainly composed of collagen (85-90%) and other types of proteins. The ECM has two mechanisms by which it affects cellular behavior: (i) by the direct interaction with the cells, and (ii) by harboring growth factors for cell proliferation and differentiation [136].

The connection between cells and ECM proteins - case (i) - is made through proteins existing on cell surface, integrins, which regulate not only the cell-to-physical matrix adhesion, but are also responsible for some intracellular signals. These proteins recognize specific peptide sequences and bind to specific peptide domains by the presence of two distinct subunits: α and β. The binding of the ligand to this intramembranous protein is dependent on the association of these two subunits, making it possible for only one integrin to recognize and connect to specific types of ECM proteins [137,138].

Huang *et al*. [139] studied the effects of mechanical factors (i.e. ECM stiffness) and presence of ECM insoluble proteins, in a combined effect, to assess their effect on the osteogenic differentiation of MSCs, cultured as two-dimensional monolayers, in basal medium. The tested ECM cell-binding proteins - type I collagen, fibronectin, vitronectin and laminin - induced the *in vitro* osteogenic differentiation of MSCs, implying that the right ECM composition is enough to induce the MSCs osteogenic differentiation. This study also showed that, although type I collagen is the main protein in bone ECM, no difference was observed in its capacity to induce more osteogenic differentiation than the other tested proteins. In fact, fibronectin showed more ability to drive osteogenic differentiation, followed by laminin, type I collagen, and vitronectin. The authors also verified that mechanical stretching of the cells improved differentiation. Another *in vitro* study by Mathews *et al*. [140] showed that type I collagen and laminin were the most successful ECM proteins in inducing the proliferation and adhesion of MSCs, and a high percentage of MSCs differentiation occurred by contact with fibronectin, vitronectin and collagen type I. Combinations of adhesive ECM proteins – fibronectin, laminin, osteocalcin – mixed with methacrylate gelatin hydrogels were suggested by Dolatshahi-Pirouz *et al*. [141] as a way to study the combinatorial role of ECM proteins and soluble factors in bone marrow MSCs, using a high-throughput strategy. Mixtures of proteins in the presence of bone-inducing cytokines led to higher osteogenic differentiation of MSCs. Gothard *et al*. [142] studied the *in vivo* effect of adding growth factors and osteoinducing

soluble molecules to an alginate/demineralized bone ECM hydrogel. All formulations, even the ones excluding growth factors or soluble factors, induced bone formation in rats. The authors hypothesized that this behavior may be related to reminiscent amounts of cytokines in the demineralized bone ECM used to synthetize the hydrogels. The UV-irradiation of the hydrogels, leading to the denaturation and fragmentation of the cytokines suggested that, indeed, this could be the explanation for the observed general bone formation.

The cytokine-matrix adhesion in bone ECM is accomplished by proteoglycans: a family of biomolecules composed of a core protein and a covalently attached sulfated glycosaminoglycan (GAG) [143]. GAGs are linear polymeric disaccharides, comprising hexosamine and hexuronic acid (except for keratan sulfate). Together with collagens, proteoglycans are the major constituents of bone organic ECM. The proteoglycans found in bone can be mostly divided in two families: (i) the small leucine-rich proteoglycans (SLRPs) and (ii) heparan sulfate proteoglycans (HSPGs). SLRPs are the most abundant proteoglycans in bone, and include decorin, biglycan, fibromodulin, lumican, osteoadherin and PG-Lb [141]. They have been associated with all phases of bone formation, and mediate signaling pathways regulating the osteogenic program, including the activities of TGF, BMPs and Wnt, which influence both the number of available osteogenic precursors and their subsequent development, differentiation, and function [143]. HSPGs are thought to be produced by osteoblasts and osteoclasts, and play an important role in cell–cell interactions between fibroblast-like cells and osteoclast-lineage cells by reserving heparin-binding growth factors and/or heparin-binding adhesion molecules, such as fibronectin [143]. HSPGs are known to regulate the availability and the biological activity of TGF-βs and FGFs, two major growth factor families involved in the regulation of bone biology.

The following table (Table 1) is a compilation of ECM proteins described as intervenient on bone modeling/remodeling.

Table 1- A list with examples of ECM proteins responsible for the bone formation and regeneration

Protein	Physiological localization	Biological function	Ligation site
Ameloblastin	• Pulp [144] • **Enamel** [144] • Hertwig's epitelial root sheath [144] • Periodontal ligament [144] • Calvarial development [144]	• Regulation of crystal growth [144] • Cell signaling [145] • Dentin and bone repair induction [145] • Bone healing stimulation *in vivo* [145] • Enhancement of proliferation and differentiation of stem cells, osteoblasts and osteoclast precursor cells (*in vitro*) [144]	• Fibronectin interaction site [144] • Heparin-binding domains [144] • CD63-interaction domains [146] • Calcium binding sites [144]
Fibronectin	• Conective tissues (including **bone**) [147] • Bodly fluids [147]	• Cells adhesion, growth, migration, and differentiation [148,149]	• Integrin (α4β1,α5β1,αVβ3,αIIbβ3,αVβ6,αVβ5) [150] • Extracellular matrix components (collagen, fibrin and heparan sulfate proteoglycans) [150]
Laminin	• Basal lamina (**bone**) [151] • Endothelial [151]	• Cell survival, proliferation, differentiation and specialized functions [152] • Although laminin is not effective at promoting osteoblast differentiation, it had some proliferative and adhesive activity on stem cells [140]	• Integrin (αVβ3,α2β1, α1β1,α3β1) [150]
Vitronectin	• **Bone** [153]	• Adhesion of endothelial cells, fibroblasts and bone-derived cells [149,154]	• integrin (αVβ3,αVβ5) [150] [154]

	• Liver [153] • Brain [153] • Fat [153] • Heart [153] • Skeletal muscle [153] • Lung [153] • Uterus [153] • Testis [153] • Thymus [153]	• Regulation of the fibrinolytic, complement and coagulation systems [155]	
Collagen type I	• Flesh and connective tissues of animals (cornea, cartilage, **bone**, blood vessels, gut, and intervertebral discs) [156]	• Regulation of bone cell phenotypes [156,157]	• Integrin (α2β1) [150]
Collagen type IV	• **Bone**- trace amounts [151]	• Collagen fibril diameter regulation [149]	• Integrin (α2β1) [150] • CD44 [150]
Collagen type X	• **Calcilfied cartilage** [158]	• Support the bone that is forming [159] • Aid in the removal of type II collagen fibrils [159] • Mineralization [159] • Vascular invasion of the cartilage matrix [159]	• Runx 2 [160] • Ca^{2+} [161]

Osteonectin (SPARC)	• **Bone** [162] • Pericellular matrix surrounding osteoblasts and osteocytes [162]	• Osteoblasts differentiation and survival [163] • Adipogenesis inhibition [163] • Regulates collagen fibril diameter [149, 164] • Cell spreading [162,165] • Collagen fibrillogenesis [166] • Ca^{2+} and hydroxyapatite binding [162]	• Hydroxyapatite [162] • Ca^{2+} [162,165] • Collagens [165] • PDGF [165] • TGFβ1 [165] • VEGF [165] • MMP2 [165] • bFGF [165] • IGF [165]
Osteocalcin	• Extracellular matrix of areas of newly formed **bone**, i.e. in the subperiosteal region [162] • Subchondral region [162] • Osteoid tissue (surface of the trabecular bone) [162] • Matrix of the bone marrow cells [162]	• Bone turnover [162] • Regulates osteoclasts [149] • Inhibits mineralization [149] • Marsk osteoblast differentiation [166] • Calcium binding [162]	• Ca^{2+} [162] • Collagen [162] • Hydroxyapatite [162]

	• Kidney [162] • Salivary and renal tube epithelium [162]		
Biglycan	• Bone [162,167] • Articular Cartilage [162] • Endothelial cells of dermal blood vessels [162] • Prickle cell layer [162]	• Cell spreading [162] • Calcium and hydroxyapatite binding [162] • Decrease the availability of active TGF-β [149,166] • Collagen fibrillogenesis promotion [149,166] • Bone formation induction [168] • Cell-cell and/or cell-protein interactions [162]	• Collagen [149] • TGF-β [162] • BMP2 [168] • Ca^{2+} [162] • Hydroxyapatite [162]
Bone sialoprotein (BSP)	• **Bone** [169]	• Mineralization regulation [149, 165, 166] • Osteoblast and osteoclasts differentiation, adhesion and function [170,171] • Angiogenesis promotion [172] • Mediates cell attachement [162]	• Integrins [165] • Collagen [165] • Ca^{2+} [165] • Hydroxyapatite [165] • MMP2 [165] • Complement factor H [165]
Osteopontin (Secreted phosphoprotein 1; OPN)	• **Bone** [162] • Kidney [162] • Endometrial glans of a	• Cell attachment [162] • Hydroxyapatite binding [165] • Mineralization and remodeling inhibition [149]	• Integrins [165] • CD44 [165] • Fibronectin [165]

	nonpregnant secretory-phase uterus [162]	• Osteoblast and osteoclasts differentiation, adhesion and function [170, 173, 174] • Hydroxyapatite nucleation regulation [175] • Inhibits mineralization and remodeling [175] • Promotes bone resorption [175]	• Hydroxyapatite [165] • Ca^{2+} [165] • Collagens [165] • MMP3 [165] • Complement factor H [165] • EGF [165] • PTH [165]
Decorin	• **Bone** [162] • Nonarticular resting cartilage [162] • Dermal collagenous matrix [162]	• Collagen binding [162] • Fibril formation regulation [162] • Decreases the availability of active TGF-β [166] • Collagen fibrillogenesis promotion [166] • Regulate collagen fibril diameter [149]	• TGF-β [149] • Collagen [162]
Thrombospondin (Type I and Type II)	• Endomysium and perimysium [176] • Basement membranes of the muscle capillaries [176] • Muscular and tendinous parts of the myotendinous junction [176] • Bone marrow [176]	• Cell attachment [149,162] • Osteoclast function regulation (type I) [177] • Inflammation regulation (type I) [166] • TGF-β activation (type I) [167] • TGF-β sequestration and collagen fibrilogenesis (type II) [167]	• Collagens [165] • Heparan sulfated proteoglycans (type I) [165] • Fibronogen (type I) [165] • Laminin (type I) [165] • Ca^{2+} (type I) [165] • Fibronectin (type I) [165]

	• Articular cartilage [175]	• MSCs proliferation inhibition (type II) [178] • Osteoblast differentiation promotion (type II) [178] • Adipogenesis inhibition (type II) [178]	• Integrins [165] • HSPG [165] • CS47 [165] • CD36 [165] • LRP [165] • Syndecan (type I) [165] • Thy-1 (type I) [165] • Calreticulin (type I) [165] • TGF-β (type I) [165] • Cathepsin (type I) [165] • Elastase (type I) [165] • PDGF [165] • bFGF (type I) [165] • MMP2 [165] • IGF-1 [165] • IGF-BP (type I) [165] • Chondroitin sulfate (type II) [165] • Proteoglycans (type II) [165]
Tenascin C	• Muscle cell endings of the myotendinous junction [176]	• Osteoblast differentiation [179] • Fibronectin desposition [164]	• Fibronectin [165] • Integrins [165]

	• Tendon cells [176] • Surfaces of the tendinous collagen fibers [176] • **Pericellular space surrounding some osteocytes** [179] • Articular cartilage [179]		• Contactin/F11 [165] • Annexin II [165] • Heparan sulfated proteoglycan [165]
Periostin	• **Bone** periosteum [180] • Periodontal ligament and tendons [180]	• Cortical bone thickness control [180] • Negative regulator of matrix mineralization [180] • Crosslinking of collagen fibrils [180] • ECM organization (especially fibronectin and tenascin C) [166] • SOST regulation [166]	• Collagen type-I [180] • Fibronectin [166] • Tenascin-C [166]
Dentin matrix acidic phosphoprotein 1 (DMP1)	• **Bone** and dentin [180]	• Target molecule for Runx2 [181] • Calcium binding [182,183] • Initiation of nucleation of crystalline hydroxyapatite [182,183] • Intra and extracellular signaling molecule [184] • Robust osteocyte marker [166] • Regulates phosphate metabolism [166]	• Ca^{2+} [182,183] • DSPP promoter [185;186]

		• Involved in osteocyte function [166]	
Collagen type III	• **Bone-trace amounts** [185] • Blood vessels [187] • Skin [187] • Lung [187]	• Promotion of bone formation [166] • Regulate collagen fibril diameter [149]	• integrins α1β1 and α2β1 [188] • vWF [189]
Versican	• **Woven bone matrix** [190]	• Defines the space destined to become bone [149]	• Glycosaminoglycan hyaluronan [190]
TGFβ receptor II interacting protein 1 (TRIP 1)	• **Bone** [191]	• Signal transduction, vesicular trafficking and cell cycle regulation [191] • Influences TGF-β [191] • Signaling by acting as a negative regulator and inhibiting positive regulation of TGF-β target genes [192] • Osteoblast proliferation and differentiation [192]	• Cytoplasmic domain of TGFβR2 [192]

6. Bone mechanobiology:

6.1. Frost's "mechanostat" theory: the role of compressive and tensile forces

Mechanical and physical signals that occur through walking, running and other types of movements have a crucial role in the induction of osteogenesis, as well as in the maintenance of healthy bone [193]. The "Mechanostat Theory", suggested by Harold Frost in the 1890's [194], correlates bone growth and loss with local elastic deformation (in the form of compression and elongation), which occurs in a life-long regime, due to peak forces exerted by surrounding muscles [195]. The control loop of bone elastic deformation is categorized in four types - disuse, adapted state, overload and fracture -, correlated with distinct deformation values, in which a 1000 μstrains equal 0.1% of the bone length [196]. The ideal frequency, intensity, and timing of loading to promote healthy bone mass growth are well reported for the *in vivo* scenario [197-199]. A current challenge for the recapitulation of the native bone niche is the optimization of such mechanical stimulation for *in vitro* settings.

6.1.1. The correlation of the "Mechanostat Theory" with bone biochemical signaling

Interesting observations have been reported during the last years, which correlate the "Mechanostat Theory" with biochemical signalling occurring during bone homeostasis**.** Tyrovola & Odont [200] reviewed several studies, in which compressive/tensile deformations were applied to bone and periodontal ligament tissues, and established a correlation between the observed behavior and the OPG/RANKL/RANK system. An example that shows the correlation of the "Mechanostat Theory" and the OPG/RANKL/RANK bone remodeling system is the one occurring in the tooth/periodontal ligament interface. The compression of tooth, during orthodontic movement, led to the increase of RANKL concentration [201,199], promoting osteoclast formation. The tensile stretching applied to the periodontal ligament promoted the increase of osteoblasts OPG concentration in a magnitude-dependent manner [203], while inducing a simultaneous RANKL concentration decrease. The relative concentrations of OPG and RANKL on both tensioned and compressed sides of tooth regulate local bone modeling, remodeling and root resorption.

6.2. Other forces affecting bone behavior: focus on flow-induced shear stress

Other physical and mechanical factors that influence bone health are the drag force and shear stress. Drag force is the sum of all the forces that oppose the flow of the blood [204]. Shear stress occurs in the bone, on the unmineralized matrix around the osteocytes, which forms canals by which the interstitial fluid passes, creating a force along the surface, on a parallel fashion [205]. A consequence of bone deformation is the generation of interstitial flow on osteocytes, creating a drag phenomenon on the fibers that connect the cells [206-210]. Weinbaum *et al*. [211] suggested a mathematical model to explain how bone cells detect mechanical loading, and how flow behaves through the pericellular matrix surrounding an osteocyte process in its canaliculus. Despite the small deformations predicted by the model, and the small dimensions of the pericellular annulus (typically $0.1\,\mu$m), the fluid flow shear stress on the membranes of the osteocyte processes was roughly the same as for the vascular endothelium in capillaries. Still little is known about the role of perfusion shear stress and interstitial flow in bone biology [212,213]. However, it is known that osteocytes are the main mechanosensing cells in bone and that, upon exposure to fluid flow, they stimulate osteoblasts, thus producing more bone tissue and prostaglandins, which are responsible for the activity of osteoblasts and osteoclasts [100]. Early studies focused on unravelling the effect of hydrostatic pressure and substrate stretching on osteocytes behaviour [214]. However, flow-induced shear stress has shown to affect osteocytes in a more relevant manner, as compared to osteoblasts [215]. A long list of biological phenomena, that has been increasing in the last years, has shown that osteocytes respond to shear stress by releasing nitric oxide (NO), adenosine triphosphate (ATP) and prostaglandinds. Moreover, gap junctions and hemichannels are open in such scenario, and several signalling pathways (e.g. Wnt/β-catenin, protein kinase A (PKA)) are initiated after shear stress induction. The mechanisms for load sensing in osteocytes are thought to depend on the dendritic process, or bending of cilia [100]. Glycocalyces on the surfaces of dendritic processes have been shown to be related with osteocytes mechanosensing; however, on the cell body, different mechanosensing mechanism are known to be active [100]. The TGF-β family - which includes BMPs, activins, and growth differentiation factors (GDFs) - has been suggested as one of the most important mediators of cellular response to physical cues via a feedback loop mechanism, reviewed by Wu *et al*. [216].

7. Tissue engineering techniques in bone strategies for bone regeneration

7.1. Analysis of the clinical needs in the regenerative medicine of bone

The complexity inherent to bone's physiology dictates the difficult regeneration of bone tissue after a critical size fracture. While bone tissue trauma normally heals by itself, the so-called "critical" defects, with average diameter of 2 cm or higher, do not show this ability [217]. Critical size defects often derive from tumor ablation, serious injury and orthopedic diseases. [218,219]. Considering physically-caused injuries, the bone healing repair failure percentage can go from 10 to 50% (data including a range of fractures from standard injury to open tibial defects) [220]. As described previously on **Section 1**, the biology of bone and fractures sites is highly complex and dynamic. Although many studies shed light into the biology of both bone healthy regulation and healing, the complete understanding of the myriad of players (including immune system, external physical factors, vasculature and osteogenic lineage cells) is yet to be fully understood. However, the failure of bone healing will ultimately culminate in the suppression of the blood supply to the tissue, which will result in the non-union of the bone (due to schemia, osteonecrosis and bone loss) [221].

Efforts to repair bone defects, excluding the ones that target bone regeneration, can be divided in two main segments: (i) implantation of bone grafts (of autologous or allogenic origins) or (ii) development of synthetic bone substitution grafts [222]. However, these two therapeutic approaches show limitations. Autologous bone grafts, although commonly applied in clinics and known to foster bone repair, can inflict morbidity of the donor's extraction site [223]. Allogenic bone grafts, coming from a different donor, can be rejected due to immune response, Moreover, the implantation of allografts requires a complex implantation technique that involves the achievement of constant vascular supply to the site, as well as a maintenance of an adequate mechanical environment to promote vessels formation [224]. Permanent substitution grafts can have some unwanted side effects, which may affect bone healing negatively. These include bone resorption, poor integration and an adverse reaction (eg: allergenic) to the material [222]. A list of current strategies based on synthetic grafts for bone healing is reviewed in references [225,226].

The listed problems associated with the current bone repair approaches show that there is a dire need for new and more efficient strategies. Unlike the previously mentioned

techniques targeting bone repair, tissue engineering seeks a complete regeneration of the damaged tissue. To achieve that, four main pillars may be used separately or combined to design strategies that promote bone regeneration: (i) biomaterials, (ii) biomolecules, (iii) cells and (iv) externally-applied stimuli.

In the following sub-sections, brief explanations of the concepts behind the use of each tissue engineering player will be provided. Representative studies in each field, as well as combined studies will be presented. Although bone regeneration studies that use unifactorial approaches are highly relevant to elucidate the role of single variables on bone cells, they do not consider the high complexity of the bone's microenvironment. Here, we review some studies that use multifactorial and, in some cases, biomimetic strategies to promote bone regeneration within the tissue engineering scope.

7.1.1. Biomaterials for bone regeneration

The re-creation of the bone original tissue requires a structure that mimics the tissue native microenvironment, so cells can attach and proliferate [227]. Biomaterials are used in tissue engineering strategies as analogous of the bone ECM, which structure is reviewed in **Section 6**. Materials suggested so far for the construction of biodegradable biomaterials for tissue regeneration are mainly composed of ceramics, glasses, polymers or composites thereof [228]. Polymeric biomaterials will be described in more detail. Detailed reviews on bioceramics and bioglasses can be found in [229,230]. Polymeric biomaterials may be of two different origins: synthetic or natural [231]. Examples of commonly applied synthetic polymers used in biomaterials composition include poly(ethylene glycol) (PEG) [232], poly(lactic acid) (PLA) [233], poly (L-lactide-*co*-glycolide) (PLGA) [234] and polyglycolic acid (PGA) [235]. Despite their lack of cell-interacting domains, synthetic materials are amenable to be chemically tailored using with precision. Natural origin materials used for tissue engineering include polyssacharides, proteins and polyhydroxyalkanoates [236]. Examples of such widely used proteins for tissue engineering include. collagen [237], its denaturated analogue gelatin [238] and silk [239]. Glycosaminoglycans **(**GAGs) are present as structure of bone ECM, forming proteoglycans. Examples of those molecules include hyaluronic acid, which is naturally present in bone [240] and chondroitin sulfate [241]. Marine-origin molecules with high similarity to GAGs, as chitosan [242], and highly tailorable algae-derived products as agarose and alginate have also seen application in the bone tissue regeneration field [243].

A wide range of natural origin polymers is used either because they are prepared from ECM proteins (see Table 1 for a list of relevant bone ECM proteins), e.g. collagen I/CHondro-Gide® (Geitlisch Pharma) and hyaluronan [2], or due to their structural similarity with ECM components [2]. Also, the implantation of acellular scaffolds, derived from decellularized allogenic or xenogenic tissues, has also been suggested for bone tissue regeneration [2].

To sustain cells for bone tissue regeneration, biomaterials have been processed in a high number of manners, which include the most common porous scaffolds, hydrogels and microparticles [5]. For the design of biomaterials for specific applications, a balance between their chemical/biochemical cues and physical properties (e.g. Stiffness, porosity, energy dissipation ability) needs to be kept. Together, all different cues exposed to cells and to the surrounding tissue contribute for the right conditions to be meet for tissue integration and induction of osteogenesis/bone regeneration [244-246].

The role of biomaterials in tissue engineering has evolved from classical cell-supporting structures to highly functional devices, designed specifically to induce a desired response, along with features for easy implantation, integration in the tissue, among others. In a recent example, Zhang *et al*. (1946) [247] created hydroxyapatite (HA) and amphiphilic poly(lactide-*co*-glycolide)-*b*-poly(ethylene glycol)-*b*-poly(lactide-*co*-glycolide) (PELGA) composites membranes with tunable decomposition rates. Such structures were stiffened when hydrated (due to enhanced PEG crystallization) and then recover their shape at body temperature, which enabled an efficient skeletal progenitor cells delivery to bone grafts. This HA-PELGA composite promoted the proliferation, attachment and osteogenesis of periosteum-derived cells *in vitro*. When implanted on a rat model, it facilitated the transference of confluent cell sheets of protein-labeled bone marrow mesenchymal stem cells (BMMSCs). Due to their shape memory behavior influenced by physiological temperatures, these membranes could be automatically folded in a tubular configuration, being distorted into a flat temporary shape that allowed for a better cell seeding/cell sheet transfer. Therefore, these membranes are promising smart materials for the usage of synthetic periosteal membranes in allograft healing.

Unlike soft tissue engineering, in which hydrogels with mechanical properties comparable to the ones of the native tissues have been developed, the fabrication of tough hydrogels with adequate mechanical properties to sustain loads present in bone is a recent trend.

Nonoyama *et al*. [248] used a double network tough hydrogel with in-gel precipitated hydroxyapatite for rat bone defects. The toughness of the hydrogel was conferred by the combination of a brittle (poly(2-acrylamido-2-methyl propanesulfonic acid)) and a ductile (poly(N,N -dimethylacrylamide)) network. Such biomaterial showed a robust bonding to the defected bones and its mechanically properties increased significantly as compared to an implanted non-mineralized hydrogel.

Biomaterials are often chemically modified [5] or impregnated/loaded with bone differentiation and formation-related molecules [5] to induce a specific bone regeneration response. A recent example by Lee *et al.* (1946) [249] focuses on the use of three-dimensional (3D) printed polycaprolactone (PCL) engrafted with a recombinant human bone morphogenic protein-2 (rhBMP2) through polydopamine (DOPA). The release of the rhBMP-2 was sustained up to 28 days and *in vitro* studies using a pre-osteoblast cell line showed the ability of such scaffold to induce cell proliferation and differentiation

Besides polymeric materials and their respective composites, graphene-based biomaterials, namely membranes and porous structures [250], have shown promising results in the treatment of bone defects. Although in this section the focus is mainly the use of polymeric materials for bone regeneration, the importance of such novel materials must also be acknowledged.

7.1.2. Cells in tissue engineering strategies for bone regeneration

In bone regeneration, cells are often included as part of a therapy, as they naturally synthesize ECM proteins responsible for the tissue reshaping.

In the tissue engineering field, osteoprogenitor cells that can differentiate into osteoblasts are mostly used [2]. Due to their multipotency, MSCs have been widely used in tissue engineering. They are usually extracted from bone marrow (BMMSCs) [251], and can be isolated, stimulated to expand to various tissues and expanded in culture [252]. They also can be retrieved with high yields after isolation from adipose tissues collected during liposuctions [253].

The regulation of bone function is dependent on the correct regulation of the crosstalk between a wide plethora of cells, as shown in **Section 5**. A study performed using MSCs, by Birmimgham *et al* (1942) [254] proved the role of the biochemical signaling between bone cells (osteocytes and osteoblasts) and MSCs, to lead osteogenic differentiation. To

determine the osteogenic differentiation, the alkaline phosphatase (ALP) activity was monitorized, as well as the calcium deposition, as well as the number of cells. The results showed that ALP peaked earlier, and a great calcium deposition was observed when the MSCs were co-cultured with osteocytes, rather than with osteoblasts. Ultimately, this finds suggest a need for a relationship with osteocytes and osteoblasts for the MSCs signaling differentiation pathway. The use of co-cultures for bone tissue regeneration induction, seems to be a good methodology to use in the clinical field.

Jeon *et al*. (1946) [255], used human induced pluripotent stem cells (hiPSC), a pluripotent stem cell type generated directly from human adult cells, that can create specific mesenchymal and macrophage precursors [256] to induce osteoblast and osteoclast differentiation. Both cell types, involved in bone resorption and formation (see **Section 5**), combined with HA-coated poly(lactic-*co*-glycolic acid)/poly(L-lactic acid) (HA–PLGA/PLLA) scaffolds, were tested in different concentrations. The 5% w/v HA-coated polymer allowed recapitulating major aspects of the tissue remodeling process of human bone *in vitro*. Afterward, the co-cultured hiPSC-MSC/-macrophage system was implanted (after culture on the scaffolds) in rodents, forming bone-like mature tissue. This study showed the importance of the osteoprogenitor cells-induced matrix deposition and tissue resorption conjugated with immunomodulation, to allow a better-quality tissue formation.

7.1.3. Physical stimuli for bone regeneration

As revised in **Sections 1** and **2**, healthy bone is exposed to stresses in a daily basis. Given that this compromises the bone environment, to promote a proliferation and differentiation of the niche cells, this mechanical loading needs to be replicated in tissue engineering [257]. Bioreactors allow mimicking such *in vivo*-occurring stimuli. Different types of bioreactors allow stimulating cells in distinct manners by inducing shear stress and flow perfusion, hydrostatic pressure and compression [258].

Spinner flasks are a basic bioreactor type, that allow an efficient mixture of oxygen and nutrients in the medium. In a specific bioreactor design adapted to the use of biomaterials, the scaffolds/samples were suspended using needles in a contained flask with the medium. Through the experiment, the scaffolds/samples were kept in place, while the medium was agitated with the use of a magnetic stirrer. The results obtained using this bioreactor showed that the system is promising for cell differentiation and proliferation, when

compared with static conditions [259]. Figure 8 shows a schematic representation of this bioreactor. However, spinner flasks have showed some limitations on mass transference, as the flow is too low to induce a homogeneous distribution of the cells by the scaffolds, residing manly on the periphery of the construct [260].

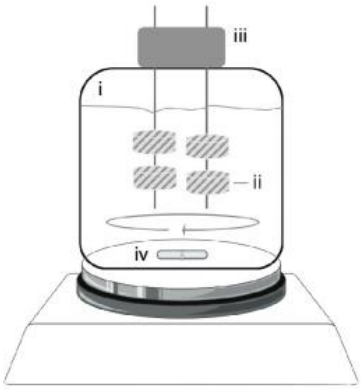

Figure 8- Spinner flask scheme. I) vessel, II) cells/scaffold; III) needles used to maintain the scaffolds in position, IV) magnetic stir bar (taken from Sladkova, M., & de Peppo, G. M. (2014) [260]

Another type of bioreactor – the rotating wall bioreactor - was created with the intention of keeping the cell culture protected from high forces during an experiment. Unlike spinner flasks, the scaffolds are completely free to move within the vessel (with medium) [261]. It is composed of chamber, shaped like a cylinder, where the walls (inner and outer, or both) can rotate in a constant angular speed [261] (see figure 9 for a schematic of this bioreactor). The velocity of the rotation speed allows for a balance between the gravitational and hydrodynamic drag forces, which allows for the scaffolds to be suspense on the medium [262]. As the tissue starts to growth, it is needed to increase the rotation, so that the previous balance can be maintained [263]. Like spinner flasks, rotating wall bioreactors allow for a better medium transportation than static 3D cell culture, as well as for a better cell distribution [259,264].

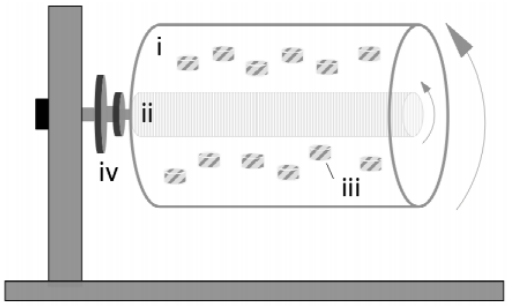

Figure 9- Rotating wall bioreactor scheme. I) rotating wall vessel, II) cylinders, III) Cells/Scaffolds, IV) rotator base (taken from Sladkova & de Peppo (2014) [260]

Spinner flasks and rotating walls have shown several limitations regarding medium perfusion into biomaterials. Flow perfusion bioreactors are constructed to surpass such problem. Using a perfusion pump, they allow a perfusion to occur in the system, and thus, for the medium to correctly flow through the scaffold [264]. The most basic perfusion bioreactor system consists of a perfusion pump, tubing to make the circuit, a chamber for the scaffold, and a media reservoir [265] (see figure 10 for a schematic of this bioreactor). The perfusion is also guaranteed by the chamber in which the scaffold is contained, since it is made in a way that the medium should flow right through the construct [261].

Perfusion bioreactors allow uniform medium mixture, so they are preferred in the tissue engineering field as they provide an optimized control of the dynamic cell culture process (environmental and cells stimulation) [264]. This is achieved by using a pump that circulates the media in the system, mimicking, as close as possible, the natural environment of the cells in the human body [265]. One of the conditions that flow perfusion bioreactors allow achieving is shear stress stimulation, which happens very often in the human body. Shear stress occurs in the bone, associated with the blood circulation, in a parallel fashion to the surface of the bone [266].

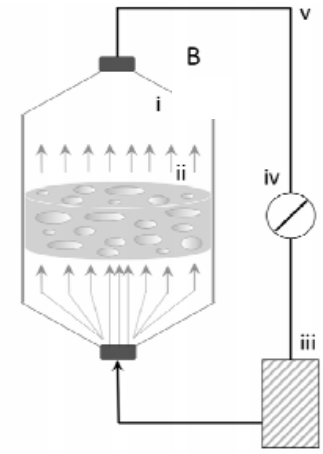

Figure 10-Perfusion bioreactor scheme. I) culture chamber, II) cells/scaffold, III) culture medium reservoir, IV) peristaltic pump, V) tubbing system (taken from Sladkova & de Peppo (2014) [260].

Bone´s microenvironment is conditioned by physical aspects, such as: bending, tension, torsion, bending, shear and compression. Compression bioreactors are usually allied with perfusion, which leads to an augmentation of the expression of osteogenic markers (eg: ALP) [267]. This bioreactor type consists of a motor, a controller, for the different magnitudes and frequencies to use, and a linear motion type system [268] (see figure 11 for a schematic of this bioreactor.) The scaffold with the cells is put on a plate, and the piston that is going to apply the force is compressed against the material [268]. This load transference should be made using flat plates, for an even load distribution. If that is not possible (as the case for multiple scaffolds), then the scaffolds should have similar heights [269].

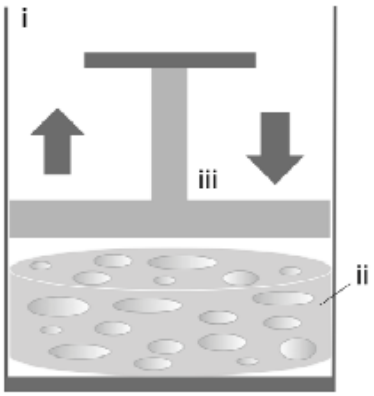

Figure 11- Compression bioreactor work schematics. I) compression chamber, II) cell/scaffold, III) piston (taken from Sladkova & de Peppo (2014) [260].

7.1.4. Biomolecules for bone regeneration

Biomolecules are essential in the bone regeneration process. As discussed in **section 7,** they are responsible for the recruitment, proliferation, differentiation and migration of the osteoprogenitor cells [2]. They are present constantly through all the bone phases, from formation to healing [2]. As it was mentioned before on **section 4**, upon bone injury, immune cells are recruited to the defect site coordinate actions triggered by the expression of cytokines and growth factors, that culminate in the recruitment of MSCs, remodeling and vascularization of the tissue [2]. BMPs are the most widely studied growth factors for bone tissue engineering. BMP-2 and BMP-7 are the most used ones, and have seen application in clinical medicine. However, they have showed limited success, owing to the reported formation of ectopic bone, as well as their high cost [269]. The release of bioactive molecules in a controlled and site-specific manner are crucial for the success of tissue engineering strategies. Herein, we will not focus on such strategies, that are described in reviews as [270], [271] and [272].

Besides soluble molecules produced during bone healing, insoluble molecules comprised in the bone ECM, namely proteins, are of utmost importance for the achievement of effective regeneration. Also, molecules mediating cell-cell contact have shown to have adjuvant and inhibiting effects on bone cell differentiation [2]. A study by Cosgrove *et al* (1946) [9] describes the use of a biomaterial-based approach to elucidate the role of cell-ECM and cell-cell contact of mesenchymal stem cells in osteogenesis driven by mechanical transduction phenomenon. The authors modified a hyaluronic acid hydrogel

with an HAVDI adhesive motif from N-cadherin (to emulate the cell-cell ligation) and a RGD adhesive motif from fibronectin (to emulate the cell-ECM ligation), for the co-presentation of these motifs. HAVDI ligation decreased the contractible state of the cells (and the nuclear YAP/TAZ location), which led cells to wrongly interpret the ECM stiffness, causing a change in the downstream cell osteogenic differentiation and proliferation.

In the study made by Dolatshahi-Pirouz *et al* (1944) [141] the authors tested several stem cell-biomaterial interactions in a high-throughput approach. Biomaterials comprised gelatin and an array of ECM proteins, dispensed in a combinatorial manner. With such a 3D hMSCs-laden gel microarray, several ECM protein combinations were assessed for their role in the induction of osteogenic differentiation. Formulations containing combined ECM proteins in their composition led to more pronounced osteodifferentition, mainly in the presence of the soluble factor BMP-2 in the medium. The use of high-throughput screening strategies allowed the multiplexed screening of biomaterials conditions, in a rapid and cost-effective manner.

7.2. Current multifactorial approaches targeting bone regeneration

Although several tissue engineering therapies for bone regeneration focus on unifactorial approaches, as reported in the previous section, novel approaches with a multifactorial approach have been developed in the last years. The study of isolated variables is of extreme importance to unravel biological effects, and has allowed the incorporation of each factor in multifactorial complex studies. However, there are few studies that consider a wide range of factors that contribute to the bone microenvironment (e.g. shear stress/flow perfusion, strain/compression, cell-cell interactions, characteristic extracellular matrix: mineralized and non-mineralized, ECM-cells interactions, soluble and insoluble factor interactions, cell-cell contact). Novel multidimensional approaches that enable a high-throughput screening analysis of a great plethora of these factors, as it can be seen in the following scheme, are in need. This may be obtained by the design and implementation of devices that (i) integrate highly functional biomaterials that replicate the native bone composition, (ii) allow culturing cells that can differentiate into multiple lineages of the bone, and (iii) permit the exposure of cell-biomaterials constructs to physiologically relevant mechanical forces.

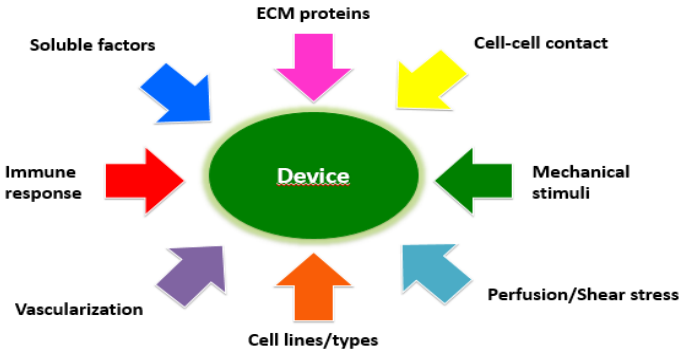

Figure 12- Summary scheme containing diverse factors that a device to use in bone tissue engineering should comprehend.

8. Conclusion

Bone tissue engineering has a high degree of complexity, due to the microenvironment of the native tissue. The bone modeling and remodeling that happens throughout an individual's life cycle helps preserving this structure, which is important for motion as well for the protection of other organs and tissues. Current tissue engineering techniques have shown to be very promising. However, they remain mostly unifactorial, not considering all the diverse interactions and stimuli occurring during bone formation and resorption. Therefore, novel techniques need to be discovered and implemented in the regenerative medicine field for the clinical treatment of bone fractures, either caused due to a disease or physical caused fracture.

References

[1] Clarke, B. (2008). Normal bone anatomy and physiology. *Clinical journal of the American Society of Nephrology*, *3*(Supplement 3), S131-S139.

[2] Quarto, R., & Giannoni, P. (2016). Bone Tissue Engineering: Past–Present–Future. *Mesenchymal Stem Cells: Methods and Protocols*, 21-33.

[3] US Department of Health and Human Services. (2004). Bone health and osteoporosis: a report of the Surgeon General. *Rockville, MD: US Department of Health and Human Services, Office of the Surgeon General*, *87*.

[4] Yin, T., & Li, L. (2006). The stem cell niches in bone. *The Journal of clinical investigation*, *116*(5), 1195-1201.

[5] Yu, X., Tang, X., Gohil, S. V., & Laurencin, C. T. (2015). Biomaterials for bone regenerative engineering. *Advanced healthcare materials*, *4*(9), 1268-1285.

[6] Marolt, D., Campos, I. M., Bhumiratana, S., Koren, A., Petridis, P., Zhang, G., & Vunjak-Novakovic, G. (2012). Engineering bone tissue from human embryonic stem cells. *Proceedings of the National Academy of Sciences*, *109*(22), 8705-8709.

[7] de Peppo, G. M., Marcos-Campos, I., Kahler, D. J., Alsalman, D., Shang, L., Vunjak-Novakovic, G., & Marolt, D. (2013). Engineering bone tissue substitutes from human induced pluripotent stem cells. *Proceedings of the National Academy of Sciences*, *110*(21), 8680-8685.

[8] Hou, L., Coller, J., Natu, V., Hastie, T. J., & Huang, N. F. (2016). Combinatorial extracellular matrix microenvironments promote survival and phenotype of human induced pluripotent stem cell-derived endothelial cells in hypoxia. *Acta Biomaterialia*, *44*, 188-199.

[9] Cosgrove, B. D., Mui, K. L., Driscoll, T. P., Caliari, S. R., Mehta, K. D., Assoian, R. K., & Mauck, R. L. (2016). N-cadherin adhesive interactions modulate matrix mechanosensing and fate commitment of mesenchymal stem cells. *Nature Materials*. 15(12):1297-1306

[10] Santos, L. J., Reis, R. L., & Gomes, M. E. (2015). Harnessing magnetic-mechano actuation in regenerative medicine and tissue engineering. *Trends in Biotechnology*, *33*(8), 471-479.

[11] Standring, S. (Ed.). (2015). *Gray's anatomy: the anatomical basis of clinical practice*. Elsevier Health Sciences.

[12] Taichman, R. S. (2005). Blood and bone: two tissues whose fates are intertwined to create the hematopoietic stem-cell niche. *Blood*, *105*(7), 2631-2639.

[13] Levrero-Florencio, F., Margetts, L., Sales, E., Xie, S., Manda, K., & Pankaj, P. (2016). Evaluating the macroscopic yield behaviour of trabecular bone using a nonlinear homogenisation approach. *journal of the mechanical behavior of biomedical materials*, *61*, 384-396.

[14] Scadden, D. T. (2006). The stem-cell niche as an entity of action. *Nature*, *441*(7097), 1075-1079.

[15] Shapiro, F. (2008). Bone development and its relation to fracture repair. The role of mesenchymal osteoblasts and surface osteoblasts. *Eur Cell Mater*, *15*(53), e76.

[16] Kini, U., & Nandeesh, B. N. (2012). Physiology of bone formation, remodeling, and metabolism. In *Radionuclide and hybrid bone imaging*. Springer Berlin Heidelberg.

[17] Steele, D. G., & Bramblett, C. A. (1988). *The anatomy and biology of the human skeleton*. Texas A&M University Press.

[18] Dallas, S. L., & Bonewald, L. F. (2010). Dynamics of the transition from osteoblast to osteocyte. *Annals of the New York Academy of Sciences*, *1192*(1), 437-443.

[19] Karsenty, G. (2003). The complexities of skeletal biology. *Nature*, *423*(6937), 316-318.
[20] Wu, M., Chen, G., & Li, Y. P. (2016). TGF-β and BMP signaling in osteoblast, skeletal development, and bone formation, homeostasis and disease. *Bone research*, *4*, 16009.
[21] Long, F. (2012). Building strong bones: molecular regulation of the osteoblast lineage. *Nature reviews Molecular cell biology*, *13*(1), 27-38.
[22] Gilbert, S. F. (2003). Paraxial and intermediate mesoderm. *Developmental Biology. Sunderland, Massachusetts.: Sinauer Associates, Inc., Publishers*.
[23] Kronenberg, H. M. (2003). Developmental regulation of the growth plate. *Nature*, *423*(6937), 332-336)
[24] Roberts, W. E., & Hartsfield, J. K. (2004). Bone development and function: genetic and environmental mechanisms. In Seminars in Orthodontics. (Vol. 10, No. 2, pp. 100-122). WB Saunders
[25] Provot, S., & Schipani, E. (2005). Molecular mechanisms of endochondral bone development. *Biochemical and biophysical research communications*, *328*(3), 658-665.
[26] Nishimura, R., Wakabayashi, M., Hata, K., Matsubara, T., Honma, S., Wakisaka, S., & Akiyama, H. (2012). Osterix regulates calcification and degradation of chondrogenic matrices through matrix metalloproteinase 13 (MMP13) expression in association with transcription factor Runx2 during endochondral ossification. *Journal of Biological Chemistry*, *287*(40), 33179-33190
[27] Akiyama, H., Chaboissier, M. C., Martin, J. F., Schedl, A., & de Crombrugghe, B. (2002). The transcription factor Sox9 has essential roles in successive steps of the chondrocyte differentiation pathway and is required for expression of Sox5 and Sox6. *Genes & development*, *16*(21), 2813-2828.
[28] Smits, P., Li, P., Mandel, J., Zhang, Z., Deng, J. M., Behringer, R. R., & Lefebvre, V. (2001). The transcription factors L-Sox5 and Sox6 are essential for cartilage formation. *Developmental cell*, *1*(2), 277-290.
[29] Ornitz, D. M., & Marie, P. J. (2002). FGF signaling pathways in endochondral and intramembranous bone development and human genetic disease. *Genes & development*, *16*(12), 1446-1465.
[30] Minina, E., Kreschel, C., Naski, M. C., Ornitz, D. M., & Vortkamp, A. (2002). Interaction of FGF, Ihh/Pthlh, and BMP signaling integrates chondrocyte proliferation and hypertrophic differentiation. *Developmental cell*, *3*(3), 439-449.
[31] Minina, E., Wenzel, H. M., Kreschel, C., Karp, S., Gaffield, W., McMahon, A. P., & Vortkamp, A. (2001). BMP and Ihh/PTHrP signaling interact to coordinate chondrocyte proliferation and differentiation. *Development*, *128*(22), 4523-4534.
[32] Schipani, E., & Provot, S. (2003). PTHrP, PTH, and the PTH/PTHrP receptor in endochondral bone development. *Birth Defects Research Part C: Embryo Today: Reviews*, *69*(4), 352-362.
[33] Vortkamp, A., Lee, K., Lanske, B., & Segre, G. V. (1996). Regulation of rate of cartilage differentiation by Indian hedgehog and PTH-related protein. *Science*, *273*(5275), 613.
[34] Kim, I. S., Otto, F., Zabel, B., & Mundlos, S. (1999). Regulation of chondrocyte differentiation by Cbfa1. *Mechanisms of development*, *80*(2), 159-170.
[35] Yoshida, C. A., Furuichi, T., Fujita, T., Fukuyama, R., Kanatani, N., Kobayashi, S., & Komori, T. (2002). Core-binding factor β interacts with Runx2 and is required for skeletal development. *Nature genetics*, *32*(4), 633-638.
[36] Semenza, G. L. (2001). HIF-1 and mechanisms of hypoxia sensing. *Current opinion in cell biology*, *13*(2), 167-171.

[37] Pfander, D., Kobayashi, T., Knight, M. C., Zelzer, E., Chan, D. A., Olsen, B. R., & Schipani, E. (2004). Deletion of Vhlh in chondrocytes reduces cell proliferation and increases matrix deposition during growth plate development. *Development*, *131*(10), 2497-2508.
[38] Huang Z, Nelson ER, Smith RL, Goodman SB (2007) The sequential expression profiles of growth factors from osteoprogenitors [correction of osteroprogenitors] to osteoblasts in vitro. Tissue Eng 13:2311-2320.
[39] Schofield, R. (1978). The relationship between the spleen colony-forming cell and the haemopoietic stem cell. *Blood cells*, *4*(1-2), 7-25.
[40] Birmingham, E., Niebur, G. L., & McHugh, P. E. (2012). Osteogenic differentiation of mesenchymal stem cells is regulated by osteocyte and osteoblast cells in a simplified bone niche.
[41]. Raggatt, L. J., & Partridge, N. C. (2010). Cellular and molecular mechanisms of bone remodeling. *Journal of Biological Chemistry*, *285*(33), 25103-25108.
[42] Jilka, R. L. (2003). Biology of the basic multicellular unit and the pathophysiology of osteoporosis. *Pediatric Blood & Cancer*, *41*(3), 182-185.
[43] Einhorn, T. A., & Gerstenfeld, L. C. (2015). Fracture healing: mechanisms and interventions. *Nature Reviews Rheumatology*, *11*(1), 45-54.
[44] Knight, M. N., & Hankenson, K. D. (2013). Mesenchymal stem cells in bone regeneration. *Advances in wound care*, *2*(6), 306-316.
[45] Mountziaris, P. M., & Mikos, A. G. (2008). Modulation of the inflammatory response for enhanced bone tissue regeneration. *Tissue Engineering Part B: Reviews*, *14*(2), 179-186.
[46] Barnes, G. L., Kostenuik, P. J., Gerstenfeld, L. C., & Einhorn, T. A. (1999). Growth factor regulation of fracture repair. *Journal of Bone and Mineral Research*, *14*(11), 1805-1815.
[47] Lieberman, J. R., Daluiski, A., & Einhorn, T. A. (2002). The role of growth factors in the repair of bone. *J Bone Joint Surg Am*, *84*(6), 1032-1044.
[48] Dimitriou, R., Tsiridis, E., & Giannoudis, P. V. (2005). Current concepts of molecular aspects of bone healing. *Injury*, *36*(12), 1392-1404.
[49] Cho, T. J., Gerstenfeld, L. C., & Einhorn, T. A. (2002). Differential temporal expression of members of the transforming growth factor β superfamily during murine fracture healing. *Journal of Bone and Mineral Research*, *17*(3), 513-520.
[50] Gerstenfeld, L. C., Cullinane, D. M., Barnes, G. L., Graves, D. T., & Einhorn, T. A. (2003). Fracture healing as a post-natal developmental process: Molecular, spatial, and temporal aspects of its regulation. *Journal of cellular biochemistry*, *88*(5), 873-884.
[51] Mountziaris, P. M., & Mikos, A. G. (2008). Modulation of the inflammatory response for enhanced bone tissue regeneration. *Tissue Engineering Part B: Reviews*, *14*(2), 179-186.
[52] Cameron, J. A., Milner, D. J., Lee, J. S., Cheng, J., Fang, N. X., & Jasiuk, I. M. (2012). Employing the biology of successful fracture repair to heal critical size bone defects. In *New perspectives in regeneration* (pp. 113-132). Springer Berlin Heidelberg.
[53] Alexander, K. A., Chang, M. K., Maylin, E. R., Kohler, T., Müller, R., Wu, A. C., & Pettit, A. R. (2011). Osteal macrophages promote in vivo intramembranous bone healing in a mouse tibial injury model. *Journal of bone and mineral research*, *26*(7), 1517-1532.
[54] van Amerongen, M. J., Harmsen, M. C., van Rooijen, N., Petersen, A. H., & van Luyn, M. J. (2007). Macrophage depletion impairs wound healing and increases left ventricular remodeling after myocardial injury in mice. *The American journal of pathology*, *170*(3), 818-829.

[55] Park, J. E., & Barbul, A. (2004). Understanding the role of immune regulation in wound healing. *The American Journal of Surgery*, *187*(5), S11-S16.
[56] Raggatt, L. J., Wullschleger, M. E., Alexander, K. A., Wu, A. C., Millard, S. M., Kaur, S., & Pettit, A. R. (2014). Fracture healing via periosteal callus formation requires macrophages for both initiation and progression of early endochondral ossification. *The American journal of pathology*, *184*(12), 3192-3204.
[57] Parihar, A., Eubank, T. D., & Doseff, A. I. (2010). Monocytes and macrophages regulate immunity through dynamic networks of survival and cell death. *Journal of innate immunity*, *2*(3), 204-215.
[58] Brown, B. N., Londono, R., Tottey, S., Zhang, L., Kukla, K. A., Wolf, M. T., & Badylak, S. F. (2012). Macrophage phenotype as a predictor of constructive remodeling following the implantation of biologically derived surgical mesh materials. *Acta biomaterialia*, *8*(3), 978-987.
[59] Claes, L., Recknagel, S., & Ignatius, A. (2012). Fracture healing under healthy and inflammatory conditions. *Nature Reviews Rheumatology*, *8*(3), 133-143.
[60] Parihar, A., Eubank, T. D., & Doseff, A. I. (2010). Monocytes and macrophages regulate immunity through dynamic networks of survival and cell death. *Journal of innate immunity*, *2*(3), 204-215.
[61] Lienau, J., Schmidt-Bleek, K., Peters, A., Haschke, F., Duda, G. N., Perka, C., & Schell, H. (2009). Differential regulation of blood vessel formation between standard and delayed bone healing. *Journal of Orthopaedic Research*, *27*(9), 1133-1140.
[62] Schlundt, C., El Khassawna, T., Serra, A., Dienelt, A., Wendler, S., Schell, H., & Duda, G. N. (2015). Macrophages in bone fracture healing: their essential role in endochondral ossification. *Bone*. S8756-3282(15)00392-0
[63] Canalis, E. (1985). Effect of growth factors on bone cell replication and differentiation. *Clinical orthopaedics and related research*, *193*, 246-263.
[64] Frost, H. M. (1989). The biology of fracture healing: an overview for clinicians. Part I. *Clinical orthopaedics and related research*, *248*, 283-293.
[65] Dighe, A. S., Yang, S., Madhu, V., Balian, G., & Cui, Q. (2013). Interferon gamma and T cells inhibit osteogenesis induced by allogeneic mesenchymal stromal cells. *Journal of Orthopaedic Research*, *31*(2), 227-234.
[66] Toben, D., Schroeder, I., El Khassawna, T., Mehta, M., Hoffmann, J. E., Frisch, J. T., & Duda, G. N. (2011). Fracture healing is accelerated in the absence of the adaptive immune system. *Journal of Bone and Mineral Research*, *26*(1), 113-124.
[67] Colburn, N. T., Zaal, K. J., Wang, F., & Tuan, R. S. (2009). A role for γ/δ T cells in a mouse model of fracture healing. *Arthritis & Rheumatology*, *60*(6), 1694-1703.
[68] Nam, D., Mau, E., Wang, Y., Wright, D., Silkstone, D., Whetstone, H., & Alman, B. (2012). T-lymphocytes enable osteoblast maturation via IL-17F during the early phase of fracture repair. *PloS one*, *7*(6), e40044.
[69] Reinke, S., Geissler, S., Taylor, W. R., Schmidt-Bleek, K., Juelke, K., Schwachmeyer, V., & Unterwalder, N. (2013). Terminally differentiated CD8+ T cells negatively affect bone regeneration in humans. *Science translational medicine*, *5*(177), 177ra36-177ra36.
[70] Benvenuto, F., Ferrari, S., Gerdoni, E., Gualandi, F., Frassoni, F., Pistoia, V., ... & Uccelli, A. (2007). Human mesenchymal stem cells promote survival of T cells in a quiescent state. *Stem cells*, *25*(7), 1753-1760.
[71] Najar, M., Raicevic, G., Boufker, H. I., Fayyad-Kazan, H., De Bruyn, C., Meuleman, N., & Lagneaux, L. (2010). Adipose-tissue-derived and Wharton's jelly–derived mesenchymal stromal cells suppress lymphocyte responses by secreting leukemia inhibitory factor. *Tissue Engineering Part A*, *16*(11), 3537-3546.

[72] Kovach, T. K., Dighe, A. S., Lobo, P. I., & Cui, Q. (2015). Interactions between MSCs and immune cells: implications for bone healing. *Journal of immunology research*, 2015:752510
[73] Yin, T., & Li, L. (2006). The stem cell niches in bone. *The Journal of clinical investigation*, *116*(5), 1195-1201.
[74] Gori, J. L., Butler, J. M., Chan, Y. Y., Chandrasekaran, D., Poulos, M. G., Ginsberg, M., & Rafii, S. (2015). Vascular niche promotes hematopoietic multipotent progenitor formation from pluripotent stem cells. *The Journal of clinical investigation*, *125*(3), 1243-1254.
[75] Zhang, J., Niu, C., Ye, L., Huang, H., He, X., Tong, W. G., & Harris, S. (2003). Identification of the haematopoietic stem cell niche and control of the niche size. *Nature*, *425*(6960), 836-841.
[76] Morrison, S. J., & Scadden, D. T. (2014). The bone marrow niche for haematopoietic stem cells. *Nature*, *505*(7483), 327-334.
[77] Ding, L., & Morrison, S. J. (2013). Haematopoietic stem cells and early lymphoid progenitors occupy distinct bone marrow niches. *Nature*, *495*(7440), 231-235.
[78] Yin, T., & Li, L. (2006). The stem cell niches in bone. *The Journal of clinical investigation*, *116*(5), 1195-1201
[79] Zhang, J., Niu, C., Ye, L., Huang, H., He, X., Tong, W. G., & Harris, S. (2003). Identification of the haematopoietic stem cell niche and control of the niche size. *Nature*, *425*(6960), 836-841.
[80] Ren, G., Esposito, M., & Kang, Y. (2015). Bone metastasis and the metastatic niche. Journal of Molecular Medicine, 93 (11), 1203-1212.
[81] Walsh, M. C., Kim, N., Kadono, Y., Rho, J., Lee, S. Y., Lorenzo, J., & Choi, Y. (2006). Osteoimmunology: interplay between the immune system and bone metabolism. *Annu. Rev. Immunol.*, *24*, 33-63.
[82] Pittenger, M. F., Mackay, A. M., Beck, S. C., Jaiswal, R. K., Douglas, R., Mosca, J. D., Marshak, D. R. (1999). Multilineage potential of adult human mesenchymal stem cells. science, 284(5411), 143-147.
[83] Capulli, M., Paone, R., & Rucci, N. (2014). Osteoblast and osteocyte: games without frontiers. *Archives of biochemistry and biophysics*, *561*, 3-12.
[84] Ducy, P., Zhang, R., Geoffroy, V., Ridall, A. L., & Karsenty, G. (1997). Osf2/Cbfa1: a transcriptional activator of osteoblast differentiation. *cell*, *89*(5), 747-754.
[85] Shapiro, F. (2007). Bone development and its relation to fracture repair. *Eur. Cells Mater.*, *15*, *53-76*
[86] Sims, N. A. (2013). New insights into osteocyte and osteoblast biology: support of osteoclast formation, PTH action and the role of Wnt16. *BoneKEY reports*, *10*, *467*.
[87] Miron, R. J., & Zhang, Y. F. (2012). Osteoinduction a review of old concepts with new standards. *Journal of dental research*, *91*(8), 736-744.
[88] Bonewald, L. F. (2011). The amazing osteocyte. *Journal of Bone and Mineral Research*, *26*(2), 229-238.
[89] Rubin, C. T., & Lanyon, L. E. (1987). Osteoregulatory nature of mechanical stimuli: function as a determinant for adaptive remodeling inbone. Journal of Orthopaedic Research, 5 (2), 300-310.
[90] Boyle, W. J., Simonet, W. S., & Lacey, D. L. (2003). Osteoclast differentiation and activation. *Nature*, *423*(6937), 337-342.
[91] Teitelbaum, S. L., & Ross, F. P. (2003). Genetic regulation of osteoclast development and function. *Nature Reviews Genetics*, *4*(8), 638-649.
[92] Matsuo, K. (2009). Cross-talk among bone cells. *Current opinion in nephrology and hypertension*, *18*(4), 292-297.

[93] Gong, Y., Slee, R. B., Fukai, N., Rawadi, G., Roman-Roman, S., Reginato, A. M., & Zacharin, M. (2001). LDL receptor-related protein 5 (LRP5) affects bone accrual and eye development. *Cell*, *107*(4), 513-523.
[94] Kato, M., Patel, M. S., Levasseur, R., Lobov, I., Chang, B. H. J., Glass, D. A., & Lang, R. A. (2002). Cbfa1-independent decrease in osteoblast proliferation, osteopenia, and persistent embryonic eye vascularization in mice deficient in Lrp5, a Wnt coreceptor. *The Journal of cell biology*, *157*(2), 303-314.
[95] Zhang, Y., Wang, Y., Li, X., Zhang, J., Mao, J., Li, Z., & Wu, D. (2004). The LRP5 high-bone-mass G171V mutation disrupts LRP5 interaction with Mesd. *Molecular and cellular biology*, *24*(11), 4677-4684.
[96] Li, J., Sarosi, I., Cattley, R. C., Pretorius, J., Asuncion, F., Grisanti, M., & Kostenuik, P. (2006). Dkk1-mediated inhibition of Wnt signaling in bone results in osteopenia. *Bone*, *39*(4), 754-766.
[97] Heiland, G. R., Zwerina, K., Baum, W., Kireva, T., Distler, J. H., Grisanti, M., ... & Schett, G. (2010). Neutralisation of Dkk-1 protects from systemic bone loss during inflammation and reduces sclerostin expression. *Annals of the rheumatic diseases*, 69(12):2152-9
[98] Bodine, P. V., Zhao, W., Kharode, Y. P., Bex, F. J., Lambert, A. J., Goad, M. B., & Komm, B. S. (2004). The Wnt antagonist secreted frizzled-related protein-1 is a negative regulator of trabecular bone formation in adult mice. *Molecular Endocrinology*, *18*(5), 1222-1237.
[99] Feng, J. Q., Zhang, J., Dallas, S. L., Lu, Y., Chen, S., Tan, X., & Macdougall, M. (2002). Dentin matrix protein 1, a target molecule for Cbfa1 in bone, is a unique bone marker gene. *Journal of Bone and Mineral Research*, *17*(10), 1822-1831.
[100] Feng, J. Q., Huang, H., Lu, Y., Ye, L., Xie, Y., Tsutsui, T. W., & Mishina, Y. (2003). The Dentin matrix protein 1 (Dmp1) is specifically expressed in mineralized, but not soft, tissues during development. *Journal of dental research*, *82*(10), 776-780.
[101] Bhatia, A., Albazzaz, M., Orías, A. A. E., Inoue, N., Miller, L. M., Acerbo, A., & Sumner, D. R. (2012). Overexpression of DMP1 accelerates mineralization and alters cortical bone biomechanical properties in vivo. *Journal of the mechanical behavior of biomedical materials*, *5*(1), 1-8.
[102] Dallas, S. L., Prideaux, M., & Bonewald, L. F. (2013). The osteocyte: an endocrine cell… and more. *Endocrine reviews*, *34*(5), 658-690.
[103] Guo, D., Keightley, A., Barragan, L., Zhao, J., Guthrie, J., & Bonewald, L. (2006). Identification of proteins involved in cytoskeletal rearrangement, antihypoxia, and membrane channels enriched in osteocytes over osteoblasts. *Journal of bone and mineral research.* 21, 168.
[104] Yang, W., Harris, M. A., Heinrich, J. G., Guo, D., Bonewald, L. F., & Harris, S. E. (2009). Gene expression signatures of a fibroblastoid preosteoblast and cuboidal osteoblast cell model compared to the MLO-Y4 osteocyte cell model. *Bone*, *44*(1), 32-45.
[105] Wetterwald, A., Hofstetter, W., Cecchini, M. G., Lanske, B., Wagner, C., Fleisch, H., & Atkinson, M. (1996). Characterization and cloning of the E11 antigen, a marker expressed by rat osteoblasts and osteocytes. *Bone*, *18*(2), 125-132.
[106] Kogianni, G., Mann, V., & Noble, B. S. (2008). Apoptotic bodies convey activity capable of initiating osteoclastogenesis and localized bone destruction. *Journal of bone and mineral research*, *23*(6), 915-927.
[107] Percival, C. J., & Richtsmeier, J. T. (2013). Angiogenesis and intramembranous osteogenesis. *Developmental Dynamics*, *242*(8), 909-922.

[108] Beamer, B., Hettrich, C., & Lane, J. (2010). Vascular endothelial growth factor: an essential component of angiogenesis and fracture healing. *HSS journal*, *6*(1), 85-94.
[109] Wu, C., Giaccia, A. J., & Rankin, E. B. (2014). Osteoblasts: a novel source of erythropoietin. *Current osteoporosis reports*, *12*(4), 428-432.
[110] Ramasamy, S. K., Kusumbe, A. P., Wang, L., & Adams, R. H. (2014). Endothelial Notch activity promotes angiogenesis and osteogenesis in bone. Nature, 507(7492), 376-380
[111] Huang, B., Wang, W., Li, Q., Wang, Z., Yan, B., Zhang, Z., & Liu, S. (2016). Osteoblasts secrete Cxcl9 to regulate angiogenesis in bone. *Nature Communications*, 14; 7:13885.
[112] Kusumbe, A. P., Ramasamy, S. K., & Adams, R. H. (2014). Coupling of angiogenesis and osteogenesis by a specific vessel subtype in bone. Nature, 507(7492), 323-328.
[113] Weitzmann, M. N., & Pacifici, R. (2007). T cells: unexpected players in the bone loss induced by estrogen deficiency and in basal bone homeostasis. *Annals of the New York Academy of Sciences*, *1116*(1), 360-375.
[114] Li, Y., Toraldo, G., Li, A., Yang, X., Zhang, H., Qian, W. P., & Weitzmann, M. N. (2007). B cells and T cells are critical for the preservation of bone homeostasis and attainment of peak bone mass in vivo. *Blood*, *109*(9), 3839-3848.
[115] Raggatt, L. J., & Partridge, N. C. (2010). Cellular and molecular mechanisms of bone remodeling. *Journal of Biological Chemistry*, *285*(33), 25103-25108.
[116] Lorenzo, J., Horowitz, M., & Choi, Y. (2008). Osteoimmunology: interactions of the bone and immune system. *Endocrine reviews*, *29*(4), 403-440.
[117] Hume, D. A. (2008). Differentiation and heterogeneity in the mononuclear phagocyte system. *Mucosal immunology*, *1*(6), 432-441.
[118] Chang, M. K., Raggatt, L. J., Alexander, K. A., Kuliwaba, J. S., Fazzalari, N. L., Schroder, K., & Pettit, A. R. (2008). Osteal tissue macrophages are intercalated throughout human and mouse bone lining tissues and regulate osteoblast function in vitro and in vivo. *The Journal of Immunology*, *181*(2), 1232-1244.
[119] Marie, P. J. (2002). Role of N-cadherin in bone formation. *Journal of cellular physiology*, *190*(3), 297-305.
[120] Cheng, S. L., Lecanda, F., Davidson, M. K., Warlow, P. M., Zhang, S. F., Zhang, L., & Civitelli, R. (1998). Human Osteoblasts Express a Repertoire of Cadherins, Which Are Critical for BMP-2–Induced Osteogenic Differentiation. *Journal of Bone and Mineral Research*, *13*(4), 633-644.
[121] Ferrari, S. L., Traianedes, K., Thorne, M., Lafage-Proust, M. H., Genever, P., Cecchini, M. G., & Suva, L. J. (2000). A role for N-cadherin in the development of the differentiated osteoblastic phenotype. *Journal of Bone and Mineral Research*, *15*(2), 198-208.
[122] Kawaguchi, J., Kii, I., Sugiyama, Y., Takeshita, S., & Kudo, A. (2001). The Transition of Cadherin Expression in Osteoblast Differentiation from Mesenchymal Cells: Consistent Expression of Cadherin-11 in Osteoblast Lineage. *Journal of Bone and Mineral Research*, *16*(2), 260-269.
[123] Lemonnier, J., Haÿ, E., Delannoy, P., Lomri, A., Modrowski, D., Caverzasio, J., & Marie, P. J. (2001). Role of N-Cadherin and Protein Kinase C in Osteoblast Gene Activation Induced by the S252W Fibroblast Growth Factor Receptor 2 Mutation in Apert Craniosynostosis. *Journal of Bone and Mineral Research*, *16*(5), 832-845
[124] Marie, P. J., & Hay, E. (2013). Cadherins and Wnt signalling: a functional link controlling bone formation. *BoneKEy reports*, *2*(4), 330.

[125] Xu, H., Gu, S., Riquelme, M. A., Burra, S., Callaway, D., Cheng, H., & Zhao, H. (2015). Connexin 43 channels are essential for normal bone structure and osteocyte viability. *Journal of Bone and Mineral Research*, *30*(3), 436-448.
[126] Pacheco-Costa, R., Hassan, I., Reginato, R. D., Davis, H. M., Bruzzaniti, A., Allen, M. R., & Plotkin, L. I. (2014). High bone mass in mice lacking Cx37 because of defective osteoclast differentiation. *Journal of Biological Chemistry*, *289*(12), 8508-8520.
[127] Plotkin, L. I., & Stains, J. P. (2015). Connexins and pannexins in the skeleton: gap junctions, hemichannels and more. *Cellular and molecular life sciences*, *72*(15), 2853-2867.
[128] Penuela, S., Gehi, R., & Laird, D. W. (2013). The biochemistry and function of pannexin channels. *Biochimica et Biophysica Acta (BBA)-Biomembranes*, *1828*(1), 15-22.
[129] Penuela, S., Gehi, R., & Laird, D. W. (2013). The biochemistry and function of pannexin channels. *Biochimica et Biophysica Acta (BBA)-Biomembranes*, *1828*(1), 15-22.
[130] Penuela, S., Bhalla, R., Gong, X. Q., Cowan, K. N., Celetti, S. J., Cowan, B. J., & Laird, D. W. (2007). Pannexin 1 and pannexin 3 are glycoproteins that exhibit many distinct characteristics from the connexin family of gap junction proteins. *Journal of cell science*, *120*(21), 3772-3783.
[131] Xiao, Z., Camalier, C. E., Nagashima, K., Chan, K. C., Lucas, D. A., Cruz, M., & Conrads, T. P. (2007). Analysis of the extracellular matrix vesicle proteome in mineralizing osteoblasts. *Journal of cellular physiology*, *210*(2), 325-335.
[132] Ishikawa, M., Iwamoto, T., Nakamura, T., Doyle, A., Fukumoto, S., & Yamada, Y. (2011). Pannexin 3 functions as an ER Ca2+ channel, hemichannel, and gap junction to promote osteoblast differentiation. *The Journal of cell biology*, 193(7), 1257-1274.
[133] Ishikawa, M., Iwamoto, T., Fukumoto, S., & Yamada, Y. (2014). Pannexin 3 inhibits proliferation of osteoprogenitor cells by regulating Wnt and p21 signaling. *Journal of Biological Chemistry*, *289*(5), 2839-2851.
[134] Iwamoto, T., Nakamura, T., Doyle, A., Ishikawa, M., de Vega, S., Fukumoto, S., & Yamada, Y. (2010). Pannexin 3 regulates intracellular ATP/cAMP levels and promotes chondrocyte differentiation. *Journal of Biological Chemistry*, *285*(24), 18948-18958.
[135] Wade, R. J., & Burdick, J. A. (2012). Engineering ECM signals into biomaterials. *Materials Today*, *15*(10), 454-459.
[136] Campbell, I. D., & Humphries, M. J. (2011). Integrin structure, activation, and interactions. *Cold Spring Harbor perspectives in biology*, *3*(3), a004994.
[137] Castillo, A. B., Blundo, J. T., Chen, J. C., Lee, K. L., Yereddi, N. R., Jang, E., & Jacobs, C. R. (2012). Focal adhesion kinase plays a role in osteoblast mechanotransduction in vitro but does not affect load-induced bone formation in vivo. *PLoS One*, *7*(9), e43291.
[138] Hidalgo-Bastida, L. A., & Cartmell, S. H. (2010). Mesenchymal stem cells, osteoblasts and extracellular matrix proteins: enhancing cell adhesion and differentiation for bone tissue engineering. *Tissue Engineering Part B: Reviews*, *16*(4), 405-412.
[139] Mbalaviele, G., Shin, C. S., & Civitelli, R. (2006). Perspective: cell–cell adhesion and signaling through cadherins: connecting bone cells in their microenvironment. *Journal of Bone and Mineral Research*, *21*(12), 1821-1827.
[140] Streuli, C. H., & Bissell, M. J. (1990). Expression of extracellular matrix components is regulated by substratum. *The Journal of cell biology*, *110*(4), 1405-1415.

[141] Huang, C. H., Chen, M. H., Young, T. H., Jeng, J. H., & Chen, Y. J. (2009). Interactive effects of mechanical stretching and extracellular matrix proteins on initiating osteogenic differentiation of human mesenchymal stem cells. *Journal of cellular biochemistry*, *108*(6), 1263-1273.
[142] Mathews, S., Bhonde, R., Gupta, P. K., & Totey, S. (2012). Extracellular matrix protein mediated regulation of the osteoblast differentiation of bone marrow derived human mesenchymal stem cells. *Differentiation*, *84*(2), 185-192.
[143] Dolatshahi-Pirouz, A., Nikkhah, M., Gaharwar, A. K., Hashmi, B., Guermani, E., Aliabadi, H., & Khademhosseini, A. (2014). A combinatorial cell-laden gel microarray for inducing osteogenic differentiation of human mesenchymal stem cells. *Scientific reports*, *4*, 3896.
[144] Hatakeyama, J., Fukumoto, S., Nakamura, T., Haruyama, N., Suzuki, S., Hatakeyama, Y., ... & Kulkarni, A. B. (2009). Synergistic roles of amelogenin and ameloblastin. *Journal of dental research*, *88*(4), 318-322.
[145] Nikitovic, D., Aggelidakis, J., Young, M. F., Iozzo, R. V., Karamanos, N. K., & Tzanakakis, G. N. (2012). The biology of small leucine-rich proteoglycans in bone pathophysiology. *Journal of Biological Chemistry*, *287*(41), 33926-33933.
[146] Lu, X., Li, W., Fukumoto, S., Yamada, Y., Evans, C. A., Diekwisch, T., & Luan, X. (2016). The ameloblastin extracellular matrix molecule enhances bone fracture resistance and promotes rapid bone fracture healing. *Matrix Biology*, *52*, 113-126.
[147] Tamburstuen, M. V., Reseland, J. E., Spahr, A., Brookes, S. J., Kvalheim, G., Slaby, I., & Lyngstadaas, S. P. (2011). Ameloblastin expression and putative autoregulation in mesenchymal cells suggest a role in early bone formation and repair. *Bone*, *48*(2), 406-413.
[148] Iizuka, S., Kudo, Y., Yoshida, M., Tsunematsu, T., Yoshiko, Y., Uchida, T., & Takata, T. (2011). Ameloblastin regulates osteogenic differentiation by inhibiting Src kinase via cross talk between integrin β1 and CD63. *Molecular and cellular biology*, *31*(4), 783-792.
[149] Gugutkov, D., Altankov, G., Rodríguez Hernández, J. C., Monleón Pradas, M., & Salmerón Sánchez, M. (2010). Fibronectin activity on substrates with controlled□ OH density. *Journal of Biomedical Materials Research Part A*, *92*(1), 322-331.
[150] Pankov, R., & Yamada, K. M. (2002). Fibronectin at a glance. Journal of cell science, 115(20), 3861-3863.
[151] Clarke, B. (2008). Normal bone anatomy and physiology. *Clinical journal of the American Society of Nephrology*, *3* (3), 131-139.
[152] Higuchi, A., Ling, Q. D., Hsu, S. T., & Umezawa, A. (2012). Biomimetic cell culture proteins as extracellular matrices for stem cell differentiation. *Chemical reviews*, *112*(8), 4507-4540.
[153] Carvalho, S., Cortez, E., Stumbo, A. C., Thole, A., Caetano, C., Marques, R., & Carvalho, L. (2008). Laminin expression during bone marrow mononuclear cell transplantation in hepatectomized rats. *Cell biology international*, *32*(8), 1014-1018.
[154] Gu, Y. C., Kortesmaa, J., Tryggvason, K., Persson, J., Ekblom, P., Jacobsen, S. E., & Ekblom, M. (2003). Laminin isoform–specific promotion of adhesion and migration of human bone marrow progenitor cells. *Blood*, *101*(3), 877-885.
[155] Kumagai, T., Lee, I., Ono, Y., Maeno, M., & Takagi, M. (1998). Ultrastructural localization and biochemical characterization of vitronectin in developing rat bone. *The Histochemical Journal*, *30*(2), 111-119.
[156] Seiffert, D. I. E. T. M. A. R. (1996). Detection of vitronectin in mineralized bone matrix. *Journal of Histochemistry & Cytochemistry*, *44*(3), 275-280.

[157] Preissner, K. T. (1991). Structure and biological role of vitronectin. *Annual review of cell biology*, *7*(1), 275-310.
[158] Gelse, K., Pöschl, E., & Aigner, T. (2003). Collagens—structure, function, and biosynthesis. *Advanced drug delivery reviews*, *55*(12), 1531-1546.
[159] Ferreira, A. M., Gentile, P., Chiono, V., & Ciardelli, G. (2012). Collagen for bone tissue regeneration. *Acta biomaterialia*, *8*(9), 3191-3200.
[160] Boskey, A. L. (1996). Matrix proteins and mineralization: an overview. *Connective tissue research*, *35*(1-4), 357-363.
[161] Rosatil, R., Horanl, G. S., Piner03, G. I., Garofalo, S., & Keene, D. R. (1994). Normal long bone growth and development in type X collagen. *Nature genetics*, *8*(2), 129-135.
[162] Zheng, Q., Zhou, G., Morello, R., Chen, Y., Garcia-Rojas, X., & Lee, B. (2003). Type X collagen gene regulation by Runx2 contributes directly to its hypertrophic chondrocyte–specific expression in vivo. *The Journal of cell biology*, *162*(5), 833-842.
[163] Kirsch, T., & von der Mark, K. (1991). Ca2+ binding properties of type X collagen. *FEBS letters*, *294*(1-2), 149-152.
[164] Young, M. F., Kerr, J. M., Ibaraki, K., Heegaard, A. M., & Robey, P. G. (1992). Structure, expression, and regulation of the major noncollagenous matrix proteins of bone. *Clinical orthopaedics and related research*, *281*, 275-294.
[165] Delany, A. M., Kalajzic, I., Bradshaw, A. D., Sage, E. H., & Canalis, E. (2003). Osteonectin-null mutation compromises osteoblast formation, maturation, and survival. *Endocrinology*, *144*(6), 2588-2596.
[166] Midwood, K. S., Williams, L. V., & Schwarzbauer, J. E. (2004). Tissue repair and the dynamics of the extracellular matrix. *The international journal of biochemistry & cell biology*, *36*(6), 1031-1037.
[167] Alford, A. I., & Hankenson, K. D. (2006). Matricellular proteins: extracellular modulators of bone development, remodeling, and regeneration. *Bone*, *38*(6), 749-757.
[168] Alford, A. I., Kozloff, K. M., & Hankenson, K. D. (2015). Extracellular matrix networks in bone remodeling. *The international journal of biochemistry & cell biology*, *65*, 20-31.
[169] Fisher, L.W., Stubbs III, J.T., Young, M.F., 1995. Antisera and cDNA probes to human andcertain animal model bone matrix noncollagenous proteins. *Acta Orthop*. 266, 61–65
[170] Chen, X.D., Fisher, L.W., Robey, P.G., Young, M.F., 2004. The small leucine-rich proteoglycan biglycan modulates BMP-4-induced osteoblast differentiation. *FASEB J.* 18, 948–958.
[171] Fisher, L. W., Torchia, D. A., Fohr, B., Young, M. F., & Fedarko, N. S. (2001). Flexible structures of SIBLING proteins, bone sialoprotein, and osteopontin. *Biochemical and biophysical research communications*, *280*(2), 460-465.
[172] Giachelli, C. M., & Steitz, S. (2000). Osteopontin: a versatile regulator of inflammation and biomineralization. *Matrix Biology*, *19*(7), 615-622.
[173] Ganss, B., Kim, R. H., & Sodek, J. (1999). Bone sialoprotein. *Critical Reviews in Oral Biology & Medicine*, *10*(1), 79-98.
[174] Bellahcène, A., Bonjean, K., Fohr, B., Fedarko, N. S., Robey, F. A., Young, M. F., & Castronovo, V. (2000). Bone sialoprotein mediates human endothelial cell attachment and migration and promotes angiogenesis. *Circulation research*, *86*(8), 885-891.
[175] Ishijima, M., Tsuji, K., Rittling, S. R., Yamashita, T., Kurosawa, H., Denhardt, D. T., & Noda, M. (2002). Resistance to Unloading-Induced Three-Dimensional Bone

Loss in Osteopontin-Deficient Mice. *Journal of Bone and Mineral Research*, *17*(4), 661-667
[176] Ihara, H., Denhardt, D. T., Furuya, K., Yamashita, T., Muguruma, Y., Tsuji, K., & Rittling, S. R. (2001). Parathyroid hormone-induced bone resorption does not occur in the absence of osteopontin. *Journal of Biological Chemistry*, *276*(16), 13065-13071.
[177] Hunter, G. K. (2013). Role of osteopontin in modulation of hydroxyapatite formation. *Calcified tissue international*, *93*(4), 348-354
[178] Kannus, P., Jozsa, L., Järvinen, T. A., Järvinen, T. L., Kvist, M., Natri, A., & Järvinen, M. (1998). Location and distribution of non-collagenous matrix proteins in musculoskeletal tissues of rat. *The Histochemical journal*, *30*(11), 799-810.
[179] Carron, J. A., Wagstaff, S. C., Gallagher, J. A., & Bowler, W. B. (2000). A CD36-binding peptide from thrombospondin-1 can stimulate resorption by osteoclasts in vitro. *Biochemical and biophysical research communications*, *270*(3), 1124-1127.
[1780] Hankenson, K. D., Bain, S. D., Kyriakides, T. R., Smith, E. A., Goldstein, S. A., & Bornstein, P. (2000). Increased Marrow-Derived Osteoprogenitor Cells and Endosteal Bone Formation in Mice Lacking Thrombospondin 2. *Journal of Bone and Mineral Res8earch*, *15*(5), 851-862.
[181] Mackie, E. J., & Murphy, L. I. (1998). The role of tenascin-C and related glycoproteins in early chondrogenesis. *Microscopy research and technique*, *43*(2), 102-110.
[182] Ravindran, S., & George, A. (2014). Multifunctional ECM proteins in bone and teeth. *Experimental cell research*, *325*(2), 148-154
[183] Feng, J. Q., Zhang, J., Dallas, S. L., Lu, Y., Chen, S., Tan, X., & Macdougall, M. (2002). Dentin matrix protein 1, a target molecule for Cbfa1 in bone, is a unique bone marker gene. *Journal of Bone and Mineral Research*, *17*(10), 1822-1831.
[184] He, G., Dahl, T., Veis, A., & George, A. (2003). Nucleation of apatite crystals in vitro by self-assembled dentin matrix protein 1. *Nature materials*, *2*(8), 552-558.
[185] He, G., & George, A. (2004). Dentin matrix protein 1 immobilized on type I collagen fibrils facilitates apatite deposition in vitro. *Journal of Biological Chemistry*, *279*(12), 11649-11656.
[186] Narayanan, K., Ramachandran, A., Hao, J., He, G., Park, K. W., Cho, M., & George, A. (2003). Dual functional roles of dentin matrix protein 1 Implications in biomineralization and gene transcription by activation of intracellular Ca2+ store. *Journal of Biological Chemistry*, *278*(19), 17500-17508.
[187] Narayanan, K., Gajjeraman, S., Ramachandran, A., Hao, J., & George, A. (2006). Dentin matrix protein 1 regulates dentin sialophosphoprotein gene transcription during early odontoblast differentiation. *Journal of Biological Chemistry*, *281*(28), 19064-19071.
[188] Keene DR, Sakai LY, Burgeson RE (1991) Human bone contains type III collagen, type VI collagen and fibrillin. J Histochem Cytochem 38:59–69
[189] Tolstoshev P, Haber R, Trapnell BC, Crystal RG (1981) Procollagen mRNA levels and activity and collagen synthesis during the fetal development of sheep lung, tendon and skin. J Biol Chem 256:9672–9679
[190] Kim, J. K., Xu, Y., Xu, X., Keene, D. R., Gurusiddappa, S., Liang, X., & Höök, M. (2005). A novel binding site in collagen type III for integrins α1β1 and α2β1. *Journal of Biological Chemistry*, *280*(37), 32512-32520.
[191] van der Plas, R. M., Gomes, L., Marquart, J. A., Vink, T., Meijers, J. C., de Groot, P. G., & Huizinga, E. G. (2000). Binding of von Willebrand factor to collagen type III: role of specific amino acids in the collagen binding domain of vWF and effects of neighboring domains. *Thrombosis and haemostasis*, *84*(6), 1005-1011.

[192] Nakamura, M., Sone, S., Takahashi, I., Mizoguchi, I., Echigo, S., & Sasano, Y. (2005). Expression of versican and ADAMTS1, 4, and 5 during bone development in the rat mandible and hind limb. *Journal of Histochemistry & Cytochemistry*, *53*(12), 1553-1562.
[193] Neer, E. J., Schmidt, C. J., Nambudripad, R., & Smith, T. F. (1994). The ancient regulatory-protein family of WD-repeat proteins. *Nature*, *371*(6495), 297-300.
[194] Choy, L., & Derynck, R. (1998). The type II transforming growth factor (TGF)-β receptor-interacting protein TRIP-1 acts as a modulator of the TGF-β response. *Journal of Biological Chemistry*, *273*(47), 31455-31462.
[195] Frost, H. M. (2001). From Wolff's law to the Utah paradigm: insights about bone physiology and its clinical applications. *The Anatomical Record*, *262*(4), 398-419.
[196] Burr, D. B., Robling, A. G., & Turner, C. H. (2002). Effects of biomechanical stress on bones in animals. *Bone*, *30*(5), 781-786.
[197] Burr, D. B., Turner, C. H., Naick, P., Forwood, M. R., Ambrosius, W., Hasan, M. S., & Pidaparti, R. (1998). Does microdamage accumulation affect the mechanical properties of bone?. *Journal of biomechanics*, *31*(4), 337-345.
[198] Duncan, R. L., & Turner, C. H. (1995). Mechanotransduction and the functional response of bone to mechanical strain. *Calcified tissue international*, *57*(5), 344-358.
[199] Rubin, C. T. (1984). Skeletal strain and the functional significance of bone architecture. *Calcified tissue international*, *36*, S11-S18.
[200] Turner, C. H., Forwood, M. R., & Otter, M. W. (1994). Mechanotransduction in bone: do bone cells act as sensors of fluid flow?. *The FASEB Journal*, *8*(11), 875-878.
[201] Robling, A. G., Hinant, F. M., Burr, D. B., & Turner, C. H. (2002). Shorter, more frequent mechanical loading sessions enhance bone mass. *Medicine and science in sports and exercise*, *34*(2), 196-202.
[202] Tyrovola, J. B., & Odont, X. X. (2015). The "mechanostat theory" of frost and the OPG/Rankl/RANK system. *Journal of cellular biochemistry*, *116*(12), 2724-2729.
[203] Shiotani, A., Shibasaki, Y., & Sasaki, T. (2001). Localization of receptor activator of NFκB ligand, RANKL, in periodontal tissues during experimental movement of rat molars. *Journal of electron microscopy*, *50*(4), 365-369.
[204] Oshiro, T., Shiotani, A., Shibasaki, Y., & Sasaki, T. (2002). Osteoclast induction in periodontal tissue during experimental movement of incisors in osteoprotegerin-deficient mice. *The Anatomical Record*, *266*(4), 218-225.
[205] Tang, L., Lin, Z., & Li, Y. M. (2006). Effects of different magnitudes of mechanical strain on osteoblasts in vitro. *Biochemical and biophysical research communications*, *344*(1), 122-128.
[206] Boutahar, N., Guignandon, A., Vico, L., & Lafage-Proust, M. H. (2004). Mechanical strain on osteoblasts activates autophosphorylation of focal adhesion kinase and proline-rich tyrosine kinase 2 tyrosine sites involved in ERK activation. *Journal of Biological Chemistry*, *279*(29), 30588-30599.
[207] Chen, K. D., Li, Y. S., Kim, M., Li, S., Yuan, S., Chien, S., & Shyy, J. Y. (1999). Mechanotransduction in response to shear stress roles of receptor tyrosine kinases, integrins, and Shc. *Journal of Biological Chemistry*, *274*(26), 18393-18400.
[208] Cowin S. C., Moss-Salentijn, L., & Moss, M. L. (1991). Candidates for the mechanosensory system in bone. *Journal of biomechanical engineering*, *113*, 191.
[209] Weinbaum, S., Cowin, S. C., & Zeng, Y. (1994). A model for the excitation of osteocytes by mechanical loading-induced bone fluid shear stresses. *Journal of biomechanics*, *27*(3), 339-360.

[210] Cowin, S. C., Weinbaum, S., & Zeng, Y. (1995). A case for bone canaliculi as the anatomical site of strain generated potentials. *Journal of biomechanics*, *28*(11), 1281-1297.
[211] Sharma U, Mikos AG, Cowin SC. (2007). Mechanosensory mechanisms in bone. In: Lanza R, Langer R, Vacanti JP, editors. Textbook of Tissue Engineering. 3rd edition. Elsevier/Academic Press.
[212] Fritton, S. P., & Weinbaum, S. (2009). Fluid and solute transport in bone: flow-induced mechanotransduction. *Annual review of fluid mechanics*, *41*, 347-374.
[213] Weinbaum, S., Cowin, S. C., & Zeng, Y. (1994). A model for the excitation of osteocytes by mechanical loading-induced bone fluid shear stresses. *Journal of biomechanics*, *27*(3), 339-360.
[214] Fritton, S. P., & Weinbaum, S. (2009). Fluid and solute transport in bone: flow-induced mechanotransduction. *Annual review of fluid mechanics*, *41*, 347-374.
[215] Xiao, Z., & Quarles, L. D. (2015). Physiological mechanisms and therapeutic potential of bone mechanosensing. *Reviews in Endocrine and Metabolic Disorders*, *16*(2), 115-129.
[216] Huang, C., & Ogawa, R. (2010). Mechanotransduction in bone repair and regeneration. *The FASEB Journal*, *24*(10), 3625-3632.
[217] Salter, D. M., Robb, J. E., & Wright, M. O. (1997). Electrophysiological responses of human bone cells to mechanical stimulation: evidence for specific integrin function in mechanotransduction. *Journal of Bone and Mineral Research*, *12*(7), 1133-1141.
[218] Wu, M., Chen, G., & Li, Y. P. (2016). TGF-β and BMP signaling in osteoblast, skeletal development, and bone formation, homeostasis and disease. *Bone research*, *4*, 16009.
[219] Hollinger, J. O., & Kleinschmidt, J. C. (1990). The critical size defect as an experimental model to test bone repair materials. *Journal of Craniofacial Surgery*, *1*(1), 60-68.
[220] Pelled, G., Ben-Arav, A., Hock, C., Reynolds, D. G., Yazici, C., Zilberman, Y., & Schwarz, E. M. (2009). Direct gene therapy for bone regeneration: gene delivery, animal models, and outcome measures. *Tissue Engineering Part B: Reviews*, *16*(1), 13-20.
[221] Kimelman, N., Pelled, G., Helm, G. A., Huard, J., Schwarz, E. M., & Gazit, D. (2007). Review: Gene-and Stem Cell–Based Therapeutics for Bone Regeneration and Repair. *Tissue engineering*, *13*(6), 1135-1150.
[222] Kimelman, N., Pelled, G., Helm, G. A., Huard, J., Schwarz, E. M., & Gazit, D. (2007). Review: Gene-and Stem Cell–Based Therapeutics for Bone Regeneration and Repair. *Tissue engineering*, *13*(6), 1135-1150.
[223] Buckwalter, J. A., Einhorn, T. A., Bolander, M. E., & Cruess, R. L. (1996). Healing of the musculoskeletal tissues. *Fractures in adults*, *1*, 267-83.
[224] Bueno, E. M., & Glowacki, J. (2009). Cell-free and cell-based approaches for bone regeneration. *Nature Reviews Rheumatology*, *5*(12), 685-697.
[225] Kneser, U., Schaefer, D. J., Polykandriotis, E., & Horch, R. E. (2006). Tissue engineering of bone: the reconstructive surgeon's point of view. *Journal of cellular and molecular medicine*, *10*(1), 7-19.
[226] Hernigou, P., Poignard, A., Manicom, O., Mathieu, G., & Rouard, H. (2005). The use of percutaneous autologous bone marrow transplantation in nonunion and avascular necrosis of bone. *Bone & Joint Journal*, *87*(7), 896-902.
[227] Szpalski, C., Barr, J., Wetterau, M., Saadeh, P. B., & Warren, S. M. (2010). Cranial bone defects: current and future strategies. *Neurosurgical focus*, *29*(6), E8.

[228] Bose, S., Roy, M., & Bandyopadhyay, A. (2012). Recent advances in bone tissue engineering scaffolds. *Trends in biotechnology*, *30*(10), 546-554.
[229] Ratner, B. D., Hoffman, A. S., Schoen, F. J., & Lemons, J. E. (2004). *Biomaterials science: an introduction to materials in medicine*. Academic press.
[230] Habibovic, P., & Barralet, J. E. (2011). Bioinorganics and biomaterials: bone repair. *Acta Biomaterialia*, *7*(8), 3013-3026.
[231] Rahaman, M. N., Day, D. E., Bal, B. S., Fu, Q., Jung, S. B., Bonewald, L. F., & Tomsia, A. P. (2011). Bioactive glass in tissue engineering. *Acta biomaterialia*, *7*(6), 2355-2373.
[232] Arcos, D., & Vallet-Regí, M. (2013). Bioceramics for drug delivery. *Acta Materialia*, *61*(3), 890-911.
[233] Baino, F., Perero, S., Ferraris, S., Miola, M., Balagna, C., Verné, E., & Ferraris, M. (2014). Biomaterials for orbital implants and ocular prostheses: overview and future prospects. *Acta biomaterialia*, *10*(3), 1064-1087.
[234] Williams, C. G., Kim, T. K., Taboas, A., Malik, A., Manson, P., & Elisseeff, J. (2003). *In vitro* chondrogenesis of bone marrow-derived mesenchymal stem cells in a photopolymerizing hydrogel. *Tissue engineering*, *9*(4), 679-688.
[235] Zhou, C., Shi, Q., Guo, W., Terrell, L., Qureshi, A. T., Hayes, D. J., & Wu, Q. (2013). Electrospun bio-nanocomposite scaffolds for bone tissue engineering by cellulose nanocrystals reinforcing maleic anhydride grafted PLA. *ACS applied materials & interfaces*, *5*(9), 3847-3854.
[236] Wang, W., Li, B., Li, Y., Jiang, Y., Ouyang, H., & Gao, C. (2010). *In vivo* restoration of full-thickness cartilage defects by poly (lactide-co-glycolide) sponges filled with fibrin gel, bone marrow mesenchymal stem cells and DNA complexes. *Biomaterials*, *31*(23), 5953-5965.
[237] Mahmoudifar, N., & Doran, P. M. (2010). Chondrogenic differentiation of human adipose-derived stem cells in polyglycolic acid mesh scaffolds under dynamic culture conditions. *Biomaterials*, *31*(14), 3858-3867.
[238] Mano, J. F., Silva, G. A., Azevedo, H. S., Malafaya, P. B., Sousa, R. A., Silva, S. S., & Neves, N. M. (2007). Natural origin biodegradable systems in tissue engineering and regenerative medicine: present status and some moving trends. *Journal of the Royal Society Interface*, *4*(17), 999-1030.
[239] Bright, C., Park, Y. S., Sieber, A. N., Kostuik, J. P., & Leong, K. W. (2006). In vivo evaluation of plasmid DNA encoding OP-1 protein for spine fusion. *Spine*, *31*(19), 2163-2172.
[240] Chang, C. H., Kuo, T. F., Lin, C. C., Chou, C. H., Chen, K. H., Lin, F. H., & Liu, H. C. (2006). Tissue engineering-based cartilage repair with allogenous chondrocytes and gelatin–chondroitin–hyaluronan tri-copolymer scaffold: a porcine model assessed at 18, 24, and 36 weeks. *Biomaterials*, *27*(9), 1876-1888.
[241] Marolt, D., Augst, A., Freed, L. E., Vepari, C., Fajardo, R., Patel, N., & Vunjak-Novakovic, G. (2006). Bone and cartilage tissue constructs grown using human bone marrow stromal cells, silk scaffolds and rotating bioreactors. *Biomaterials*, *27*(36), 6138-6149.
[242 Fan, H., Tao, H., Wu, Y., Hu, Y., Yan, Y., & Luo, Z. (2010). TGF-β3 immobilized PLGA-gelatin/chondroitin sulfate/hyaluronic acid hybrid scaffold for cartilage regeneration. *Journal of biomedical materials research Part A*, *95*(4), 982-992.
[243] Deng, T., Lv, J., Pang, J., Liu, B., & Ke, J. (2014). Construction of tissue-engineered osteochondral composites and repair of large joint defects in rabbit. *Journal of tissue engineering and regenerative medicine*, *8*(7), 546-556.

[244] Nettles, D. L., Elder, S. H., & Gilbert, J. A. (2002). Potential use of chitosan as a cell scaffold material for cartilage tissue engineering. *Tissue engineering*, *8*(6), 1009-1016.
[245] Thorpe, S. D., Buckley, C. T., Vinardell, T., O'Brien, F. J., Campbell, V. A., & Kelly, D. J. (2010). The response of bone marrow-derived mesenchymal stem cells to dynamic compression following TGF-β3 induced chondrogenic differentiation. *Annals of biomedical engineering*, *38*(9), 2896-2909.
[246] Oliveira, M. B., Song, W., Martín, L., Oliveira, S. M., Caridade, S. G., Alonso, M., & Mano, J. F. (2011). Development of an injectable system based on elastin-like recombinamer particles for tissue engineering applications. *Soft Matter*, *7*(14), 6426-6434.
[247] Engler, A. J., Sen, S., Sweeney, H. L., & Discher, D. E. (2006). Matrix elasticity directs stem cell lineage specification. *Cell*, *126*(4), 677-689
[248] Zhang, B., Filion, T. M., Kutikov, A. B., & Song, J. (2016). Facile Stem Cell Delivery to Bone Grafts Enabled by Smart Shape Recovery and Stiffening of Degradable Synthetic Periosteal Membranes. *Advanced Functional Materials*].
[249] Nonoyama, T., Wada, S., Kiyama, R., Kitamura, N., Mredha, M., Islam, T., ... & Yasuda, K. (2016). Double-Network Hydrogels Strongly Bondable to Bones by Spontaneous Osteogenesis Penetration. *Advanced Materials*, *28*(31), 6740-6745.
[250] Lee, S. J., Lee, D., Yoon, T. R., Kim, H. K., Jo, H. H., Park, J. S., & Park, S. A. (2016). Surface modification of 3D-printed porous scaffolds via mussel-inspired polydopamine and effective immobilization of rhBMP-2 to promote osteogenic differentiation for bone tissue engineering. *Acta biomaterialia*, *40*, 182-191.
[251] Lu, J., Cheng, C., He, Y. S., Lyu, C., Wang, Y., Yu, J., & Li, D. (2016). Multilayered Graphene Hydrogel Membranes for Guided Bone Regeneration. *Advanced Materials*, *28*(21), 4025-4031.
[252] Albrektsson, T., & Johansson, C. (2001). Osteoinduction, osteoconduction and osseointegration. *European Spine Journal*, *10*, S96-S101
[253] Bianco, P., & Robey, P. G. (2000). Marrow stromal stem cells. *The Journal of clinical investigation*, *105*(12), 1663-1668.
[254] Mizuno, H., Zuk, P. A., Zhu, M., Lorenz, P. H., Benhaim, P., & Hedrick, M. H. (2002). Myogenic differentiation by human processed lipoaspirate cells. *Plastic and reconstructive surgery*, *109*(1), 199-209.
[255] Birmingham, E., Niebur, G. L., & McHugh, P. E. (2012). Osteogenic differentiation of mesenchymal stem cells is regulated by osteocyte and osteoblast cells in a simplified bone niche. *Eur Cell Mater*, 23:13-27
[256] Jeon, O. H., Panicker, L. M., Lu, Q., Chae, J. J., Feldman, R. A., & Elisseeff, J. H. (2016). Human iPSC-derived osteoblasts and osteoclasts together promote bone regeneration in 3D biomaterials. *Scientific reports*, *6*, 26761
[257] Lou, X. (2015). Induced pluripotent stem cells as a new strategy for osteogenesis and bone regeneration. *Stem Cell Reviews and Reports*, *11*(4), 645-651.
[258] Ren, L., Yang, P., Wang, Z., Zhang, J., Ding, C., & Shang, P. (2015). Biomechanical and biophysical environment of bone from the macroscopic to the pericellular and molecular level. *Journal of the mechanical behavior of biomedical materials*, *50*, 104-122.
[259] Sladkova, M., & de Peppo, G. M. (2014). Bioreactor systems for human bone tissue engineering. *Processes*, *2*(2), 494-525.
[260] Birla, R. (2014). *Introduction to tissue engineering: applications and challenges*. John Wiley & Sons.

[261] Sucosky, P., Osorio, D. F., Brown, J. B., & Neitzel, G. P. (2004). Fluid mechanics of a spinner-flask bioreactor. *Biotechnology and bioengineering*, *85*(1), 34-46.
[262] Gelinsky, M., Bernhardt, A., & Milan, F. (2015). Bioreactors in tissue engineering: Advances in stem cell culture and three-dimensional tissue constructs. *Engineering in Life Sciences*, *15*(7), 670-677
[263] Schwarz, R.P.; Thomas, J.; Wolf, D.A. Cell culture for three-dimensional modeling in rotating-wallvessels: An application of simulated microgravity. *J. Tissue Cult. Methods* 1992, *14*, 51–55
[264] Freed, L. E., & Vunjak-Novakovic, G. (2002). Spaceflight bioreactor studies of cells and tissues. *Advances in space biology and medicine*, *8*, 177-195.
[265] Hansmann, J., Groeber, F., Kahlig, A., Kleinhans, C., & Walles, H. (2013). Bioreactors in tissue engineering—principles, applications and commercial constraints. *Biotechnology journal*, *8*(3), 298-307.
[266] Bilodeau, K., & Mantovani, D. (2006). Bioreactors for tissue engineering: focus on mechanical constraints. A comparative review. *Tissue engineering*, *12*(8), 2367-2383.
[267] Zydney, A. L. (2016). Continuous downstream processing for high value biological products: A Review. *Biotechnology and bioengineering*, *113*(3), 465-475.
[268] Gaspar, D. A., Gomide, V., & Monteiro, F. J. (2012). The role of perfusion bioreactors in bone tissue engineering. *Biomatter*, *2*(4), 167-175.
[269] Yeatts, A. B., & Fisher, J. P. (2011). Bone tissue engineering bioreactors: dynamic culture and the influence of shear stress. *Bone*, *48*(2), 171-181.
[270] El Haj, A. J., & Cartmell, S. H. (2006). Mechanical bioreactors for tissue engineering. *Bioreactors for Tissue Engineering*.
[271] El Haj, A. J., Wood, M. A., Thomas, P., & Yang, Y. (2005). Controlling cell biomechanics in orthopaedic tissue engineering and repair. *Pathologie Biologie*, *53*(10), 581-589.
[272] Wood, M. A., Yang, Y., Baas, E., Meredith, D. O., Richards, R. G., Kuiper, J. H., & El Haj, A. J. (2008). Correlating cell morphology and osteoid mineralization relative to strain profile for bone tissue engineering applications. *Journal of The Royal Society Interface*, *5*(25), 899-907.
[273] Wong, D. A., Kumar, A., Jatana, S., Ghiselli, G., & Wong, K. (2008). Neurologic impairment from ectopic bone in the lumbar canal: a potential complication of off-label PLIF/TLIF use of bone morphogenetic protein-2 (BMP-2). *The Spine Journal*, *8*(6), 1011-1018.
[274] Vo, T. N., Kasper, F. K., & Mikos, A. G. (2012). Strategies for controlled delivery of growth factors and cells for bone regeneration. *Advanced drug delivery reviews*, *64*(12), 1292-1309.
[275] Koutsopoulos, S., Unsworth, L. D., Nagai, Y., & Zhang, S. (2009). Controlled release of functional proteins through designer self-assembling peptide nanofiber hydrogel scaffold. *Proceedings of the National Academy of Sciences*, *106*(12), 4623-4628.
[276] Monteiro, N., Martins, A., Reis, R. L., & Neves, N. M. (2015). Nanoparticle-based bioactive agent release systems for bone and cartilage tissue engineering. *Regenerative Therapy*, *1*, 109-118.

Chapter II- Materials and methods

1. Objectives

1.1. Main objective

The main objective of this study was the validation and development of a perfusion bioreactor for the high-throughput analysis of biomaterials/stem cells combinations.

1.2. Secondary objectives

- ✓ Development of an arrayed hollow platform with 3D porous biomaterials
- ✓ Biomaterial modification with 32 different combinations of proteins
- ✓ Assembly of a bioreactor using widely available labware

2. Materials and methods

2.1. Preparation of hollow arrayed platform

A polydimethylsiloxane (PDMS, Elastomer Kit, Dow Corning) solution in a ratio of 5:1 (PDMS:curing agent) was prepared and degassed under vacuum for 1 hour. A volume of 3 mL was pipetted onto a mold, schematically represented on Figure 1. The molds containing the PDMS solution were again degassed under vacuum for 1 hour, and cured in an oven (Oven/Laboratory dryer, Ecocell 55 Frilabo), at 70ºC for 1 hour. The hollow PDMS structure shown in Figure 2 was obtained after removing the cured PDMS from the mold using tweezers. The final platform had approximately 2 mm height and 4 x 4 cm^2 area. The hollowed platform had 1 mm diameter circular by 1 mm, as represented in Figure 1.

2.2. Microarrayed platforms containing chitosan scaffolds

A 0.9% chitosan (Sigma-Aldrich) solution was prepared using glacial acetic acid (LabChem) at 1% (w/v). We tested several chitosan concentrations, from the range of 0,125% to 1%. We chose 0,9% in the end, since this was the concentration that allowed the construction of a porous and robust scaffold, for the previously mentioned concentration range. A volume of 3 µL was pipetted onto individual wells of the PDMS platform. The platform containing chitosan solution in the wells was frozen at -20ºC for 4 hours, and then freeze-dried (LyoQuest Plus Eco,VWR) overnight. The scaffolds were then neutralized by adding droplets of 1 M sodium hydroxide (NaOH, Eka, AkzoNobel) solution prepared in 70% (%vol) ethanol (Valente & Ribeiro). Different neutralization and washing approaches were developed and optimized to minimize chitosan scaffolds shrinking after neutralization. After 10 minutes neutralization, scaffolds were washed with distilled water for

30 minutes (the water was changed three times). The samples were frozen again at -20ºC for 4 hours and freeze-dried overnight. The platforms were sterilized prior to cell culture by exposure to UV irradiation for 30 minutes in each side of the device (Laminar Flow Cabinet S@femate Eco 1.2m, EuroClone®).

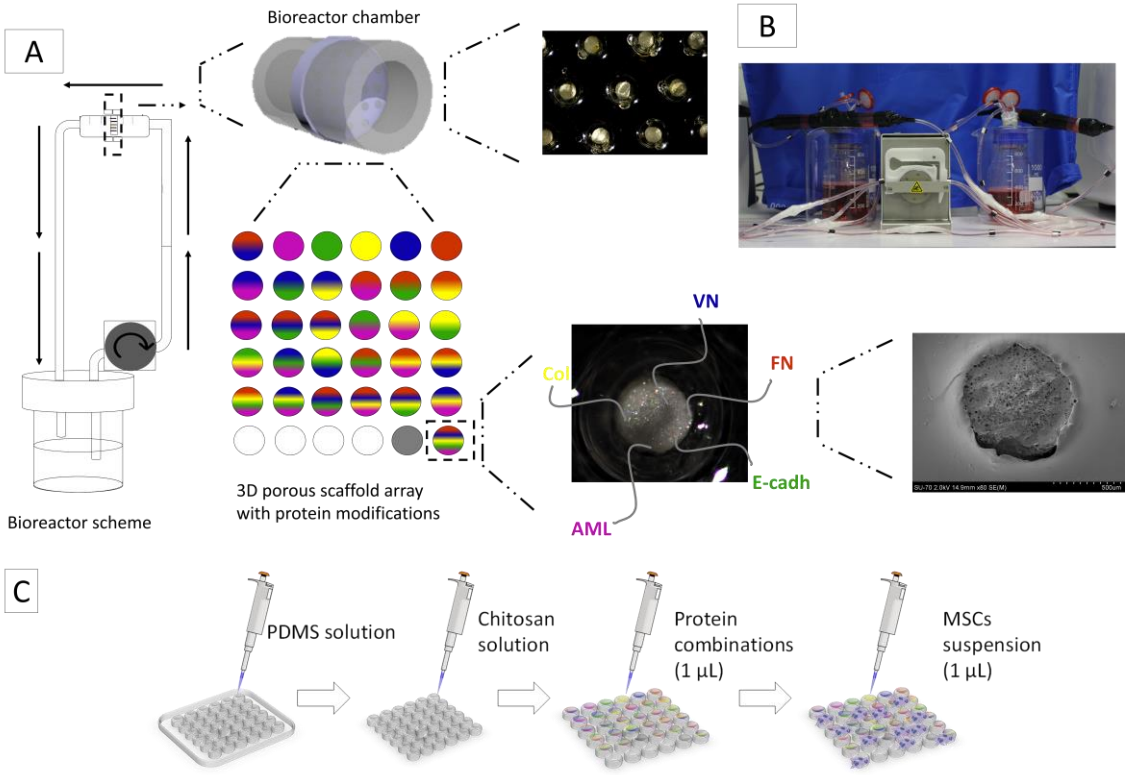

Figure 1- (A) Schematic representation of the assembled bioreactor. (B) Final aspect of an assembled bioreactor, with two experiments taking place at the same time. (C) Schematic modification of the 3D scaffolds in the hollow arrays

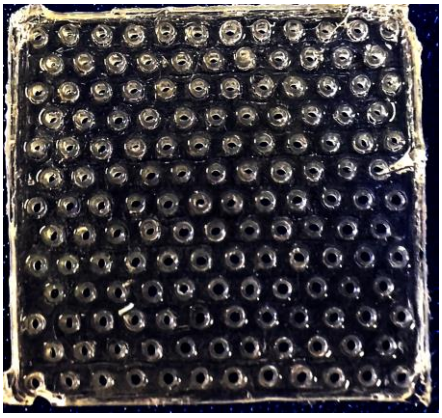

Figure 2- Picture of a hollow platform. Each individual spot was later filled with chitosan solution, to prepare a minaturized porous scaffold.

2.3. Preparation of protein solutions

Five human proteins were used in this study: fibronectin (F, Sigma Aldrich), vitronectin (V, Sigma Aldrich), E-cadherin (E, Advanced BioMatrix), collagen type I (C, Sigma Aldrich) and amelogenin (A, Abcam). Solutions of the 5 proteins were prepared by dissolution of the stock solution in a phosphate buffered saline solution (PBS, ThermoScientific). The protein solutions were all diluted to the same final concentration, 0.05 mg/mL. Protein solutions used for immobilization on chitosan scaffolds were prepared with equal proportions of each protein. The final protein solutions had the same final mass of protein.

2.4. Protein immobilization onto miniaturized chitosan 3D scaffolds

Solutions of *N*-Hydroxysuccinimide (NHS, Aldrich Laborspirit) and N-(3-Dimethylaminopropyl)-N′-ethylcarbodiimide hydrochloride (EDC, Sigma (Fluka)) were added to the protein solutions, in a proportion of 1:1:2, (v/v) EDC-NHS:protein solution, accordingly to a previously reported method [1]. EDC and NHS concentrations in the protein solutions were 2 mM and 5 mM, respectively. A volume of 1 μL of each protein mixture was pipetted onto single scaffolds, and left to react for one hour at room temperature. The chips were then washed three times in sterile PBS.

The covalent immobilization of the proteins to the scaffolds was crucial, since in preliminary approaches consisting in the physical adsorption of the proteins to the scaffolds, we observed a complete loss of adhered cells to the scaffolds after a 3-day time point. The reasons for proteins activity loss and eventual cell detachment on this approach were not explored in this work.

2.5. Cell expansion

Bone Marrow-Derived Mesenchymal Stem Cells (BMSCs) were purchased from LGC Standards, ATCC. The undifferentiated cells were cultured and expanded under basal condition, using Minimum Essential alpha Medium (alpha-MEM, Sigma, USA), supplemented with 10% (v/v) fetal bovine serum (ThermoFisher Scientific) and 1% (v/v) penicillin-streptomycin.

2.6. Cell seeding

A 5000 cells/μL BMSCs suspension was pipetted, at a volume of 1 μL, onto the scaffolds with previously immobilized proteins. Cells were left to attach to the material for 30 min at 37ºC. After this seeding step, the chips were washed once with PBS and incubated (CO_2 Incubator, Model C170, Binder) at 37ºC, 5% CO_2, in cell supplemented culture medium. Cells were used on passages of P2 to P6, and cell culture was exchanged every 2 days.

2.7. Bioreactor assembly

A perfusion bioreactor (figure 1) was assembled to withstand parallel replicates of each individual setup depending solely on the available channels of the peristaltic pump used to perfuse the medium. Each individual set of the bioreactor comprised: (i) one chamber with cell culture medium and capable of holding the hollow PDMS platform containing 3D scaffolds arrays and respective adhered cells, (ii) tubes (Tygon ST R3607, Ismatec, 3.17 mm outer diameter) for medium transportation, (iii) one reservoir of cell culture medium (Schott, 250 mL), and (iv) one peristaltic pump (REGLO digital MS-2/6-160) (figure 1). The tubes were connected to the cell culture medium reservoir through a commercially available screw cap (Screw cap HPLC, GL 45, 4 ports, Duran®) with four ports (3.0 mm diameter). The inlet tube, that drove medium flux to the bioreactor chamber, was inserted inside the cell culture medium; the outlet tube, which recirculated the cell culture medium back to the reservoir, was left about 1 cm above the cell culture medium meniscus. The tubes connecting the medium reservoir and the bioreactor chamber were assembled in the channels of a peristaltic pump. Gas exchange in the cell culture medium was promoted through the assembly of two 0.2 μm sterile cellulose acetate syringe filters (30 mm diameter; Whatmann™/GE Healthcare) in the two remaining entries of the reservoir cap. The bioreactor chamber was composed of two sterile 20 mL polypropylene syringes (VWR) without the respective pistons. Tubes were connected to the outlet of the syringes, and both syringes were assembled together containing the perforated arrayed platform in between both syringes. The chamber was sealed using sterile Parafilm® and insulation tape on outer layers. All tube-tube and syringe-tube junctions were also sealed with Parafilm® and insulation tape. The schematic representation of the

bioreactor assembly is depicted in Figure 1A. A picture of the bioreactor containing two parallel setups, assembled to the same peristaltic pump, can be seen in Figure 1B.

2.8. Dynamic and static (control) cell culture

The arrayed platforms containing seeded cells were placed in the bioreactor chamber using sterile tweezers. BMSCs were cultured in the platforms for 24 hours, under static conditions, prior to the assembly in the bioreactor. For static control experiments, cell culture was continued under static conditions inside suspension Petri dishes, with 8 mL supplemented cell culture medium. On dynamic culture, after the complete bioreactor sealing, the bioreactor reservoirs and chambers were placed on an incubator at 37ºC and 5% CO_2. The bioreactor chambers were placed in a horizontal position. The peristaltic pump was set with a flow of 0.68 mL/min. This flow is in a range of 0.2 – 1 mL/min, previously shown by Bancroft *et al*. [2] to induce BMSCs cell growth, proliferation and differentiation into the osteogenic lineage on two-dimensional cell culture conditions. The experiments were then carried out for 24 hours and 5 days of incubation. To remove the scaffold arrays from the bioreactor, the parafilm® and insulating tape shell used to seal the syringes chamber was cut, inside a laminar flow chamber, with a sterile scalpel. The platform was then carefully removed using sterile tweezers. All scaffold arrays were washed with sterile PBS, and immediately analyzed for cell viability.

2.9. Live/Dead analysis

The scaffold arrays retrieved from static and dynamic cell culture were immersed in 2 mL of sterile PBS containing 4 µL of calcein AM (Thermo Fisher Scientific) and 2 µL of propidium iodide (PI, Thermo Fisher Scientific) in the incubator at 37ºC, 5% CO_2, for 30 minutes. The platforms were then analyzed using a fluorescence microscope (Axio Imager M2, Zeiss) with both EGFP/PI filters, at a fixed exposure time of 800 ms. Images were acquired in each individual spot of the platform, and tiled automated high-content image acquisition of whole chips was also performed. After the analysis, the chips were fixed with formalin at 4% (Sigma), at 4ºC, for 24 hours. The semi-quantitative results for calcein AM signal quantification were calculated by dividing the detected intensity in each formulation by the one detected in the protein-free control in each individual time point. Higher ratios represented conditions with higher detected calcein AM signal.

2.10. ALP quatification analysis

After fixation with formalin, the platforms were washed twice with distilled water for 30 minutes, and then immersed in a ALP substract solution (1-Step™ NBT/BCIP Substrate Solution,

ThermoScientific). The reaction took place at 37ºC, for 4 hours. The ALP present in the array was stained in purple. However, a method based on fluorescence analysis was developed to perform rapid and easy analyses of ALP presence in each individual scaffold. Whole platform images were acquired automatically using a fluorescence microscope equipped with a xyz-controlled table, at an exposure time of 60 ms, using the EGFP filter. The whole array and scaffolds have autofluorescence. The places stained for ALP show a non-fluorescent signal, and black spots can be observed in the exact places where ALP is visibly stained. The relative semi-quantitative assessment of ALP per scaffold was performed by increasing the fluorescent signal of the all images equally, and by quantifying the fluorescent signal in each individual scaffold. Scaffolds with lower detected fluorescence were the ones with higher amounts of ALP. The semi-quantitative results for ALP quantification were calculated by dividing the detected intensity in each formulation by the one detected in the protein-free control. Lower ratios represented conditions with higher amount of detected ALP.

References

[1] Custódio, C. A., Alves, C. M., Reis, R. L., & Mano, J. F. (2010). Immobilization of fibronectin in chitosan substrates improves cell adhesion and proliferation. *Journal of tissue engineering and regenerative medicine*, *4*(4), 316-323.

[2] Bancroft, G. N., Sikavitsas, V. I., Van Den Dolder, J., Sheffield, T. L., Ambrose, C. G., Jansen, J. A., & Mikos, A. G. (2002). Fluid flow increases mineralized matrix deposition in 3D perfusion culture of marrow stromal osteoblasts in a dose-dependent manner. *Proceedings of the National Academy of Sciences*, *99*(20), 12600-12605.

Chapter III- Design of a perfusion bioreactor for the high-throughput analysis of combinations of ECM proteins on human mesenchymal stem cells behaviour in dynamic 3D conditions

Screening for the combined influence of protein microenvironments and flow perfusion on the adhesion and osteogenic commitment of mesenchymal stem cells on 3D scaffolds

Diana Lopes[1], Mariana B. Oliveira[1*], João F. Mano[1*]

[1] Department of Chemistry, CICECO – Aveiro Institute of Materials. 3810- Aveiro.

*Corresponding author e-mail: mboliveira@ua.pt, jmano@ua.pt

Abstract

Extracellular matrix (ECM) and cell-cell adhesion mediating proteins have been used to tailor stem cells biological response. Bioinspired biomaterial models that combine different proteins and modulate biophysical aspects co-relatable with the native ECM have been explored for cell expansion and differentiation purposes, both in traditional 2D and closer-to-native niche 3D models. Despite the efforts to understand crucial effects of tissue native niches, biomaterials multivariate arrays often lack the ability to emulate dynamic mechanical aspects that occur in specific biological milieus. Although there is *in vitro* evidence of the adjuvant role of biomimetic flow enabling stem cells to differentiate into different lineages, the screening of rationally designed large arrays of ECM-like 3D matrices stimulated by *in vivo*-mimetic mechanical stimulation is still needed. Here, a system comprising a tailor-made bioreactor and 32 different biomaterial combinations based on the ECM and cell-cell contact proteins is assembled to study mesenchymal stem cells (MSCs) adhesion and alkaline phosphatase (ALP) expression under flow perfusion. The bioreactor was assembled from widely available affordable labware, and permitted retrieved data from 32 experimental conditions in a single experiment. This system may find applications in the development of biomaterials for tissue regeneration and as a disease model platform.

1. Introduction

The poor isolation of the role of individual factors and their respective interplay affecting human tissues healing processes hinders the development of simplified, yet relevant and effective, implantable tissue engineering systems and *in vitro* testing devices [1]. Although bioinspiration can be a powerful source to drive novel biomaterial designs, the rational and controlled testing of compositional variates and their synergic role with other native niche aspects (such as mechanical stimuli) is necessary to successfully combine biology know-how and the design of effective engineering systems [2]. The extracellular matrix (ECM) is accepted as a cornerstone aspect for the maintenance of tissues function and regeneration capability [3], because it is the three-dimensional (3D) matter that embeds cells and, besides providing mechanical cues and physical/structural support to tissues [4], is composed of molecules secreted by the tissues' own cells and regulates

several signaling pathways [3]. Such phenomena involve cell-cell and cell-matrix adhesion mediation proteins, which also have significant roles in the recruitment and binding of growth factors that trigger signaling cascades, commonly involved in cell differentiation signaling [4]. ECM structural and biochemical properties are, in part, dictated by distinct protein contents, which closely relate with defined functional properties of each tissue. One of the most common limitations associated with *in vitro* studies targeting tissue regeneration is the standard 2D culture conditions adopted to test the potential of biomaterials. It has been proven, though, that mimicking the 3D structure of native ECM is of utmost importance to achieve *in vitro*/*in vivo* correlating results [5-7]. As such, to fully understand the complexity dictating regeneration, target aspects of tissue 3D microenvironments need to be identified and emulated *in vitro* [8-11].

Mechanical factors have proven to be a powerful adjuvant of regeneration techniques [12]. Such stimuli occur naturally in human tissues and their application is highly relevant for the development of *in vitro* regeneration strategies [13]. Bioreactors are a useful tool due to their ability to maintain 3D ECM-mimetic constructs under stress [14]. Perfusion bioreactors enhance the homogeneous distribution of the cells inside scaffolds, and provide increased fluid circulation inside the biomaterial structure, providing high oxygen and nutrients availability to cells [15,16]. These systems can be operated in a continuous way, allowing a continuous shear flow stimulation [17,18] and/or consistent medium perfusion through the scaffolds [19]. Bancroft *et al*. described for the first time the use of a perfusion bioreactor for stem cells stimulation while seeded on 3D polymeric scaffolds targeting bone regeneration [20]. Healthy bone remodels in response to mechanical stresses: in the absence of loading bone resorption is increased, while in its presence - felt by cells as flow perfusion through the movement of extracellular fluid radially toward the bone cortex [21] - , bone is known to remodel. Subsequent studies focusing on the role of perfusion on primary bone cells and stem cells behavior have shown increased mineralized matrix deposition in a dose-dependent manner [22-24].

High-throughput screening techniques have allowed the multivariate testing of tissue engineering systems, in a cost- and time-saving manner [25-30]. Targeting bone regeneration and ECM proteins combinations, Dolatshahi-Pirouz *et al.* designed a high-throughput system using type-I collagen hydrogels loaded with combinations of ECM proteins, including fibronectin, vitronectin, laminin and osteocalcin. The effect of pro-osteogenic soluble growth factors on the system was also assessed on the osteogenic differentiation of bone marrow-derived stem cells (MSCs) [31]. Other high-throughput screening platforms were used to assess the osteogenic potential of biomaterials [32-35]. Although these studies provided valuable information about biomaterials composition and

cellular responses, all these experiments were performed under static cell culture conditions. The combined effect of dynamic flow and biomaterials composition on the triggering of cellular responses is still poorly explored, as flow perfusion studies have been limited to experiments using a low number of conditions.

Here, we report the design of a novel device that allowed performing a high-throughput study of the role of 32 ECM proteins combinations along with a continuous perfusion stimulus. Chitosan scaffolds with average diameter of 1 mm were patterned on a poly(dimethylsiloxane) hollow platform. Each individual scaffold was chemically modified with different protein combinations, comprising mixtures of ECM adhesive proteins (fibronectin - F, vitronectin - V and type I collagen - C), cell-cell contact protein (E-cadherin - E) and an enamel ECM protein (amelogenin - A). MSCs were seeded on each individual scaffold, and the role of each protein combination under (i) static conditions and (ii) flow perfusion conditions (at a flow rate of 0.03 mL/min) were assessed for cell adhesion and osteogenic early marker alkaline phosphatase (ALP) expression after 1 and 5 days of cell culture. The dynamic environment was achieved by the construction of a bioreactor, using regular labware materials, by a simple assembly and of low cost construction. The technology reported herein allowed disclosing combined effects of dynamic perfusion environments with combinatorial biomaterial compositions on stem cells differentiation.

2. Materials and methods

2.1. Preparation of hollow arrayed platform

A polydimethylsiloxane (PDMS, Elastomer Kit, Dow Corning) solution in a ratio of 5:1 (PDMS:curing agent) was prepared and degassed under vacuum for 1 hour. A volume of 3 mL was pipetted onto a mold, schematically represented on Figure 1. The molds containing the PDMS solution were again degassed under vacuum for 1 hour, and cured in an oven (Oven/Laboratory dryer, Ecocell 55 Frilabo), at 70ºC for 1 hour. The final platform had approximately 2 mm height and 4 x 4 cm^2 area. The hollowed had 1 mm diameter circular by 1 mm, as represented in Figure 1.

2.2. Microarrayed platforms containing chitosan scaffolds

A 0.9% chitosan (Sigma-Aldrich) solution was prepared using glacial acetic acid (LabChem) at 1% (w/v). A volume of 3 μL was pipetted onto individual wells of the PDMS platform. The platform containing chitosan solution in the wells was frozen at -20ºC for 4 hours, and then freeze-dried (LyoQuest Plus Eco,VWR) overnight. The scaffolds were then neutralized by adding droplets of 1 M sodium hydroxide (NaOH, Eka, AkzoNobel) solution prepared in 70% (%vol) ethanol (Valente

& Ribeiro). After 10 minutes neutralization, they were washed with distilled water for 30 minutes (the water was changed three times). The samples were frozen again at -20ºC for 4 hours and freeze-dried overnight. The platforms were sterilized prior to cell culture by exposure to UV irradiation for 30 minutes in each side of the device (Laminar Flow Cabinet S@femate Eco 1.2m, EuroClone®).

2.3. Preparation of protein solutions

Five human proteins were used in this study: fibronectin (F, Sigma Aldrich), vitronectin (V, Sigma Aldrich), E-cadherin (E, Advanced BioMatrix), collagen type I (C, Sigma Aldrich) and amelogenin (A, Abcam). Solutions of the 5 proteins were prepared by dissolution of the stock solution in a phosphate buffered saline solution (PBS, ThermoScientific). The protein solutions were all diluted to the same final concentration, 0.05 mg/mL. Protein solutions used for immobilization on chitosan scaffolds were prepared with equal proportions of each protein. The final protein solutions had the same final mass of protein.

2.4. Protein immobilization onto miniaturized chitosan 3D scaffolds

Solutions of *N*-Hydroxysuccinimide (NHS, Aldrich Laborspirit) and N-(3-Dimethylaminopropyl)-N′-ethylcarbodiimide hydrochloride (EDC, Sigma (Fluka)) were added to the protein solutions, in a proportion of 1:1:2, (v/v) EDC-NHS:protein solution, accordingly to a previously reported method [36]. EDC and NHS concentrations in the protein solutions were 2 mM and 5 mM, respectively. A volume of 1 μL of each protein mixture was pipetted onto single scaffolds, and left to react for one hour at room temperature. The chips were then washed three times in sterile PBS.

2.5. Cell expansion

Bone Marrow-Derived Mesenchymal Stem Cells (BMSCs) were purchased from LGC Standards, ATCC. The undifferentiated cells were cultured and expanded under basal condition, using Minimum Essential alpha Medium (alpha-MEM, Sigma, USA), supplemented with 10% (v/v) fetal bovine serum (ThermoFisher Scientific) and 1% (v/v) penicillin-streptomycin.

2.6. Cell seeding

A 5000 cells/μL BMSCs suspension was pipetted, at a volume of 1 μL, onto the scaffolds with previously immobilized proteins. Cells were left to attach to the material for 30 min at 37ºC. After this seeding step, the chips were washed once with PBS and incubated (CO_2 Incubator, Model

C170, Binder) at 37ºC, 5% CO_2, in cell supplemented culture medium. Cells were used on passages of P2 to P6, and cell culture medium was exchanged every 2 days.

2.7. Bioreactor assembly

A perfusion bioreactor (figure 1) was assembled to withstand parallel replicates of each individual setup depending solely on the available channels of the peristaltic pump used to perfuse the medium. Each individual set of the bioreactor comprised: (i) one chamber with cell culture medium and capable of holding the hollow PDMS platform containing 3D scaffolds arrays and respective adhered cells, (ii) tubes (Tygon ST R3607, Ismatec, 3.17 mm outer diameter) for medium transportation, (iii) one reservoir of cell culture medium (Schott, 250 mL), and (iv) one peristaltic pump (REGLO digital MS-2/6-160). The tubes were connected to the cell culture medium reservoir through a commercially available screw cap (Screw cap HPLC, GL 45, 4 ports, Duran®) with four ports (3.0 mm diameter). The inlet tube, that drove medium flux to the bioreactor chamber, was inserted inside the cell culture medium; the outlet tube, which recirculated the cell culture medium back to the reservoir, was left about 1 cm above the cell culture medium meniscus. The tubes connecting the medium reservoir and the bioreactor chamber were assembled in the channels of a peristaltic pump. Gas exchange in the cell culture medium was promoted through the assembly of two 0.2 μm sterile cellulose acetate syringe filters (30 mm diameter; Whatmann^{TM}/GE Healthcare) in the two remaining entries of the reservoir cap. The bioreactor chamber was composed of two sterile 20 mL polypropylene syringes (VWR) without the respective pistons. Tubes were connected to the outlet of the syringes, and both syringes were assembled together containing the perforated arrayed platform in between both syringes. The chamber was sealed using sterile Parafilm® and insulation tape on outer layers. All tube-tube and syringe-tube junctions were also sealed with Parafilm® and insulation tape. The schematic representation of the bioreactor assembly is depicted in Figure 1A. A picture of the bioreactor containing two parallel setups, assembled to the same peristaltic pump, can be seen in Figure 1B.

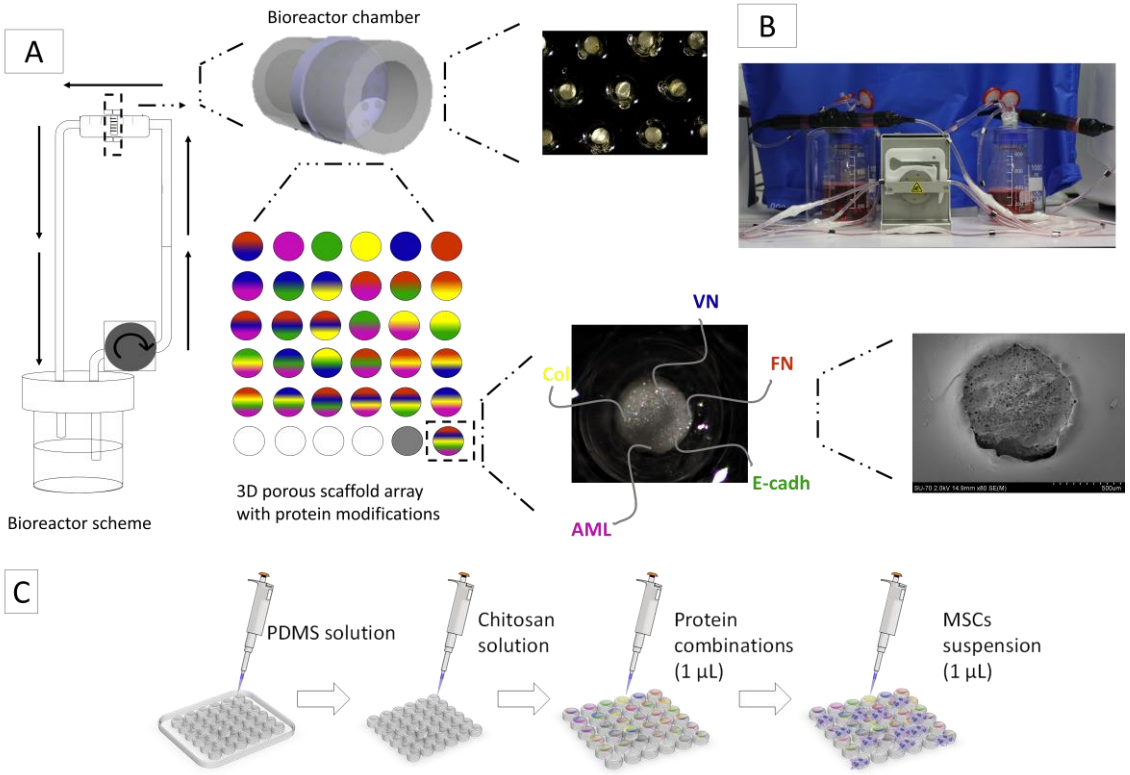

Figure 1- (A) Schematic representation of the assembled bioreactor. (B) Final aspect of an assembled bioreactor, with two experiments taking place at the same time. (C) Schematic modification of the 3D scaffolds in the hollow arrays

2.8. Dynamic and static (control) cell culture

The arrayed platforms containing seeded cells were placed in the bioreactor chamber using sterile tweezers. BMSCs were cultured in the platforms for 24 hours, under static conditions, prior to the assembly in the bioreactor. For static control experiments, cell culture was continued under static conditions inside suspension Petri dishes, with 8 mL supplemented cell culture medium. On dynamic culture, after the complete bioreactor sealing, the bioreactor reservoirs and chambers were placed on an incubator at 37ºC and 5% CO_2. The bioreactor chambers were placed in a horizontal position. The peristaltic pump was set with a flow of 0.68 mL/min. This flow is in a range of 0.2 – 1 mL/min, previously shown by Bancroft *et al*. [37] to induce BMSCs cell growth, proliferation and differentiation into the osteogenic lineage on two-dimensional cell culture conditions. The experiments were then carried out for 24 hours and 5 days of incubation. To remove the scaffold arrays from the bioreactor, the parafilm® and insulating tape shell used to seal the syringes chamber was cut, inside a laminar flow chamber, with a sterile scalpel. The platform was then carefully removed using sterile tweezers. All scaffold arrays were washed with sterile PBS, and immediately analyzed for cell viability.

2.9. Live/Dead analysis

The scaffold arrays retrieved from static and dynamic cell culture were immersed in 2 mL of sterile PBS containing 4 μL of calcein AM (Thermo Fisher Scientific) and 2 μL of propidium iodide (PI, Thermo Fisher Scientific) in the incubator at 37ºC, 5% CO_2, for 30 minutes. The platforms were then analyzed using a fluorescence microscope (Axio Imager M2, Zeiss) with both EGFP/PI filters, at a fixed exposure time of 800 ms. Images were acquired in each individual spot of the platform, and tiled automated high-content image acquisition of whole chips was also performed. After the analysis, the chips were fixed with formalin at 4% (Sigma), at 4ºC, for 24 hours. The semi-quantitative results for calcein AM signal quantification were calculated by dividing the detected intensity in each formulation by the one detected in the protein-free control in each individual time point. Higher ratios represented conditions with higher detected calcein AM signal.

2.10. ALP quantification analysis

After fixation with formalin, the platforms were washed twice with distilled water for 30 minutes, and then immersed in a ALP substract solution (1-Step™ NBT/BCIP Substrate Solution, ThermoScientific). The reaction took place at 37ºC, for 4 hours. The ALP present in the array was stained in purple. However, a method based on fluorescence analysis was developed to perform

rapid and easy analyses of ALP presence in each individual scaffold. Whole platform images were acquired automatically using a fluorescence microscope equipped with a xyz-controlled table, at an exposure time of 60 ms, using the EGFP filter. The whole array and scaffolds have autofluorescence. The places stained for ALP show a non-fluorescent signal, and black spots can be observed in the exact places where ALP is visibly stained. The relative semi-quantitative assessment of ALP per scaffold was performed by increasing the fluorescent signal of the all images equally, and by quantifying the fluorescent signal in each individual scaffold. Scaffolds with lower detected fluorescence were the ones with higher amounts of ALP. The semi-quantitative results for ALP quantification were calculated by dividing the detected intensity in each formulation by the one detected in the protein-free control. Lower ratios represented conditions with higher amount of detected ALP.

3. Results and discussion

3.1. Design of a miniaturized perfusable platform for the characterization of proteins-BMSCs interactions on 3D environments

A PDMS platform with 1 mm diameter hollows and approximately 2 mm height was conceived so 3D miniaturized porous scaffolds could be patterned inside each spot. Unlike most high-throughput devices, which allow physical access to biomaterials from a top view perspective, the homogeneously dispersed biomaterials in the platform developed here were physically accessible from both parallel faces of the platform (up and down sides). The possible control over PDMS crosslinking extent, through the application of tailored curing temperature or amount of curing agent, may allow the production of platforms with diversified stiffness and flexibility, which may allow these platforms to find application in other bioreactor settings, or in more complex design experiments. Also, the height, hollows' diameter and distance may be easily tailored to achieve larger scaffolds models, which may later be used, for example, for *in vivo* implantation.

The miniaturized freeze-dried chitosan scaffolds were covalently modified with 31 combinations of five proteins: fibronectin - F, vitronectin - V, collagen type-I - C, E-cadherin - E, and amelogenin – A; standard EDC/NHS chemistry was applied to promote the covalent reaction of chitosan amines groups with protein carboxylic groups [38]. One protein-free condition (chitosan only) was used as a control for all experiments, leading to a total of 32 total conditions studied per array. Fibronectin, vitronectin and collagen type-I are cell adhesive proteins present in the ECM, and are known to mediate cell-matrix interactions through different membrane integrins [39]. They are present in several human tissues, namely in bone. Amelogenin is an enamel protein that has been positively

associated with the osteogenic commitment of MSCs [40], and is associated with improved bone regeneration [41]. E-cadherin has been used to simulate cell-cell contact on biomaterials surfaces [42]. Initial assays performed with adsorbed protein led to cell aggregation and subsequent cell loss from the surface of the scaffolds after 3 days of cell culture (data not shown). Custódio *et al*. [36] showed that fibronectin immobilized onto chitosan membranes through EDC/NHS chemistry retains its function for a longer period than adsorbed protein.

The combinatorial effect of cell-matrix and cell-cell interactions in osteogenic commitment of stem cells is still poorly studied. Previous studies have focused on the exposure of 3D encapsulated mesenchymal stem cells to ECM adhesive proteins and soluble growth factors [43]. The interplay of other types of proteins, namely cell-cell contact ones, and other aspects of bone physiology as flow perfusion [44] have not been undisclosed yet. The designed platform with an array of chitosan scaffolds allowed the study of several protein combinations simultaneously, in a time, space and cost-effective manner.

3.2. Design of a perfusion bioreactor compatible with high-throughput protein-MSCs interactions study

The arrayed PDMS platforms containing miniaturized chitosan scaffolds were incorporated into a newly designed bioreactor that allowed the continuous perfusion of each individual scaffold with cell culture medium, as shown in Figure 1. The bioreactor was assembled with common, affordable and disposable labware. Sterile disposable polypropylene syringes were used to create the main bioreactor chamber, which accommodated the array platform. Plastic tubes, glass bottles, HPLC screw caps with ports, sterile filters and one peristaltic pump were the additional material needed to develop the final device. The wide availability of these materials, as well as the independence from tailor-made pieces, facilitates the assembly of this device in any laboratory. The bioreactor chamber was easily closed and isolated by using sterile parafilm and insulation tape; the use of micromachined chamber, O-rings and other commonly used accessories was avoided, decreasing costs and handling steps that may culminate in microbial contaminations of the whole setup.

Several perfused chambers containing PDMS perforated arrayed platforms can be cultured in parallel by using commercially available multichannel perfusion pumps. The parallelizable nature of this bioreactor allows for (i) increasing time effectiveness of the experiments, because several independent platforms can be studied in simultaneous, (ii) the study of replicate conditions, as several platforms prepared under the same conditions can be simultaneously assessed using stem cells from controlled batches, and (iii) the effective high-throughput versatility of this system, because a virtually unlimited number of platforms can be studied in parallel. The diameter and

volume capacity of the syringes used to assemble the bioreactor chamber may be modulated, enabling the exposure of a different number of scaffolds to the flow perfusion conditions. This versatility may be useful to increase the number of studied conditions per independent experiments, allowing the retrieval of high amounts of experimental data in single experiments. On the contrary, it may be useful to limit the volume of cell culture medium necessary to perform each experiment, especially in the case of supplemented cell culture media with recombinant molecules, such as growth factors.

The perfusion bioreactor described here was used to test 32 distinct protein-BMSCs combinations under a perfusion flow of 0.68 mL/minute. This flow is in the range of 0.3 to 1 mL/min, previously described by Bancroft *et al.* [45] as effective on the stimulation of the proliferation and induction of the osteogenic differentiation of bone marrow-derived mesenchymal stem cells.

3.3. BMSCs *in vitro* response characterization

The behavior of BMSCs while cultured on the 3D scaffold arrays was characterized using image analysis. The fluorescence signal intensity of calcein AM detected in each individual spot was used as a semi-quantitative indicator of cell number in each biomaterial. Calcein-AM is a fluorescent dye frequently used to evaluate cell viability. This compound enters the cell cytoplasm through the cell membrane, and the calcein-AM bond is broken into the two free compounds by intracellular esterases [46]. Free calcein remains inside viable cells with an integrate membrane, and emits a fluorescent signal (~515 nm), allowing the localization and detection of live cells through fluorescence microscopy methods. ALP is an enzyme which higher activity has been widely reported as an indication of early osteogenic differentiation of MSCs [47]. The loss of autofluorescence from the scaffolds resulting from reacted ALP was used as a semi-quantitative method to with the presence of the protein in each spot. All results were normalized to the protein-free control, and they allowed to infer about the role of additive proteins to the chitosan scaffolds, as well as synergic effects between protein formulations and dynamic flow regime.

3.4. Cell number assessment – Calcein signal quantification

All formulations in the platforms were stained under the same conditions, and later analyzed using fluorescence microscopy with the same exposure time. Single images of each miniaturized spot were acquired for quantification purposes. Nonetheless, automated data acquisition was also possible using a by the Zeiss M2 microscope (Zeiss) with a controlled x-y-z table, as depicted in Figure 2. For image analysis, the area of the scaffolds was selected, and the image was later treated as a “region of interest” (ROI), in which the green fluorescence was measured directly, without any

image treatment, using the ZEN software (Zeiss). The ratio between the calcein signal intensity quantified in the protein-free spot (here, "0") and the calcein signal intensity detected on the protein-containing formulations was calculated for all independent platform experiments (Figure 2). Figure 3 shows some of the conditions that induced promising cell response for calcein, for the different studied timepoints and environments and figure 4 the conditions that had lower cell adhesion. Figure 5 and 6 show the conditions that lead to a higher and lower ALP quantification, respectively. The average ratios can be found as a heatmap in Figure 7, and box plot charts showing medians, minimum and maximum measured values are depicted in Supplementary information-section C.

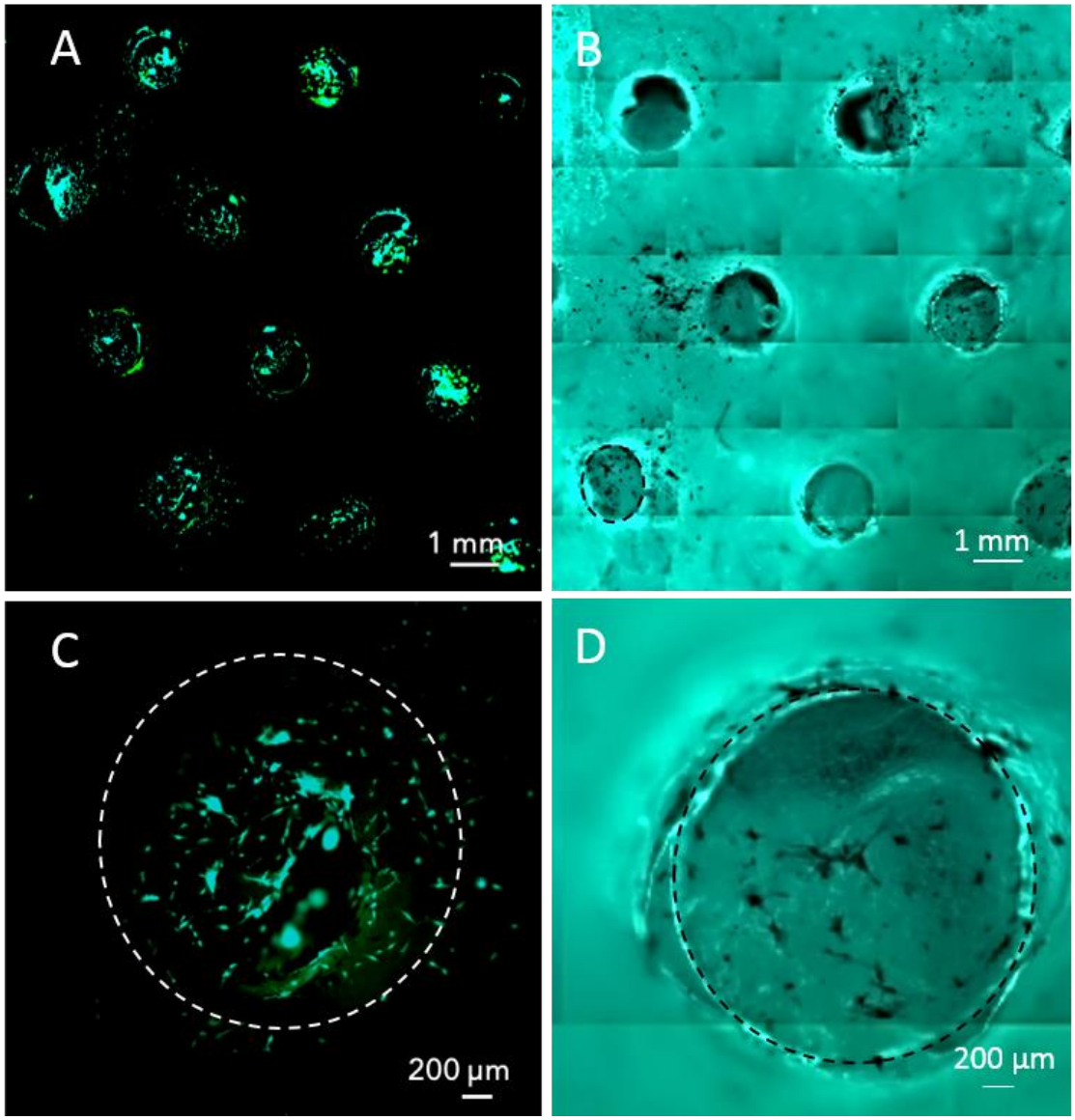

Figure 2- Live/dead and ALP analysis of one array platform under flow perfusion conditions, at day 1. Live cells are stained in green. Cells with ALP are black. A) Tile image acquisition of a part of the platform for Calcein. B) Tile image acquisition of a part of the platform for ALP. C) Amplified view of a single condition for Calcein and D) for ALP

After one day of cell culture under static environment, the E, EC, VE, VA, FC, VEC, FCA, VECA and FECA conditions showed higher calcein fluorescence signal. One of the most recurrent components of these mixtures is the cell-adhesive proteins type I collagen, which is present in the human native ECM [48]. The presence of collagen in the chitosan scaffolds by itself, however, was not enough to trigger a higher cell number in the scaffolds as compared to the protein-free control (Figure 7). Another protein with high predominance in the formulations that elicited higher calcein signal was E-cadherin. E-cadherin is responsible for calcium-dependent cell-cell adhesion [49], and biologically it is known to be present in cells from the epithelial lineage, such as epithelial stem cells (ESCs) [50]. For biomaterial-modification purposes, it has been suggested as a component of biomaterials capable of inducing MSCs proliferation and inhibiting apoptosis [51]. E-cadherin is involved in cell adhesion, proliferation, migration and differentiation [52], and its function is reported to go beyond the establishment of cell-cell junctions; it is known that it takes part in signaling pathways, including the Rho GTPase signaling [53,54]. Here, the modification of chitosan scaffolds with E-cadherin alone was enough to detect a higher calcein signal. When allied with cell adhesion proteins (mainly collagen and vitronectin), E-cadherin showed improved cell adhesion capacity: its conjugation with ECM integrin-mediated adhesive proteins, namely vitronectin, fibronectin and collagen showed also an increased ability to promote cell attachment (Figure 7). The mixture of E-cadherin with ECM adhesive proteins was effective on binary, ternary and quaternary combinations, indicating that the proteins kept their function even in lower proportion in the formulations. In general, initial MSCs adhesion to chitosan scaffolds seems to be enhanced in combinatorial protein combinations, instead of single protein formulations. ECM adhesive proteins and E-cadherin, also in the presence of amelogenin in certain formulations, seem to have a synergistic effect on this phenomenon. After 5 days under static conditions, the platform spots showing increased calcein signal when compared to the protein-free conditions were the following: EA, VC, FEC, FEA, FVE, ECA, VECA, FVEA. As observed at day 1, conditions with the combination of fibronectin, vitronectin, E-cadherin and amelogenin promote a higher number of adherent cells (Figure 7).

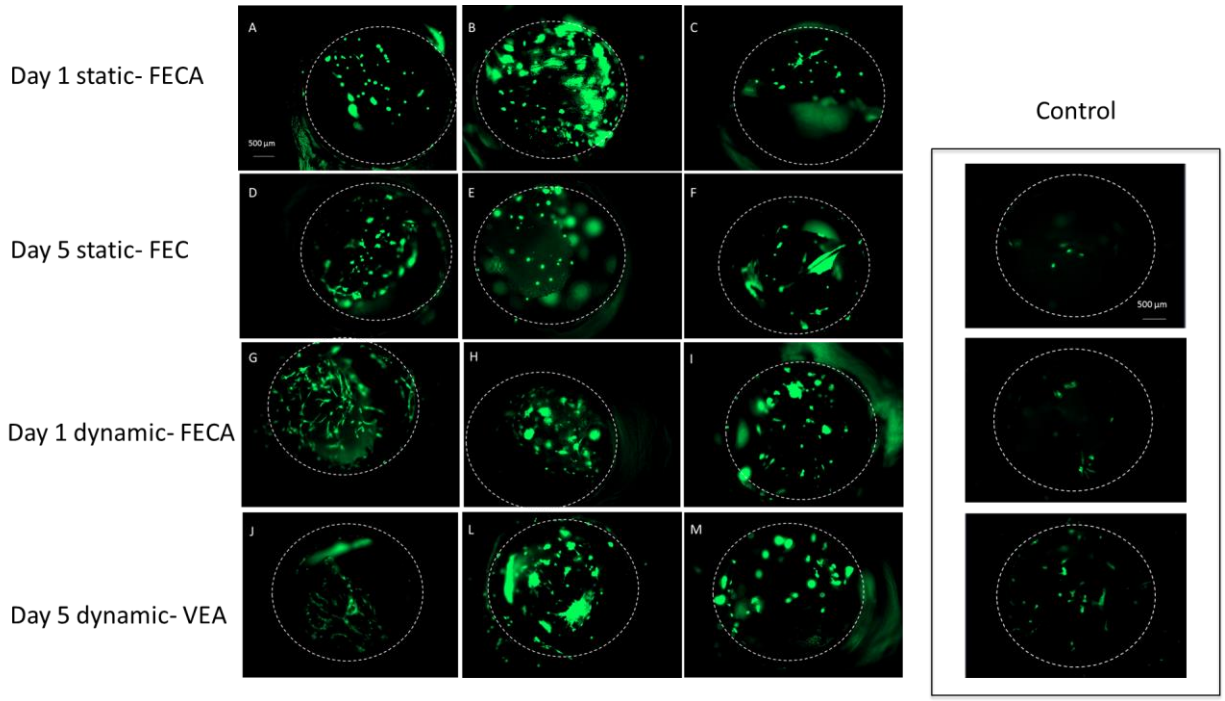

Figure 3- Examples of conditions with higher calcein values, for the different studied environments and timepoints. A),B),C) Replicates of FECA for day 1, static environment. D), E), F) Replicates of FEC for day 5, static environment. G), H), I) Replicates of FECA for day 1, dynamic environment. J), L), M) Replicates of VEA for day 5, dynamic environment.

The analysis of calcein fluorescence intensity for platforms cultured under dynamic conditions (Figure 7) showed that after 1 day of cell culture the conditions with highest calcein signal were F, A, VEC, VEA, FVCA and FECA. The interaction between ECM adhesive proteins, along with E-cadherin and amelogenin, seem to dictate higher cell adhesion. The recurrent presence of amelogenin in these formulations may indicate a correlation between this cell adhesion protein [55] and mechanotransduction phenomenon observed in the dynamic conditions assays. For 5 days of cell culture under dynamic flow stimulation, FA, FC and, FEA, VEC and VEA conditions showed the highest calcein intensity. As observed on previous time points, specific conditions with interactions between adhesive proteins (as fibronectin and vitronectin) with E-cadherin and amelogenin promote a higher number of adhered live cells in the scaffolds. Statistical analysis of effects of each individual protein or groups of proteins on the calcein signal detected in each scaffold shows that on all time points amelogenin shows a general positive effect on the number of cells present in the scaffold (Figure 7). After 5 days of static culture, the presence of amelogenin and E-cadherin in the protein mixtures are the major driving forces for increased cell number (Figure 7). In opposition to static culture, the effect of vitronectin alone on protein formulations was robust enough to be shown on the effect list, both for day 1 and day 5 of cell culture (Figure 7).

Interactions of E-cadherin and adhesive proteins also contributed significantly for increased cell number.

Although the integrin-mediated interactions between cells and ECM proteins as fibronectin, vitronectin and type I collagen are widely reported [56], the specific cell interaction mechanism of amelogenin is still yet not fully understood. A study made by Kirkham *et al*., showed that amelogenin interacts with cells through the cell membrane [57]. Lokappa *et al*. later showed that this interaction was made at the membrane phospholipids [58], and that the N-terminal of amelogenin may be the responsible for this interaction, since enamel malformations of the amelogenin's N-terminal in the disease amelogenesis imperfecta (AI) lead to a faulty interaction between cells and the protein [59]. The improving effect of amelogenin on the cell number in the scaffolds, both on static and dynamic culture conditions, may be related to its adhesive interactions with cells through mechanisms that differ from the other proteins. Another possibility to explain the adjuvant effect observed relies on the possible configurational and structural alterations that amelogenin may induce in other proteins present in the mixtures used to modify the surface of the chitosan scaffolds. Protein-protein interactions have been reported to induce structural and functional changes in different combinations of proteins [60-62]. The interaction of each protein with different cell types also dictates the role of each protein. In a particular example, Heydarkhan-Hagvall *et al*. reported that scaffolds coated in vitronectin showed higher cell adhesion rates of embryonic stem cells, other than those coated in fibronectin, on a 3D environment [63].

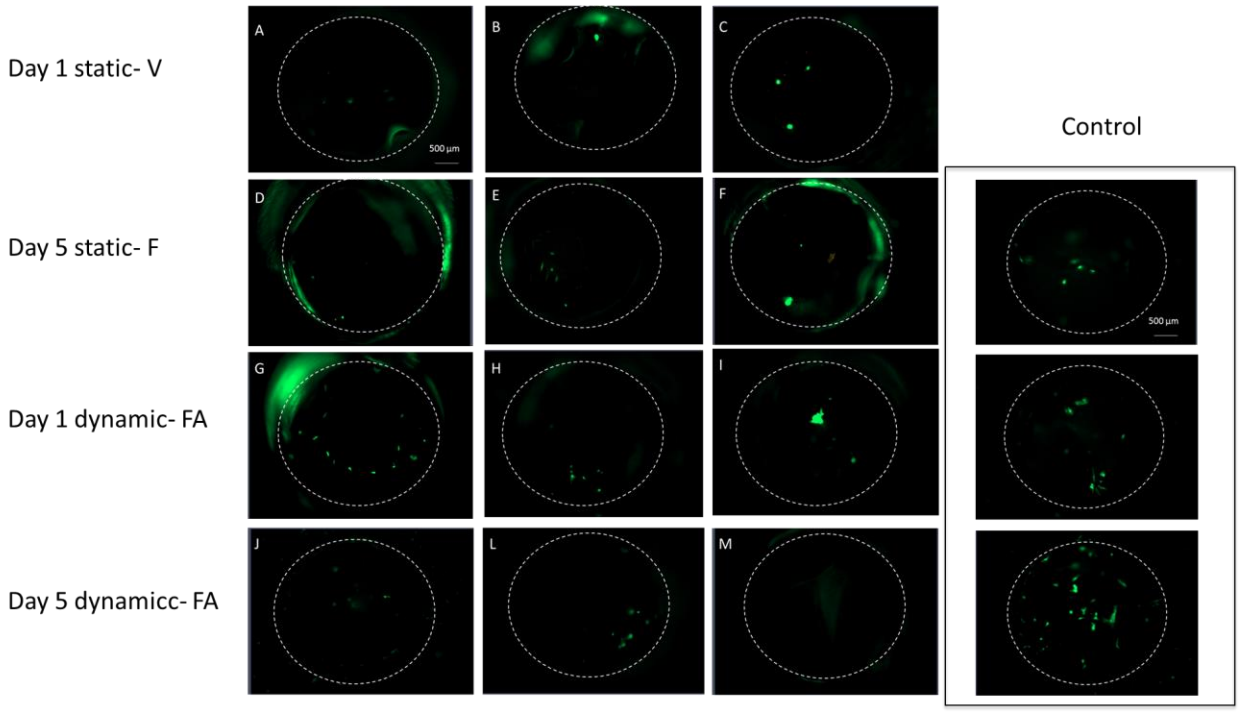

Figure 4- Examples of conditions with lower calcein values, for the different studied environments and timepoints. A),B),C) Replicates of V for day 1 static environment. D), E), F) Replicates of F for day 5 static environment. G),H), I) Replicates of FA for day 1 dynamic environment. J), L), M) Replicates of A for day 5, dynamic environment.

3.5. ALP quantification analysis

An innovative approach was developed to assess the amount of ALP in each individual spot of the platforms. After the enzyme-substrate reaction, ALP in the platforms was stained with a purple color. Under the green fluorescent beam used to analyze calcein signal, the ALP stained cells (figure 2 D) emit a non-fluorescent signal, while by increasing the lamp's exposure time, the chitosan scaffolds showed green autofluorescence (Figure 7). Pictures of the whole platform were acquired using a fixed exposure time, and the lowering of the fluorescence values in each spot was inversely correlated with the presence of ALP.

After one day of static cell culture, the conditions that led higher ALP quantification were: FV, FE, VA, ECA and FVEC. For this timepoint and under static conditions, none of the proteins alone led to an increase on ALP quantification (Figure 7). Amelogenin has been reported as capable of inducing osteogenic differentiation of embryonic stem cells through the activation of the Wtn pathway [64]. E-cadherin was also high predominant in the mixtures triggering higher ALP levels (Figure 7). Despite different mesenchymal cadherins are known to mediate bone formation in vivo [65], the role of E-cadherin has not been disclosed yet. Despite its role as an individual protein has not induced an increase in ALP quantification, here we observed that its mixture with ECM adhesive proteins as fibronectin and collagen has led to improved effects.

After 5 days of cell culture under static conditions, ALP quantification levels were, in general, lower than at day 1, as compared to the protein-free control (Figure 7). The major positive effects on ALP quantification were observed in the conditions FV and FVA. For this timepoint, fibronectin clearly has a pronounced effect, as it appears several times on the conditions leading ALP increased expression. Tang *et al.*, verified that human plasma fibronectin coated on scaffold surfaces enhanced odontoblast-like cells proliferation, differentiation and mineralization [66]. Conditions containing both vitronectin and amelogenin also led increased ALP quantification. Despite type I collagen has previously shown adjuvant effects on osteogenic differentiation of MSCs [67], this effect was not observed here, which may be related to the porous scaffolds system developed here, and/or with the interactions established in the protein mixtures leading to functional loss of each individual protein. Despite their ability to trigger osteogenic differentiation of BMSCs, different proteins have been proved to act through different pathways. For example, adult mesenchymal stem cells were grown in 2D substrates treated with adsorbed vitronectin and type I collagen [68], and osteogenesis on vitronectin correlated with enhanced focal adhesion formation, the activation of focal adhesion kinase (FAK) and paxillin, and the diminished activation of extracellular signal-regulated kinase (ERK) and phosphatidylinositol-3 kinase (PI3K) pathways. On type-I collagen, the osteogenic differentiation occurred with lower focal adhesion formation, reduced activation of FAK and paxillin, and increased activation of ERK and PI3K). The simultaneous stimulation of different pathways in combinatorial biomaterial formulations, along with 3D culture conditions (in opposition to conventionally used 2D platforms) may hide the cues to explain the complex results observed in the studied array.

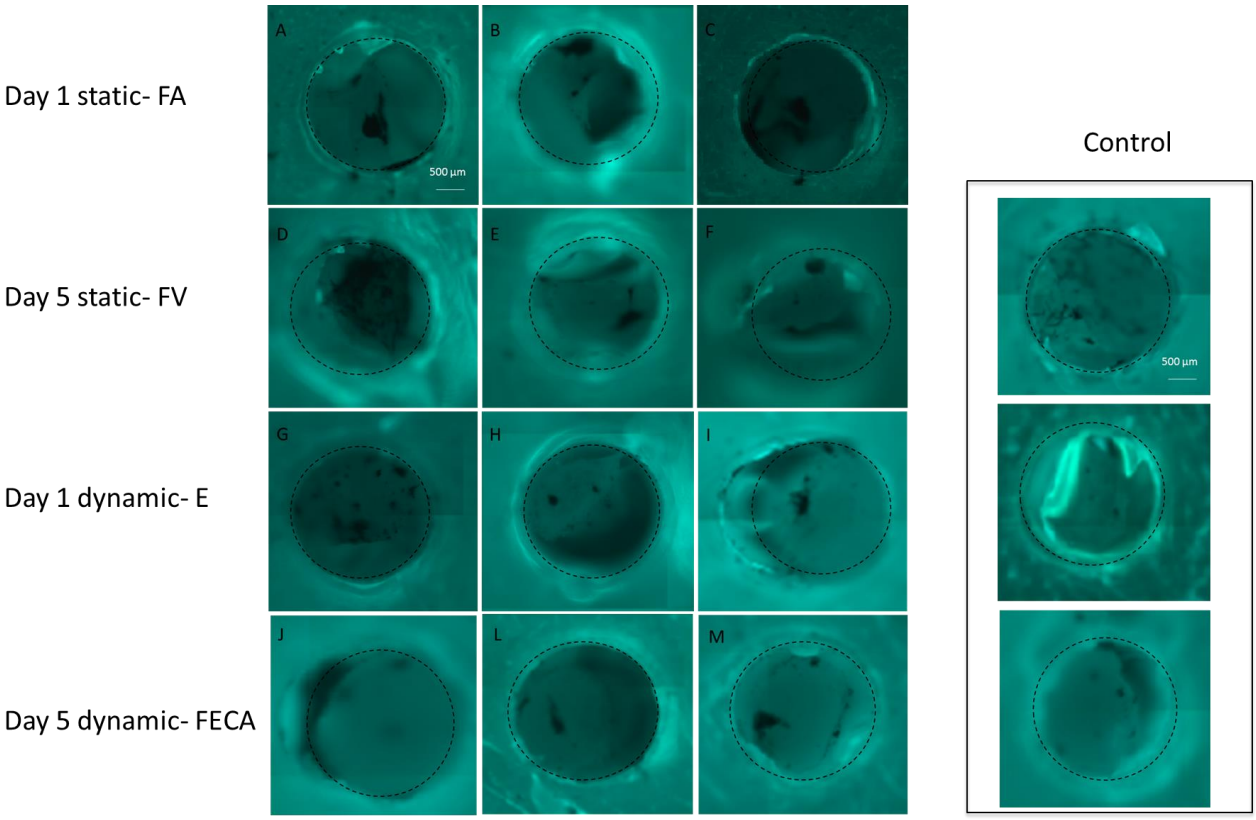

Figure 5- Examples of conditions with higher ALP values, for the different studied environments and timepoints. A),B),C) Replicates of FA for day 1, static environment. D), E), F) Replicates of FV for day 5, static environment. G), H), I) Replicates of E for day 1, dynamic environment. J), L), M) Replicates of FECA for day 5, dynamic environment.

After one day under flow, the formulations A, E, FA, VC, ECA, and FECA led the highest expressions of ALP (Figure 7). Here, the effect of amelogenin alone and in combination with other conditions is visible, and was statistically detected on the effect assessment (Figure 7). Conditions that promoted the highest osteogenic pathway response indicate a possibly positive effect of collagen in coordination with amelogenin in the dynamic flow conditions, in opposition to the static culture setup, in which collagen did not show any adjuvant effect on the osteogenic induction of BMSCs. The relevance of amelogenin in this process is evidenced by, for example, analyzing cell response to EC composition, which rendered one of the lowest ALP quantification ratios, in opposition to the highly ALP inducing ECA.

The adjuvant and predominant effect of amelogenin and some of its combinations is visible after 5 days of cell culture in the bioreactor (Figure 7). The highest ALP quantification was observed for VE. FA, ECA, FVA and FECA conditions. In a similar way to the observations on static conditions, fibronectin in combination with other proteins shows a relevant role after 5 days of cell culture, in opposition to day 1, in which its presence does not lead the increase of ALP quantification. In accordance with the results from day 1, the presence of amelogenin in the hit spotted formulations is observed, and this trend is visible in the effect list (Figure 7).

In summary, after one day of cell culture higher ALP quantification seems to be dictated, both on static and dynamic conditions, by formulations rich in either amelogenin and/or E-cadherin in combination with ECM proteins as fibronectin and vitronectin. At day 5, the role of fibronectin is more preponderant, which is probably associated with the ability of this protein to induce cell adhesion and proliferation when covalently immobilized in chitosan substrates [36]. On the dynamic culture conditions, the presence of amelogenin seems to promote an enhanced pre-osteogenic commitment, indicating a possible synergic relationship between the protein and the applied flow.

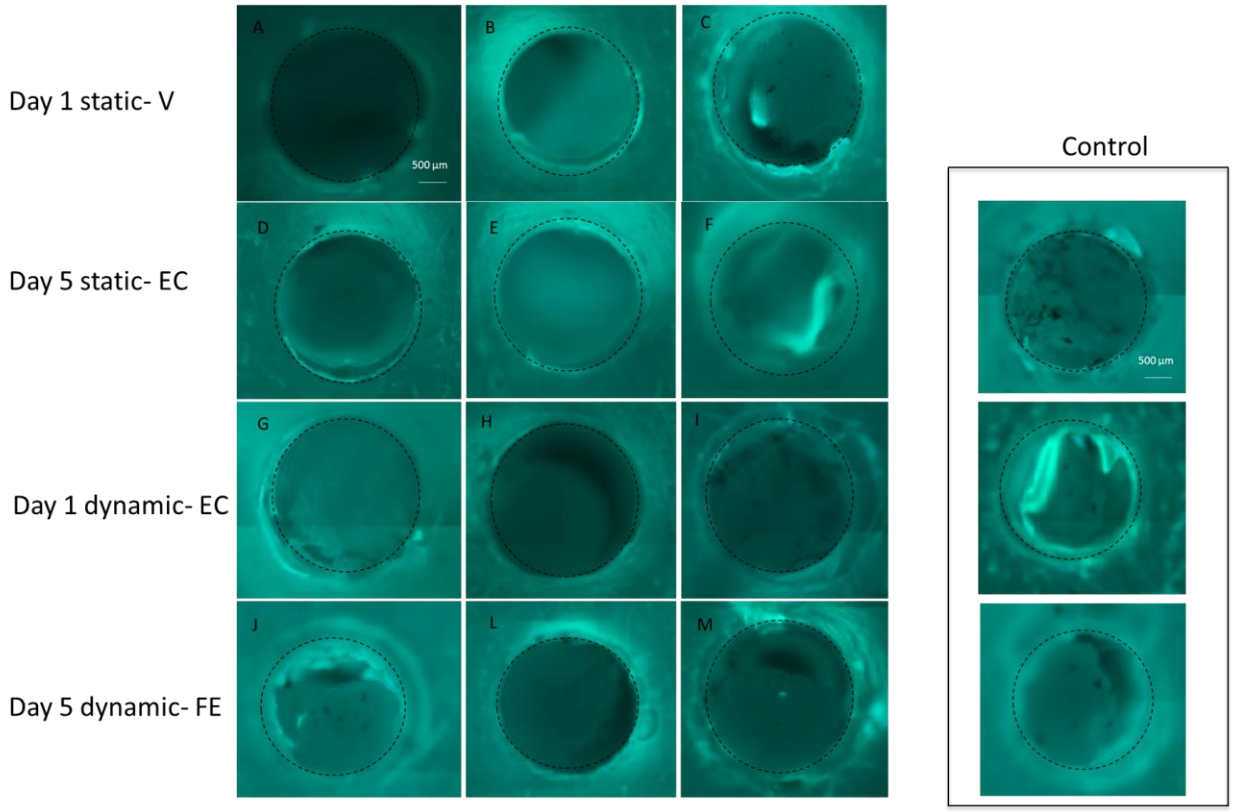

Figure 6- Examples of conditions with lower ALP values, for the different studied environments and timepoints. A),B),C) Replicates of V for day 1, static environment. D), E), F) Replicates of EC for day 5, static environment. G), H), I) Replicates of EC for day 1, dynamic environment. J), L), M) Replicates of FE for day 5, dynamic environment.

The comparison of the ALP quantification trends (Figure 7) with the normalized ALP ratios by calcein intensity ratios (Figure 7) shows similar results. This indicates that, in the case of the analysis conducted in this study, the total cell amount in each biomaterial did not influence the comparative amounts of ALP and, consequently, the respective analysis.

Biomaterials application targeting rapid tissue regeneration may benefit from improved cell number attached to the scaffold, along with a rapid triggering of a desired differentiation response. The identification of biomaterials formulations and culture conditions that withstand both high cell

number and high ALP quantification are shown in Supplementary Information, section A and B, inside the dashed rectangles. A threshold of calcein ratio above 1.1 and ALP below 0.8 (given that lower ALP ratios correspond to higher amount of the protein present in the scaffolds) was set. Flow perfused conditions allowed assessing a higher number of formulations enabling both high cell number and ALP activity, as compared to static conditions.

The technology developed in this work allowed the affordable and rapid assessment of protein-BMSCs interactions under static and dynamic flow perfusion conditions. Although protein combinations and cell suspensions were dispensed in each individual platform spot manually, the flat configuration and precise array position of the 3D scaffolds in the developed chips make them compatible with the use of automatized robots, commonly used in the preparation of high-throughput devices. The analysis performed in this work was based on the assessment of early markers of osteogenesis. We envision the further use of the developed system on long-term studies targeting osteogenesis and other tissue regeneration pathways. The versatility of the method makes it a potential device for the future testing of more protein and surface-modification molecules, along with other cell types, driving new discoveries in the fields of biomaterials development for tissue regeneration, drug discovery and disease models design.

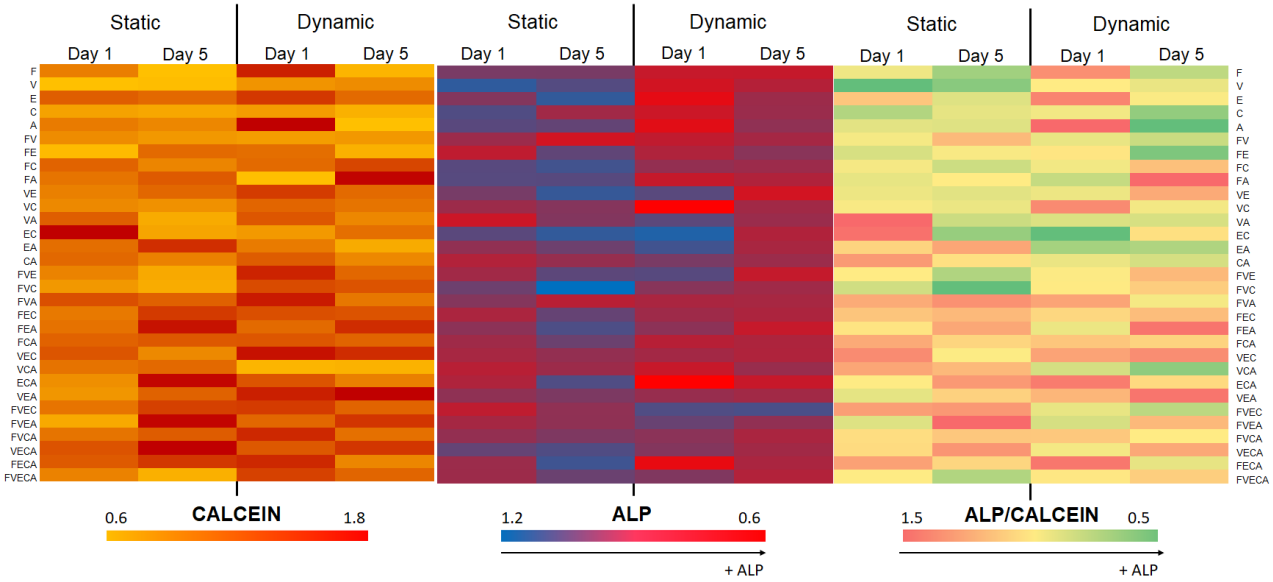

Figure 7- Heatmaps of the average ratio values obtained by dividing the acquired calcein AM or ALP signal for each condition by the value of the protein-free condition in that time point (here, condition "0"). Higher values are represented in red. All values were acquired in sets of 5 to 8 independent experiments. Due to sample loss that occurred mainly after formalin fixation of the platforms (probably due to shrinkage of the chitosan scaffolds and subsequent loss to the medium), all samples represented in this heatmap are the mean value of, at least, 3 scaffolds and, maximum, 8 scaffolds.

4. Conclusion

In this work, an arrayed hollow platform was developed to incorporate 3D porous biomaterials that were modified with 32 different combinations of proteins present in bone ECM, cell-cell contact junctions and enamel. The interactions between each individual biomaterial combination and human BMSCs were tested under static cell culture conditions, as well as under a dynamic perfusion flow. A bioreactor was assembled using widely available labware, based mainly on disposable plastic material. Two syringes were assembled to work as a chamber in which the developed arrayed platform was incorporated. The system allowed different flows, controlled through the movement of a peristaltic pump. A high-throughput study was performed by testing 32 biomaterials-cells interactions in a single platform. By using a programmable table with controlled xyz positioning, images of the whole platforms could be acquired in a single automatized step. Image analysis was used to establish comparisons of cell number in each biomaterial condition, and of the expression of an osteogenic early marker: alkaline phosphatase. The results obtained in this study, with 64 conditions assessed per time point, allowed concluding about the importance of multiprotein formulations on the triggering of cell adhesion and osteogenic commitment of BMSCs. Hit-spotted formulations leading to high cell adhesion and ALP quantification consisted of mixtures of ECM-adhesive proteins (namely, fibronectin, type-I collagen and vitronectin) with cell-cell contact proteins (E-cadherin) and, with a high consistency, amelogenin. Cell response and hit-spotted biomaterial formulations were dependent on the application of flow perfusion on the whole system, and the application of dynamic flow drove cells to express high amounts of ALP as compared to protein-free conditions. This proof-of-concept work allowed proving the potential of the developed high-throughput system to test cell-biomaterials interactions under flow. Each component of the bioreactor shows versatility, which opens the possibility of testing a higher number of biomaterials per independent experiment, patterning biomaterials with distinct shapes and sized (by modulating the hollows of the array platform), and exposing the system to distinct flows. Also, different cell types (and even co-culture setups) and biomaterials combinations are amenable to be tested in future works using this platform, which makes it an appealing tool to be used for novel breakthrough discoveries on healthcare fields, including regenerative medicine, drug discovery and disease model/organ-on-a-chip development.

References

[1] Eming, S. A., Martin, P., & Tomic-Canic, M. (2014). Wound repair and regeneration: mechanisms, signaling, and translation. *Science translational medicine*, *6*(265), 265sr6-265sr6.
[2] Harrison, R. H., St-Pierre, J. P., & Stevens, M. M. (2014). Tissue engineering and regenerative medicine: a year in review. *Tissue Engineering Part B: Reviews*, *20*(1), 1-16.
[3] Xue, M., & Jackson, C. J. (2015). Extracellular matrix reorganization during wound healing and its impact on abnormal scarring. *Advances in wound care*, *4*(3), 119-136.
[4] Frantz, C., Stewart, K. M., & Weaver, V. M. (2010). The extracellular matrix at a glance. *J Cell Sci*, *123*(24), 4195-4200.
[5] Bosi, S., Rauti, R., Laishram, J., Turco, A., Lonardoni, D., Nieus, T., ... & Ballerini, L. (2015). From 2D to 3D: novel nanostructured scaffolds to investigate signalling in reconstructed neuronal networks. *Scientific Reports (Nature Publisher Group)*, *5*, 9562.
[6] Gupta, N., Liu, J. R., Patel, B., Solomon, D. E., Vaidya, B., & Gupta, V. (2016). Microfluidics-based 3D cell culture models: Utility in novel drug discovery and delivery research. *Bioengineering & Translational Medicine*, *1*(1), 63-81.
[7] Hinderer, S., Layland, S. L., & Schenke-Layland, K. (2016). ECM and ECM-like materials—biomaterials for applications in regenerative medicine and cancer therapy. *Advanced drug delivery reviews*, *97*, 260-269.
[8] Zhang, Y., Chopp, M., Zhang, Z. G., Katakowski, M., Xin, H., Qu, C., ... & Xiong, Y. (2016). Systemic administration of cell-free exosomes generated by human bone marrow derived mesenchymal stem cells cultured under 2D and 3D conditions improves functional recovery in rats after traumatic brain injury. *Neurochemistry international*.
[9] Kang, H. W., Lee, S. J., Ko, I. K., Kengla, C., Yoo, J. J., & Atala, A. (2016). A 3D bioprinting system to produce human-scale tissue constructs with structural integrity. *Nature biotechnology*, *34*(3), 312-319.
[10] Kamei, K. I., Koyama, Y., Tokunaga, Y., Mashimo, Y., Yoshioka, M., Fockenberg, C., ... & Chen, Y. (2016). Characterization of Phenotypic and Transcriptional Differences in Human Pluripotent Stem Cells under 2D and 3D Culture Conditions. *Advanced healthcare materials*, *5*(22), 2951-2958.
[11] González, S., Mei, H., Nakatsu, M. N., Baclagon, E. R., & Deng, S. X. (2016). A 3D culture system enhances the ability of human bone marrow stromal cells to support the growth of limbal stem/progenitor cells. *Stem cell research*, *16*(2), 358-364
[12] Ozcivici, E., Luu, Y. K., Adler, B., Qin, Y. X., Rubin, J., Judex, S., & Rubin, C. T. (2010). Mechanical signals as anabolic agents in bone. *Nature Reviews Rheumatology*, *6*(1), 50-59.
[13] Wang, X., Nyman, J. S., Dong, X., Leng, H., & Reyes, M. (2010). Fundamental biomechanics in bone tissue engineering. *Synthesis Lectures on Tissue Engineering*, *2*(1), 1-225.
[14] Vetsch, J. R., Müller, R., & Hofmann, S. (2015). The evolution of simulation techniques for dynamic bone tissue engineering in bioreactors. *Journal of tissue engineering and regenerative medicine*, *9*(8), 903-917.
[15] Ding, M., Henriksen, S. S., Wendt, D., & Overgaard, S. (2016). An automated perfusion bioreactor for the streamlined production of engineered osteogenic grafts. *Journal of Biomedical Materials Research Part B: Applied Biomaterials*, *104*(3), 532-537.
[16] Carpentier, B., Layrolle, P., & Legallais, C. (2011). Bioreactors for bone tissue engineering. *The International journal of artificial organs*, *34*(3), 259-270.
[17] de Peppo, G. M., Marcos-Campos, I., Kahler, D. J., Alsalman, D., Shang, L., Vunjak-Novakovic, G., & Marolt, D. Engineering bone tissue substitutes from human induced

pluripotent stem cells. *Proceedings of the National Academy of Sciences*, *110*(21), 8680-8685 (2013).
[18] Zydney, A. L. (2016). Continuous downstream processing for high value biological products: a review. *Biotechnology and bioengineering*, *113*(3), 465-475.
[19] Yeatts, A. B., & Fisher, J. P. (2011). Bone tissue engineering bioreactors: dynamic culture and the influence of shear stress. *Bone*, *48*(2), 171-181.
[20] Bancroft, G. N., Sikavitsas, V. I., & Mikos, A. G. (2003). Design of a flow perfusion bioreactor system for bone tissue-engineering applications. *Tissue engineering*, *9*(3), 549-554.
[21] Sikavitsas, V. I., Temenoff, J. S., & Mikos, A. G. (2001). Biomaterials and bone mechanotransduction. *Biomaterials*, *22*(19), 2581-2593.
[22] Bancroft, G. N., Sikavitsas, V. I., Van Den Dolder, J., Sheffield, T. L., Ambrose, C. G., Jansen, J. A., & Mikos, A. G. (2002). Fluid flow increases mineralized matrix deposition in 3D perfusion culture of marrow stromal osteoblasts in a dose-dependent manner. *Proceedings of the National Academy of Sciences*, *99*(20), 12600-12605.
[23] Sikavitsas, V. I., Bancroft, G. N., Holtorf, H. L., Jansen, J. A., & Mikos, A. G. (2003). Mineralized matrix deposition by marrow stromal osteoblasts in 3D perfusion culture increases with increasing fluid shear forces. *Proceedings of the National Academy of Sciences*, *100*(25), 14683-14688.
[24] Datta, N., Pham, Q. P., Sharma, U., Sikavitsas, V. I., Jansen, J. A., & Mikos, A. G. (2006). In vitro generated extracellular matrix and fluid shear stress synergistically enhance 3D osteoblastic differentiation. *Proceedings of the National Academy of Sciences of the United States of America*, *103*(8), 2488-2493.
[25] Abraham, V. C., Taylor, D. L., & Haskins, J. R. (2004). High content screening applied to large-scale cell biology. *Trends in biotechnology*, *22*(1), 15-22.
[26] Guillemot, F., Souquet, A., Catros, S., Guillotin, B., Lopez, J., Faucon, M., ... & Chabassier, P. (2010). High-throughput laser printing of cells and biomaterials for tissue engineering. *Acta biomaterialia*, *6*(7), 2494-2500.
[27] Beachley, V. Z., Wolf, M. T., Sadtler, K., Manda, S. S., Jacobs, H., Blatchley, M. R., ... & Elisseeff, J. H. (2015). Tissue matrix arrays for high-throughput screening and systems analysis of cell function. *Nature methods*, *12*(12), 1197-1204.
[28] Nam, K. H., Smith, A. S., Lone, S., Kwon, S., & Kim, D. H. (2015). Biomimetic 3D tissue models for advanced high-throughput drug screening. *Journal of laboratory automation*, *20*(3), 201-215.
[29] Oliveira, M. B., & Mano, J. F. (2014). High-throughput screening for integrative biomaterials design: exploring advances and new trends. *Trends in biotechnology*, *32*(12), 627-636.
[30] Chen, Y. Y., Silva, P. N., Syed, A. M., Sindhwani, S., Rocheleau, J. V., & Chan, W. C. (2016). Clarifying intact 3D tissues on a microfluidic chip for high-throughput structural analysis. *Proceedings of the National Academy of Sciences*, *113*(52), 14915-14920.
[31] Dolatshahi-Pirouz, A., Nikkhah, M., Gaharwar, A. K., Hashmi, B., Guermani, E., Aliabadi, H., ... & Khademhosseini, A. (2014). A combinatorial cell-laden gel microarray for inducing osteogenic differentiation of human mesenchymal stem cells. *Scientific reports*, *4*.
[32] Desbordes, S. C., Placantonakis, D. G., Ciro, A., Socci, N. D., Lee, G., Djaballah, H., & Studer, L. (2008). High-throughput screening assay for the identification of compounds regulating self-renewal and differentiation in human embryonic stem cells. *Cell stem cell*, *2*(6), 602-612.
[33] Oliveira, M. B., & Mano, J. F. (2014). High-throughput screening for integrative biomaterials design: exploring advances and new trends. *Trends in biotechnology*, *32*(12), 627-636.

[34] Zhou, Q., Kühn, P. T., Huisman, T., Nieboer, E., Van Zwol, C., Van Kooten, T. G., & Van Rijn, P. (2015). Directional nanotopographic gradients: a high-throughput screening platform for cell contact guidance. *Scientific reports*, *5*, 16240.
[35] Simon, C. G., & Lin-Gibson, S. (2011). Combinatorial and High-Throughput Screening of Biomaterials. *Advanced materials*, *23*(3), 369-387.
[36] Custódio, C. A., Alves, C. M., Reis, R. L., & Mano, J. F. (2010). Immobilization of fibronectin in chitosan substrates improves cell adhesion and proliferation. *Journal of tissue engineering and regenerative medicine*, *4*(4), 316-323.
[37] Bancroft, G. N., Sikavitsas, V. I., Van Den Dolder, J., Sheffield, T. L., Ambrose, C. G., Jansen, J. A., & Mikos, A. G. (2002). Fluid flow increases mineralized matrix deposition in 3D perfusion culture of marrow stromal osteoblasts in a dose-dependent manner. *Proceedings of the National Academy of Sciences*, *99*(20), 12600-12605.
[38] Olbrich, K. C., Andersen, T. T., Blumenstock, F. A., & Bizios, R. (1996). Surfaces modified with covalently-immobilized adhesive peptides affect fibroblast population motility. *Biomaterials*, *17*(8), 759-764.
[39] Reticker-Flynn, N. E., Malta, D. F. B., Winslow, M. M., Lamar, J. M., Xu, M. J., Underhill, G. H., ... & Bhatia, S. N. (2012). A combinatorial extracellular matrix platform identifies cell-extracellular matrix interactions that correlate with metastasis. *Nature communications*, *3*, 1122.
[40] Tanimoto, K., Huang, Y. C., Tanne, Y., Kunimatsu, R., Michida, M., Yoshioka, M., ... & Tanne, K. (2012). Amelogenin enhances the osteogenic differentiation of mesenchymal stem cells derived from bone marrow. *Cells Tissues Organs*, *196*(5), 411-419.
[41] Haze, A., Taylor, A. L., Haegewald, S., Leiser, Y., Shay, B., Rosenfeld, E., ... & Gibson, C. W. (2009). Regeneration of bone and periodontal ligament induced by recombinant amelogenin after periodontitis. *Journal of cellular and molecular medicine*, *13*(6), 1110-1124.
[42] Yang, K., Lee, J., & Cho, S. W. (2012). Engineering biomaterials for feeder-free maintenance of human pluripotent stem cells. *International journal of stem cells*, *5*(1), 1.
[43] Hou, L., Coller, J., Natu, V., Hastie, T. J., & Huang, N. F. (2016). Combinatorial extracellular matrix microenvironments promote survival and phenotype of human induced pluripotent stem cell-derived endothelial cells in hypoxia. *Acta biomaterialia*, *44*, 188-199.
[44] Nii, M., Lai, J. H., Keeney, M., Han, L. H., Behn, A., Imanbayev, G., & Yang, F. (2013). The effects of interactive mechanical and biochemical niche signaling on osteogenic differentiation of adipose-derived stem cells using combinatorial hydrogels. *Acta biomaterialia*, *9*(3), 5475-5483.
[45] Bancroft, G. N., Sikavitsas, V. I., Van Den Dolder, J., Sheffield, T. L., Ambrose, C. G., Jansen, J. A., & Mikos, A. G. (2002). Fluid flow increases mineralized matrix deposition in 3D perfusion culture of marrow stromal osteoblasts in a dose-dependent manner. *Proceedings of the National Academy of Sciences*, *99*(20), 12600-12605.
[46] Weston SA, Parish CR. *New fluorescent dyes for lymphocyte migration studies. Analysis by flow cytometry and fluorescence microscopy.* J Immunol Methods *1990; 133: 87–97.*
[47] Prins, H. J., Braat, A. K., Gawlitta, D., Dhert, W. J., Egan, D. A., Tijssen-Slump, E., ... & Martens, A. C. (2014). In vitro induction of alkaline phosphatase levels predicts in vivo bone forming capacity of human bone marrow stromal cells. *Stem cell research*, *12*(2), 428-440.
[48] Frantz, C., Stewart, K. M., & Weaver, V. M. (2010). The extracellular matrix at a glance. *J Cell Sci*, *123*(24), 4195-4200.
[49] Gumbiner BM. Regulation of cadherin-mediated adhesion in morphogenesis. Nat Rev Mol Cell Biol. 2005;6:622–634.

[50] Eastham AM, Spencer H, Soncin F, Ritson S, Merry CL, Stern PL, Ward CM. Epithelial-mesenchymal transition events during human embryonic stem cell differentiation. Cancer Res. 2007;67:11254–62.
[51] Zhang, Y., Mao, H., Qian, M., Hu, F., Cao, L., Xu, K., ... & Yang, J. (2016). Surface modification with E-cadherin fusion protein for mesenchymal stem cell culture. *Journal of Materials Chemistry B*, *4*(24), 4267-4277.
[52] Li, L., Bennett, S. A., & Wang, L. (2012). Role of E-cadherin and other cell adhesion molecules in survival and differentiation of human pluripotent stem cells. *Cell adhesion & migration*, *6*(1), 59-73.
[53] Pieters, T., & Van Roy, F. (2014). Role of cell–cell adhesion complexes in embryonic stem cell biology. *J Cell Sci*, *127*(12), 2603-2613.
[54] Cavallaro, U., & Christofori, G. (2004). Cell adhesion and signalling by cadherins and Ig-CAMs in cancer. *Nature Reviews Cancer*, *4*(2), 118-132.
[55] Hoang, A. M., Klebe, R. J., Steffensen, B., Ryu, O. H., Simmer, J. P., & Cochran, D. L. (2002). Amelogenin is a cell adhesion protein. *Journal of dental research*, *81*(7), 497-500.
[56] Flaim, C. J., Chien, S., & Bhatia, S. N. (2005). An extracellular matrix microarray for probing cellular differentiation. *Nature methods*, *2*(2), 119-125.
[57] Kirkham, J., Andreev, I., Robinson, C., Brookes, S. J., Shore, R. C., & Smith, D. A. (2006). Evidence for direct amelogenin–target cell interactions using dynamic force spectroscopy. *European journal of oral sciences*, *114*(s1), 219-224.
[58] Lokappa, S. B, Balakrishna Chandrababu, K., Dutta, K., Perovic, I., Spencer Evans, J., & Moradian-Oldak, J. (2015). Interactions of amelogenin with phospholipids. *Biopolymers*, *103*(2), 96-108.
[59] Lokappa, S. B., Chandrababu, K. B., & Moradian-Oldak, J. (2015). Tooth enamel protein amelogenin binds to ameloblast cell membrane-mimicking vesicles via its N-terminus. *Biochemical and biophysical research communications*, *464*(3), 956-961.
[60] Prigodich, R. V., & Vesely, M. R. (1997). Characterization of the complex between bovine osteocalcin and type I collagen. *Archives of Biochemistry and Biophysics*, *345*(2), 339-341.
[61] Dzamba, B. J., Wu, H., Jaenisch, R., & Peters, D. M. (1993). Fibronectin binding site in type I collagen regulates fibronectin fibril formation. *The Journal of cell biology*, *121*(5), 1165-1172.
[62] Charonis, A. S., Tsilibary, E. C., Yurchenco, P. D., & Furthmayr, H. (1985). Binding of laminin to type IV collagen: a morphological study. *The Journal of cell biology*, *100*(6), 1848-1853.
[63] Heydarkhan-Hagvall, S., Gluck, J. M., Delman, C., Jung, M., Ehsani, N., Full, S., & Shemin, R. J. (2012). The effect of vitronectin on the differentiation of embryonic stem cells in a 3D culture system. *Biomaterials*, *33*(7), 2032-2040.
[64] Warotayanont, R., Frenkel, B., Snead, M. L., & Zhou, Y. (2009). Leucine-rich amelogenin peptide induces osteogenesis by activation of the Wnt pathway. *Biochemical and biophysical research communications*, *387*(3), 558-563.
[65] Di Benedetto, A., Watkins, M., Grimston, S., Salazar, V., Donsante, C., Mbalaviele, G., ... & Civitelli, R. (2010). N-cadherin and cadherin 11 modulate postnatal bone growth and osteoblast differentiation by distinct mechanisms. *J Cell Sci*, *123*(15), 2640-2648.
[66] Tang, J., & Saito, T. (2017). Human plasma fibronectin promotes proliferation and differentiation of odontoblast. *Journal of Applied Oral Science*, *25*(3), 299-309.
[67] Salasznyk, R. M., Williams, W. A., Boskey, A., Batorsky, A., & Plopper, G. E. (2004). Adhesion to vitronectin and collagen I promotes osteogenic differentiation of human mesenchymal stem cells. *BioMed Research International*, *2004*(1), 24-34.

[68] Kundu, A. K., & Putnam, A. J. (2006). Vitronectin and collagen I differentially regulate osteogenesis in mesenchymal stem cells. *Biochemical and biophysical research communications*, *347*(1), 347-357.

Chapter IV- Conclusion and future work

1. Conclusion and Future work

The high complexity associated with bone's physiology is an important factor driving the difficult regeneration of this tissue after trauma. Bone defects are capable of healing by themselves on small-scale injuries. However, severe damage leading to defects with diameters larger than 2 cm show impaired self-healing ability. To achieve fully functional bone regenerative therapies, it is necessary to understand the individual distinctive biological processes and structural features of bone biology. Bone must not be overlooked as a dynamic and complex system in which highly regulated crosstalk occurs. In this study, we suggest the development of a perfusion bioreactor for the high-throughput analysis of several protein combinations and their effect on human BMSCs response under flow perfusion. The studied protein array comprised bone ECM, cell-cell contact junction and enamel proteins. We created an arrayed hollow platform, developed to incorporate 3D porous biomaterials modified with 32 different combinations of proteins. A bioreactor was assembled using widely available labware, based mainly on disposable plastic material. Two syringes were assembled to work as a chamber in which the developed arrayed platform was incorporated. The system is versatile to allow the application of different flows, simply controlled through the movement of a peristaltic pump. By using a programmable table with controlled xyz positioning, images of the whole platforms could be acquired in a single automatized step. Image analysis was used to establish comparisons of cell number in each biomaterial condition, and of the expression of an osteogenic early marker: alkaline phosphatase (ALP). The results obtained in this study, with 64 conditions assessed per time point allowed concluding about the importance of multiprotein formulations on the triggering of cell adhesion and osteogenic commitment of BMSCs, and their combined role with dynamic flow stimulation. Hit-spotted formulations leading to high cell adhesion and ALP quantification consisted of mixtures of ECM-adhesive proteins (namely, fibronectin, type-I collagen and vitronectin) with cell-cell contact proteins (E-cadherin) and, with a high consistency, amelogenin. Cell response was highly dependent on the application of flow perfusion, which showed synergic effects with different protein combinations.

The present work has shown the potential of a novel perfusion bioreactor for applications on healthcare field, namely for the development of regenerative medicine *in vitro* systems. The developed system provided the implementation of high-throughput analysis of biomaterials targeting bone regeneration through the use of bone and enamel microenvironment proteins. The most relevant novelty associated with the developed device is associated with the ability to locally induce mechanical stimuli to cells cultured in 3D scaffolds, in a mimetic approach of the native bone flow perfusion. *In vivo*, such mechanical stimulation is crucial to enable healthy bone maintenance and to induce healing. Despite the potential of the developed

system for tissue regeneration, the work developed here was a proof-of-concept targeting osteogenic stem cell differentiation on early time points (5 days of cell culture). The application of this system for time points targeting mature osteogenic differentiation, such as 21 days of cell culture, is a needed step in future work. Moreover, only chitosan 3D scaffolds were studied, as well as fixed proportions of proteins. The potential of this high-throughput platform for the study of larger arrays of biomaterials (processed with different techniques and with distinct features), cells and co-cultures under perfused environment, with different perfusion flows in discrete/continuous mode, would allow to prove the full potential of the developed bioreactor as a high-throughput versatile device for tissue regeneration, or even for disease model studies.

Supplementary information

A- Detailed fluorescence images of calcein, for the several conditions and timepoints

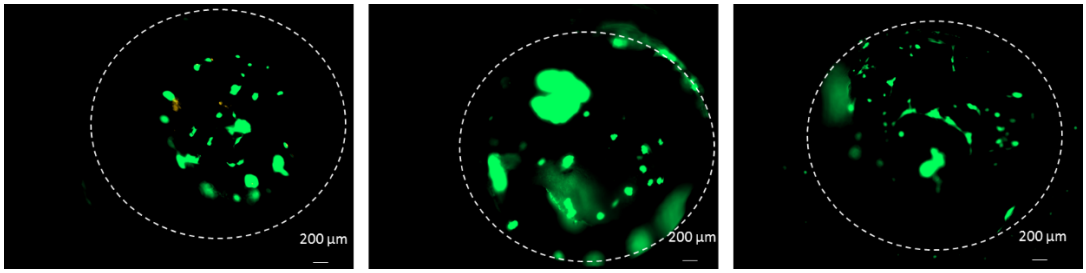

Figure A1- Fluorescence of 3 replicates of E condition for static environment day 1

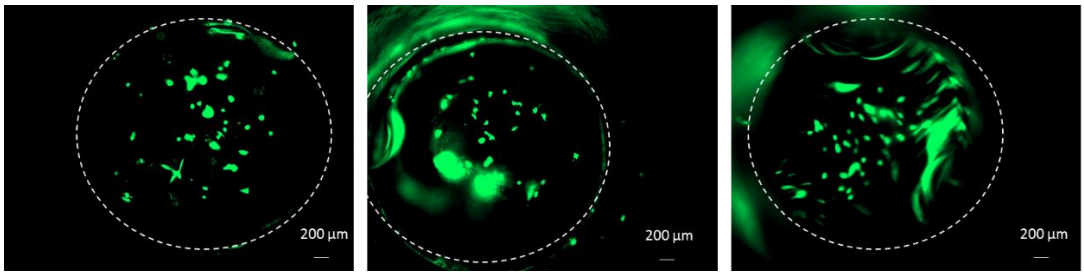

Figure A2- Fluorescence of 3 replicates of FC condition for static environment day 1

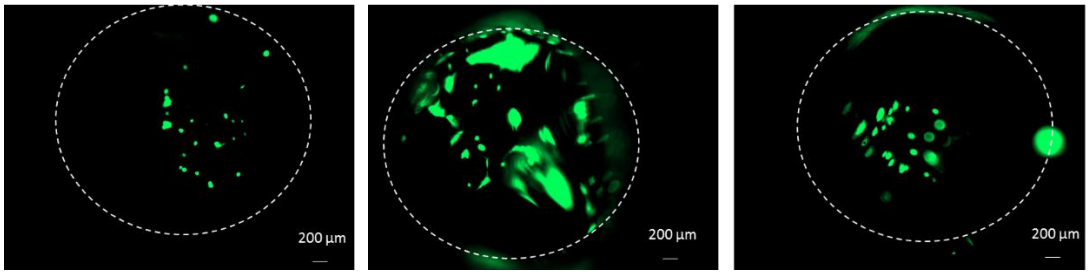

Figure A3- Fluorescence of 3 replicates of VE condition for static environment day 1

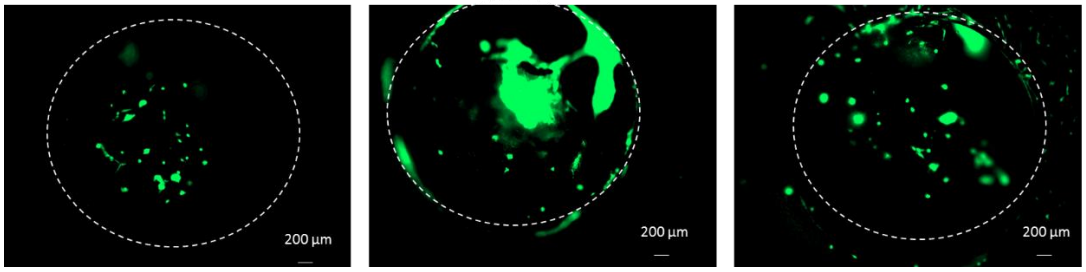

Figure A4- Fluorescence of 3 replicates of VA condition for static environment day 1

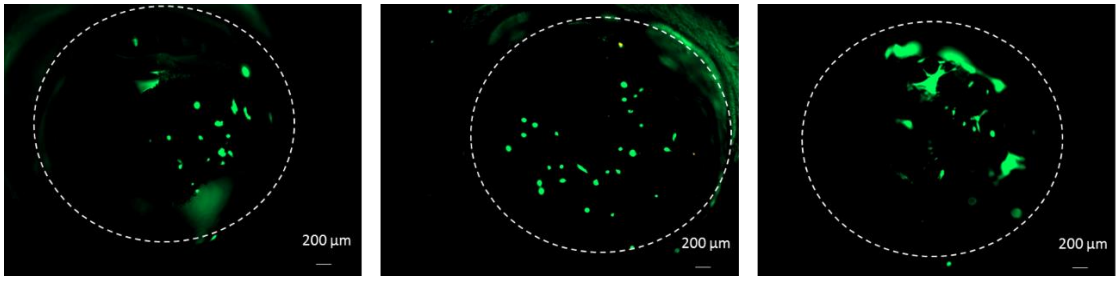

Figure A5- Fluorescence of 3 replicates of EC condition for static environment day 1

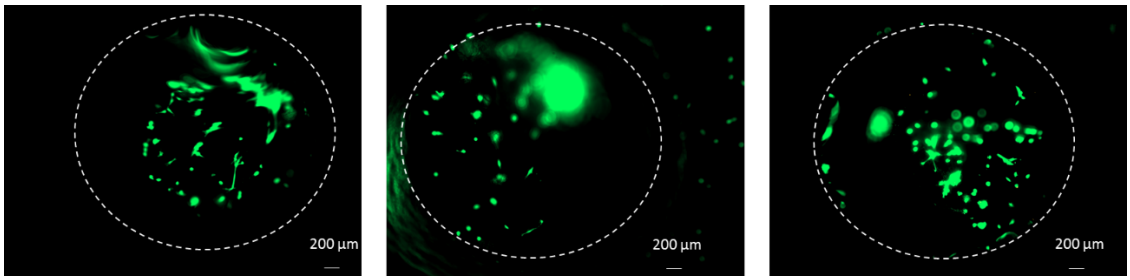

Figure A6- Fluorescence of 3 replicates of FCA condition for static environment day 1

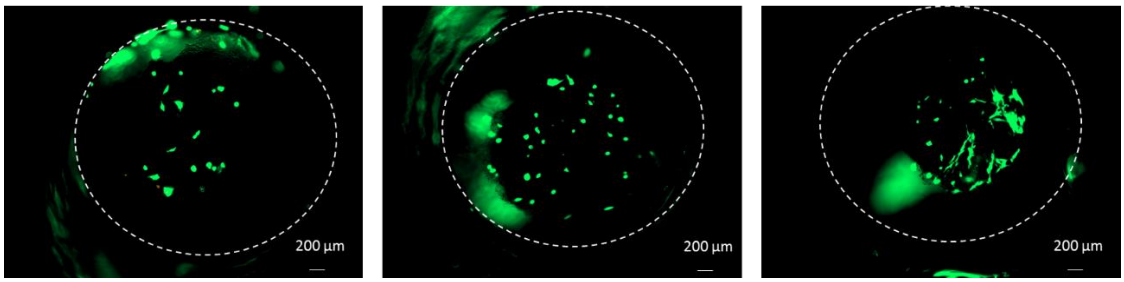

Figure A7- Fluorescence of 3 replicates of VEC condition for static environment day 1

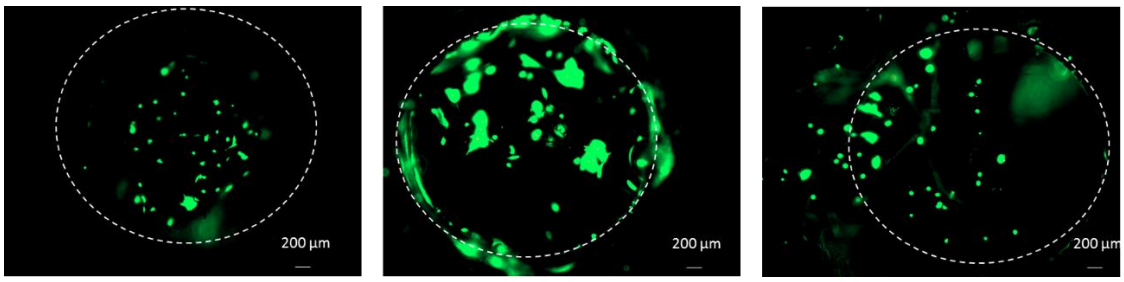

Figure A8- Fluorescence of 3 replicates of VECA condition for static environment day 1

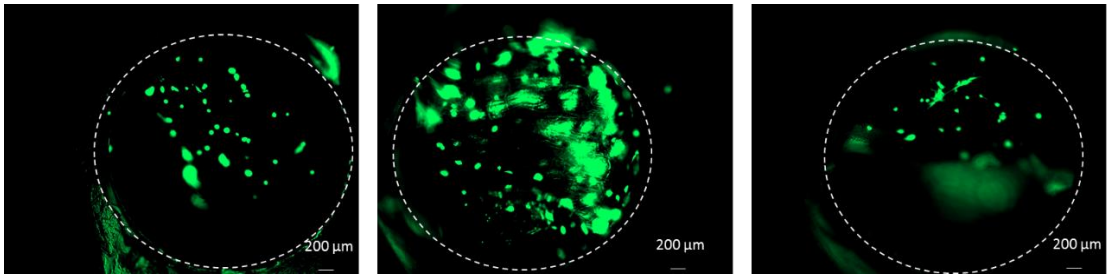

Figure A9- Fluorescence of 3 replicates of FECA condition for static environment day 1

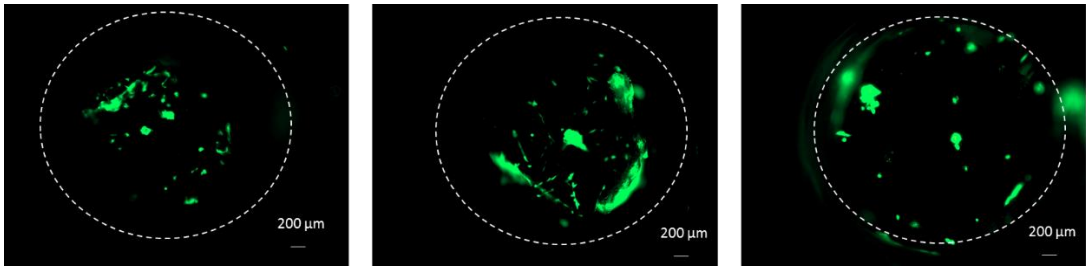

Figure A10- Fluorescence of 3 replicates of VC condition for static environment day 5

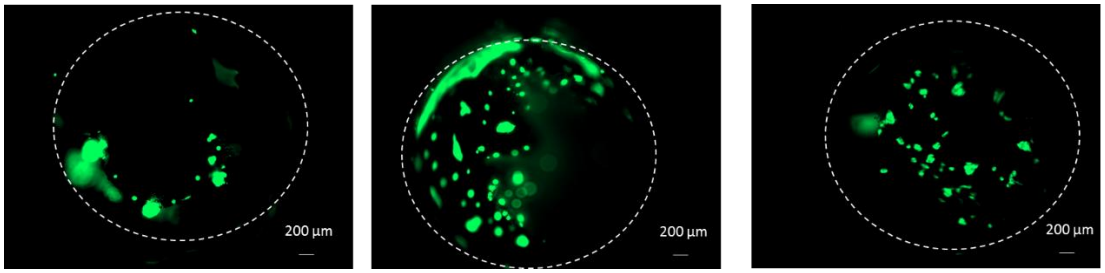

Figure A11- Fluorescence of 3 replicates of EA condition for static environment day 5

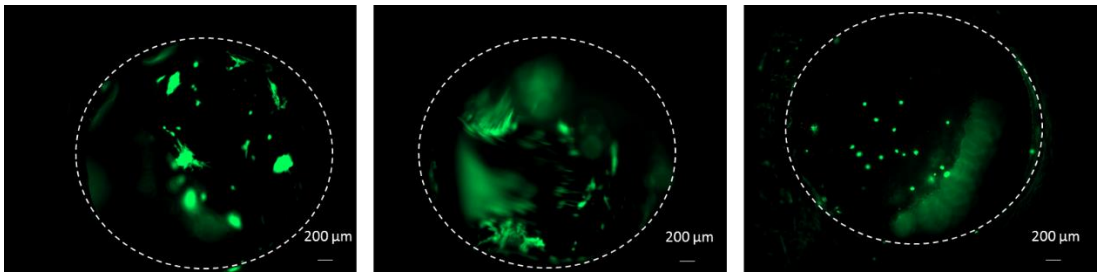

Figure A12- Fluorescence of 3 replicates of FVE condition for static environment day 5

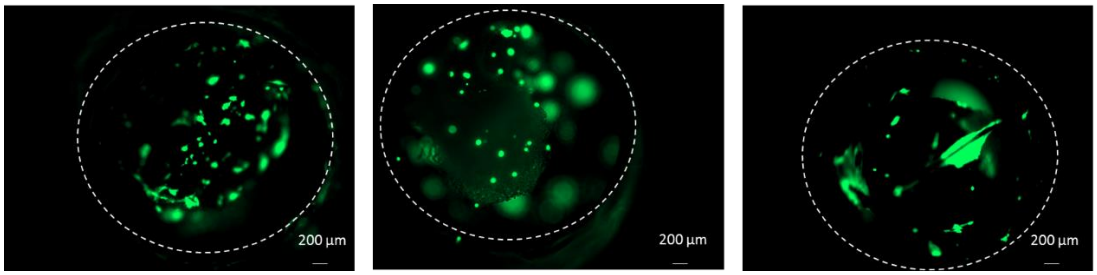

Figure A13- Fluorescence of 3 replicates of FEC condition for static environment day 5

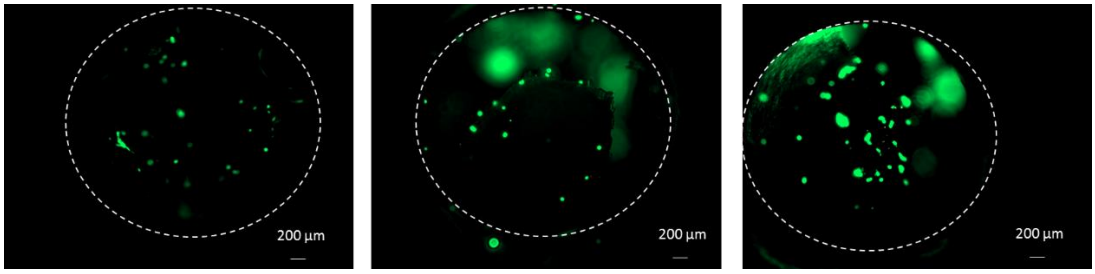

Figure A14- Fluorescence of 3 replicates of FEA condition for static environment day 5

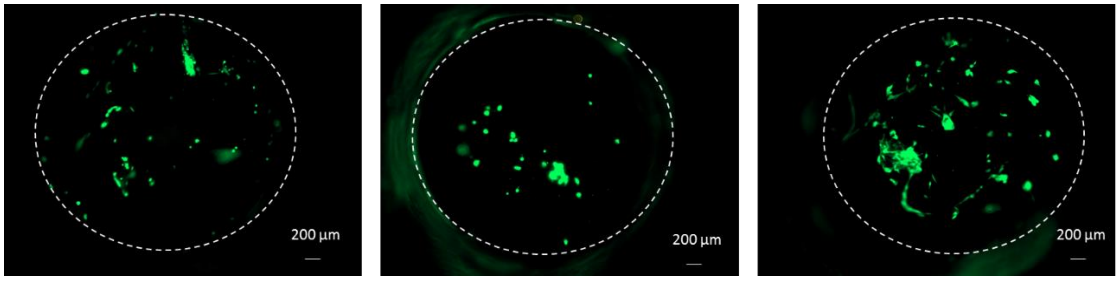

Figure A15- Fluorescence of 3 replicates of ECA condition for static environment day 5

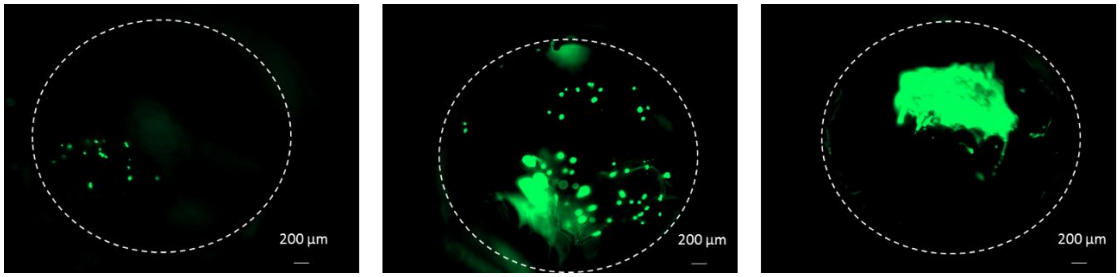

Figure A16- Fluorescence of 3 replicates of FVEA condition for static environment day 5

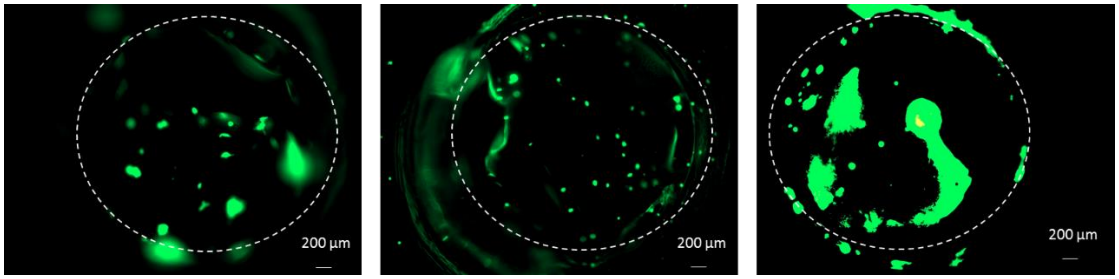

Figure A17- Fluorescence of 3 replicates of VECA condition for static environment day 5

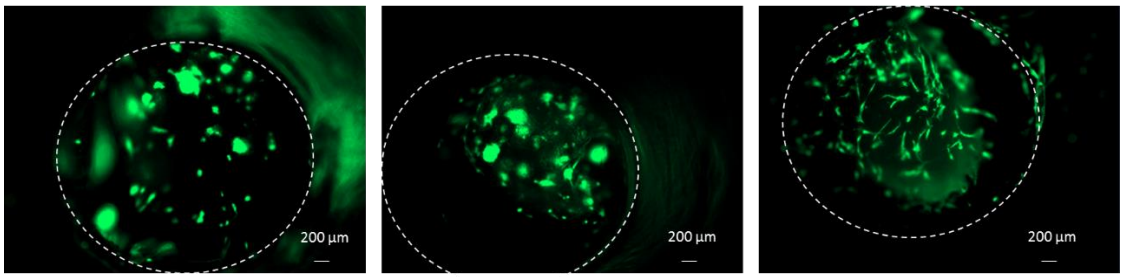

Figure A18- Fluorescence of 3 replicates of FECA condition for dynamic environment day 1

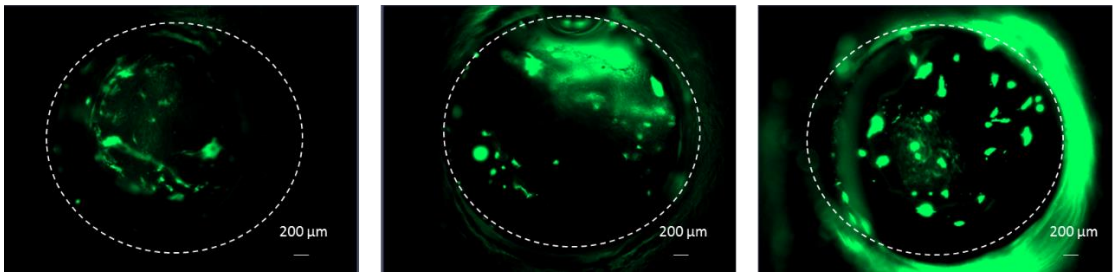

Figure A19- Fluorescence of 3 replicates of VECA condition for dynamic environment day 1

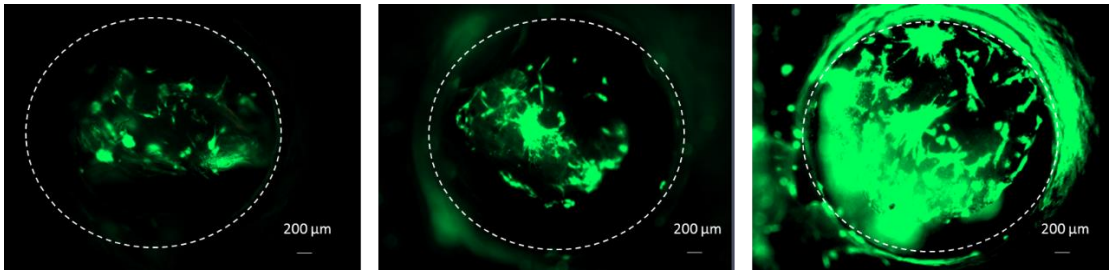

Figure A20- Fluorescence of 3 replicates of FVCA condition for dynamic environment day 1

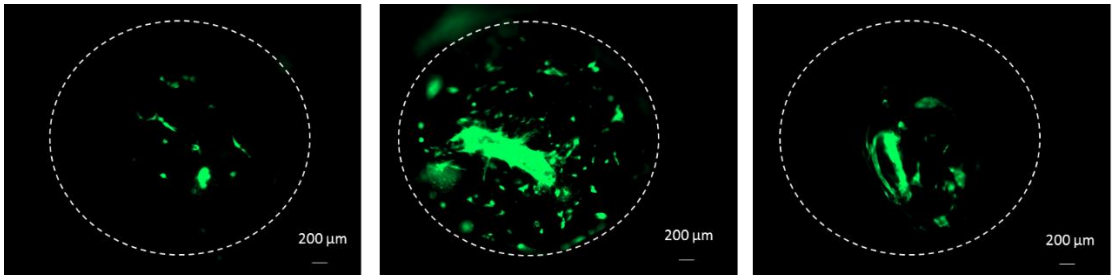

Figure A21- Fluorescence of 3 replicates of FA condition for dynamic environment day 5

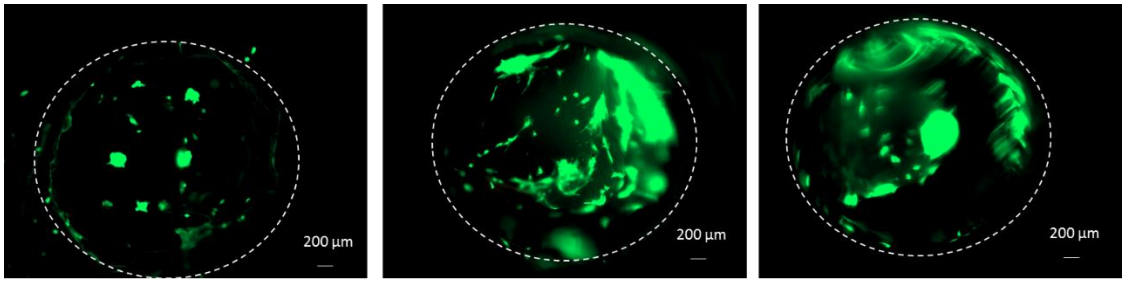

Figure A22- Fluorescence of 3 replicates of VE condition for dynamic environment day 5

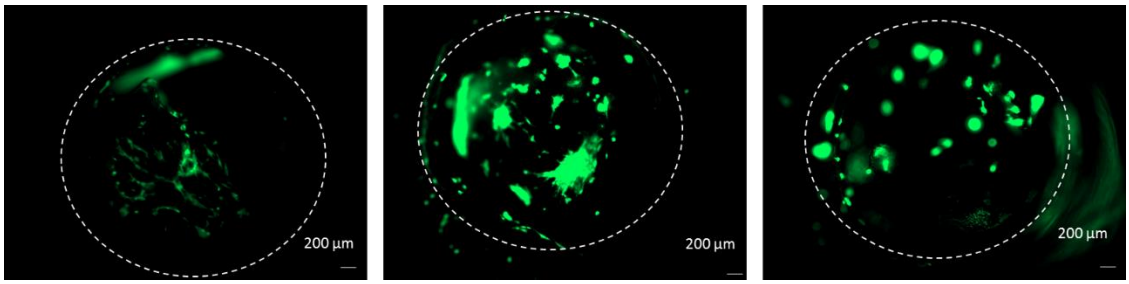

Figure A23- Fluorescence of 3 replicates of VEA condition for dynamic environment day 5

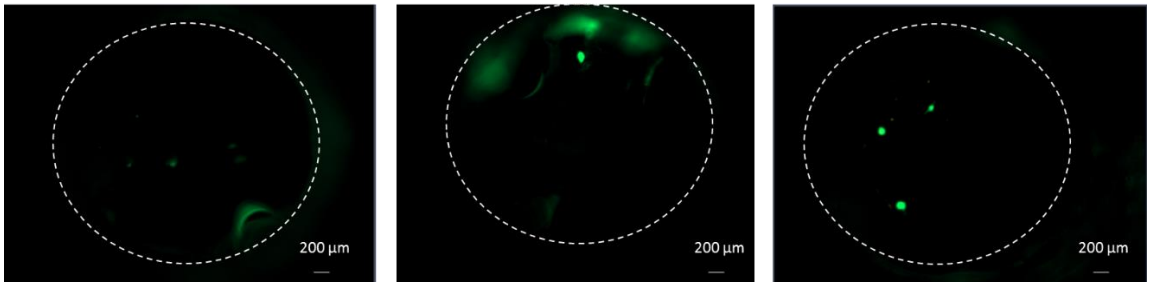

Figure A 24- Fluorescence of 3 replicates of V condition for static environment day 1

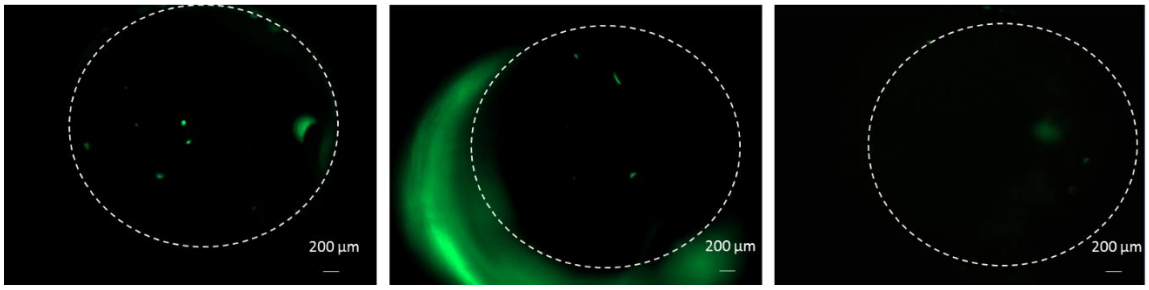

Figure A25- Fluorescence of 3 replicates of FE condition for static environment day 1

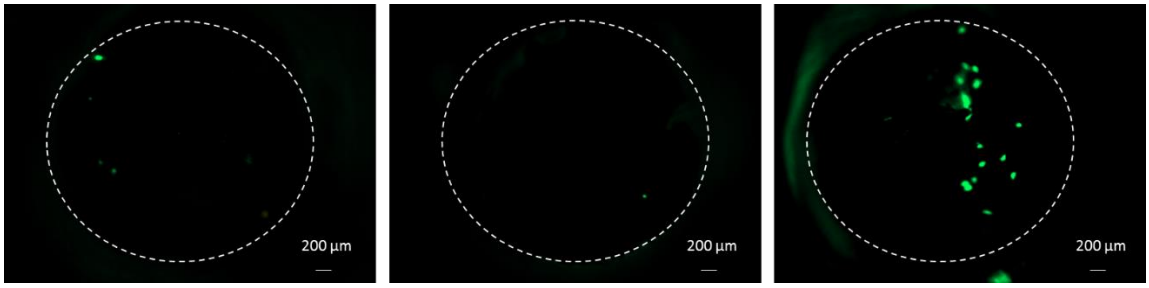

Figure A26- Fluorescence of 3 replicates of FVEA condition for static environment day 1

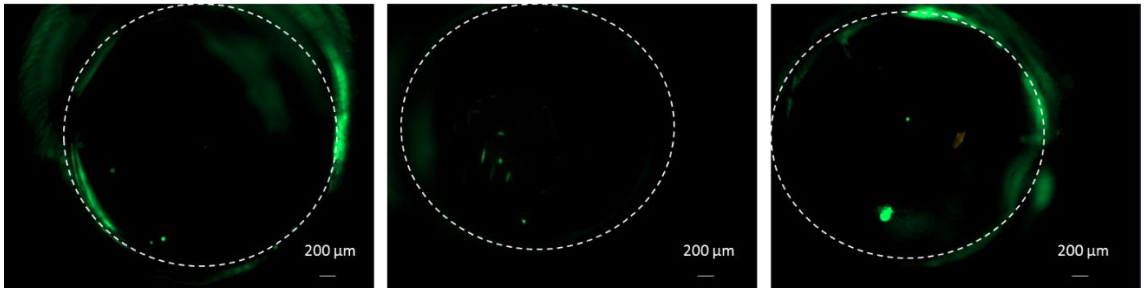

Figure A27- Fluorescence of 3 replicates of F condition for static environment day 5

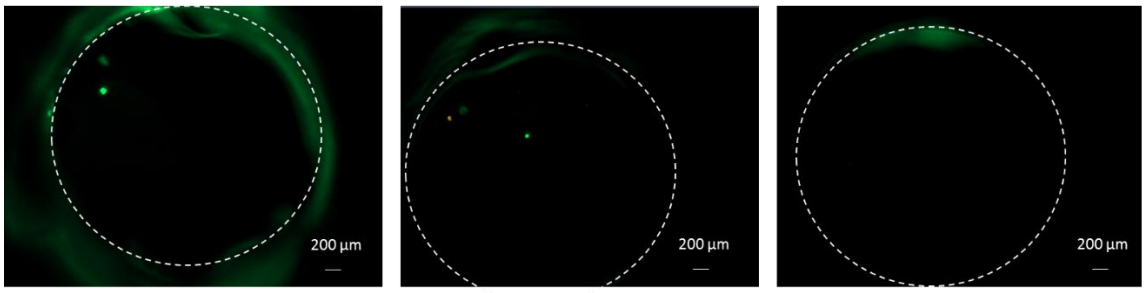

Figure A28- Fluorescence of 3 replicates of V condition for static environment day 5

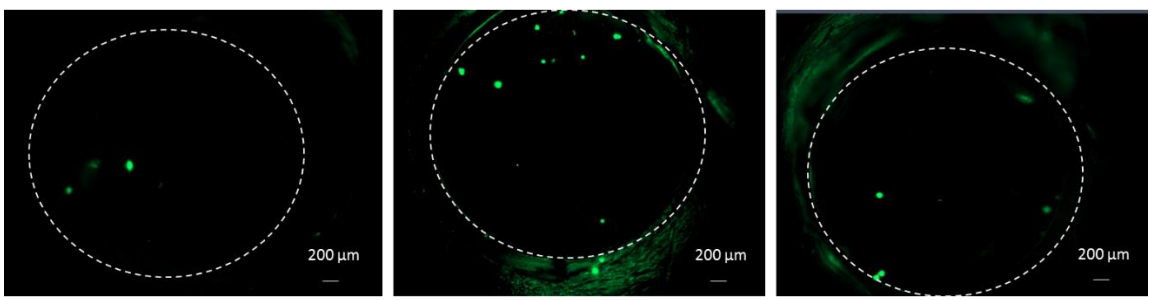

Figure A29- Fluorescence of 3 replicates of FVECA condition for static environment day 5

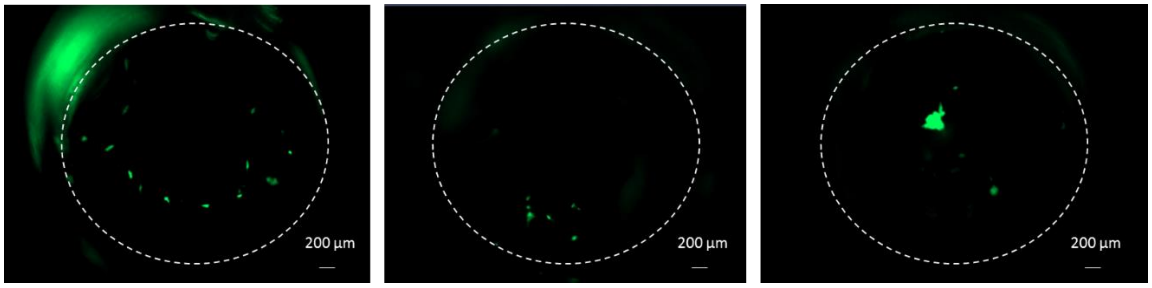

Figure A30- Fluorescence of 3 replicates of FA condition for dynamic environment day 1

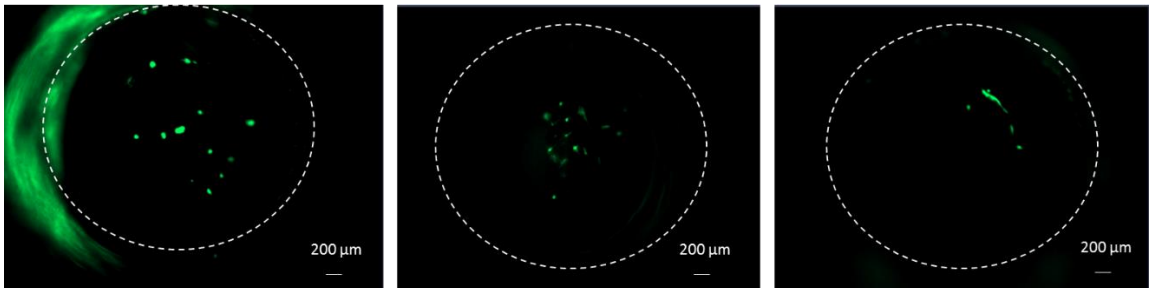

Figure A31- Fluorescence of 3 replicates of FV condition for dynamic environment day 1

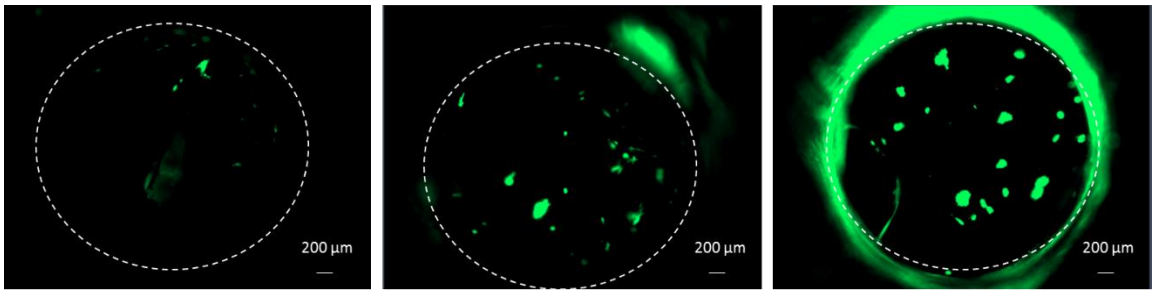

Figure A32- Fluorescence of 3 replicates of VCA condition for dynamic environment day 1

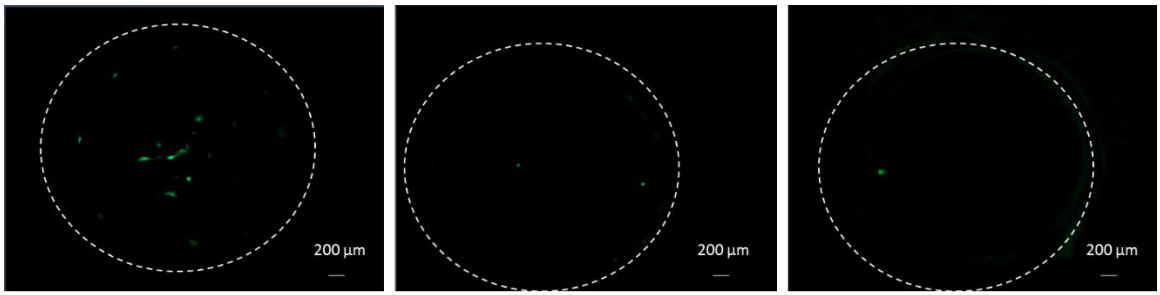

Figure A33- Fluorescence of 3 replicates of A condition for dynamic environment day 5

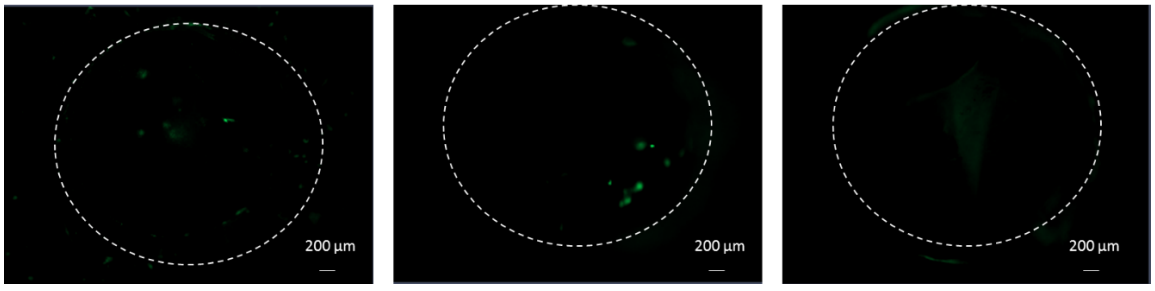

Figure A34- Fluorescence of 3 replicates of FE condition for dynamic environment day 5

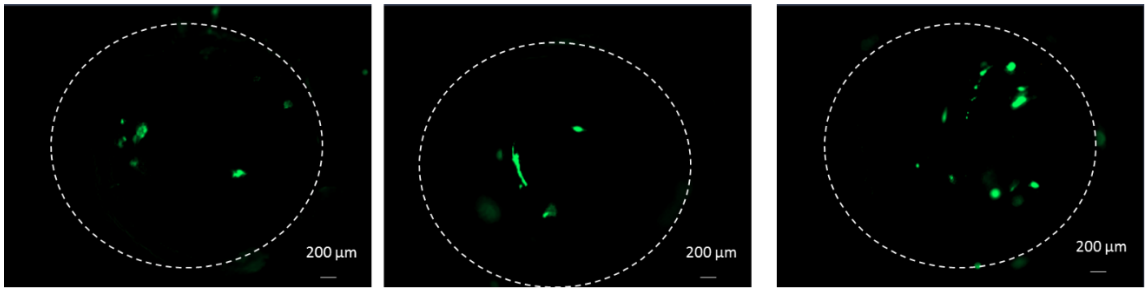

Figure A35- Fluorescence of 3 replicates of VCA condition for dynamic environment day 5

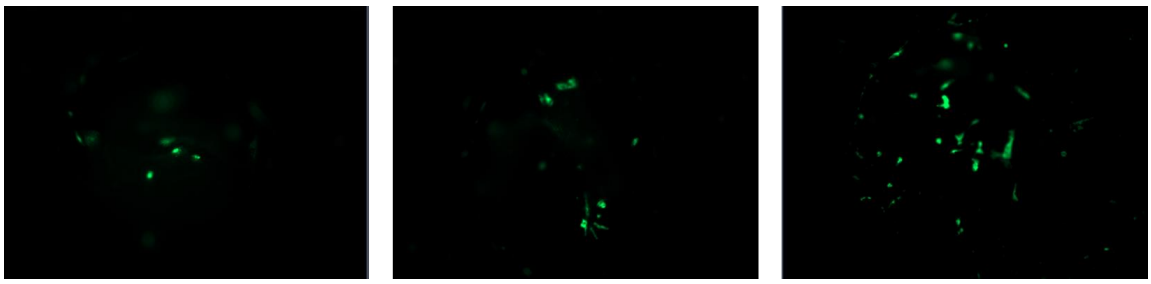

Figure A36- Fluorescence of 3 replicates of the condition with no proteins (control)

B- Detailed fluorescence images of ALP conditions for the several timepoints and different environments

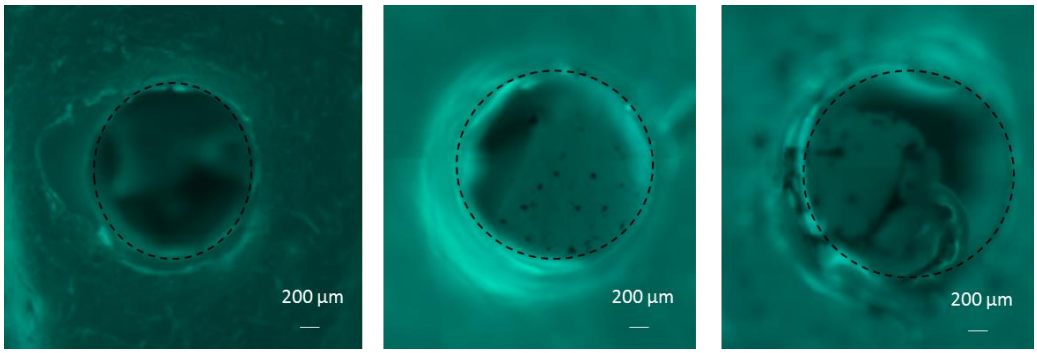

Figure B1- Fluorescence of 3 replicates of FE condition for static environment day 1

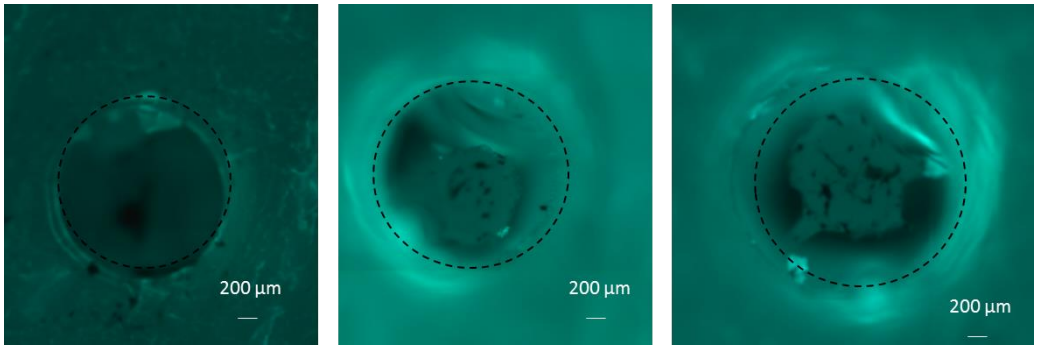

Figure B2- Fluorescence of 3 replicates of VA condition for static environment day 1

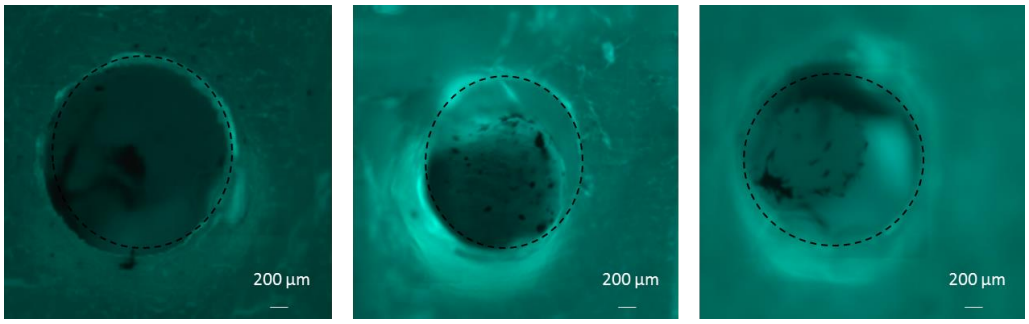

Figure B3- Fluorescence of 3 replicates of ECA condition for static environment day 1

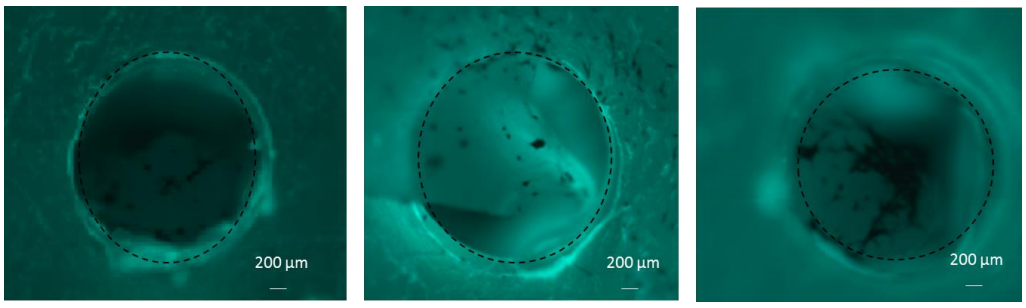

Figure B4- Fluorescence of 3 replicates of FVEC condition for static environment day 1

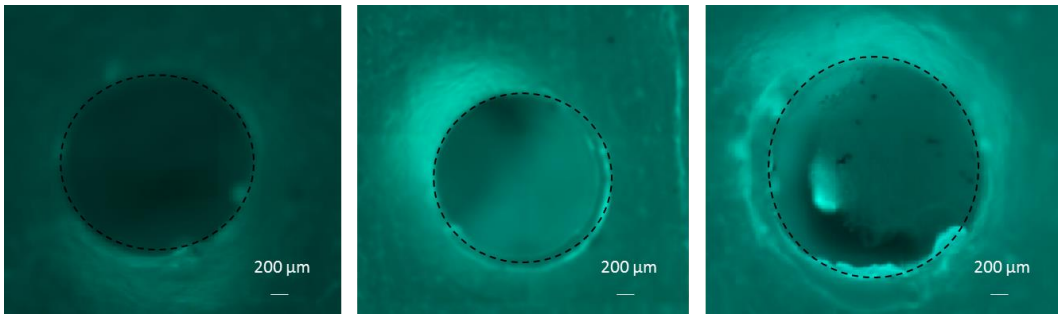

Figure B5- Fluorescence of 3 replicates of V condition for static environment day 1

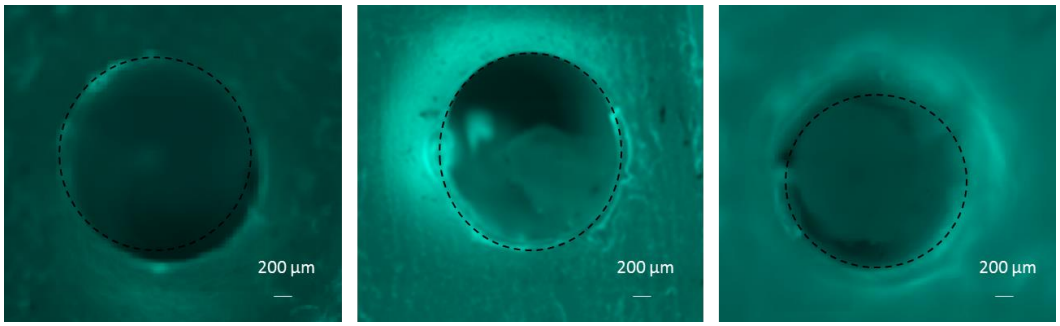

Figure B6- Fluorescence of 3 replicates of C condition for static environment day 1

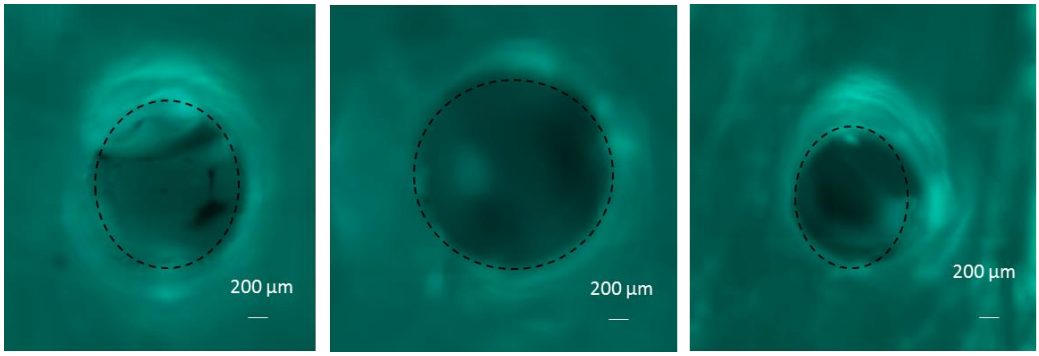

Figure B7- Fluorescence of 3 replicates of VE condition for static environment day 5

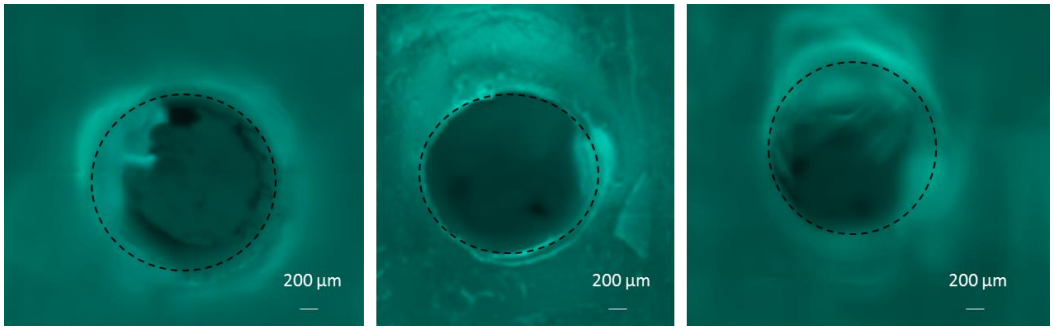

Figure B8- Fluorescence of 3 replicates of ECA condition for static environment day 5

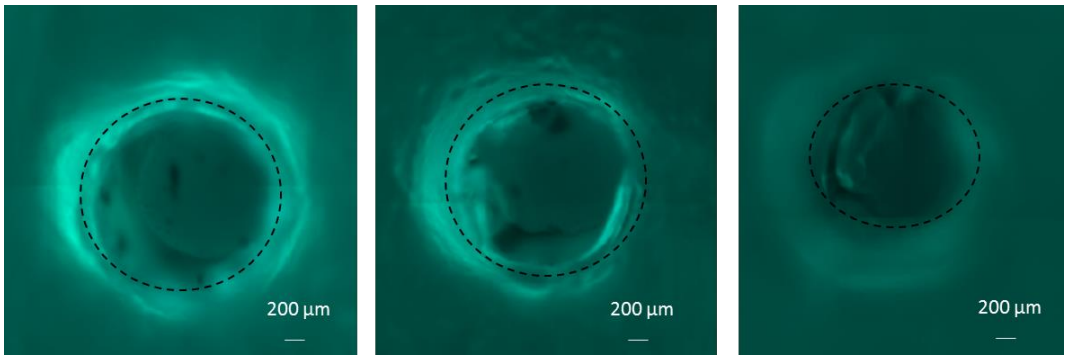

Figure B9- Fluorescence of 3 replicates of FVA condition for static environment day 5

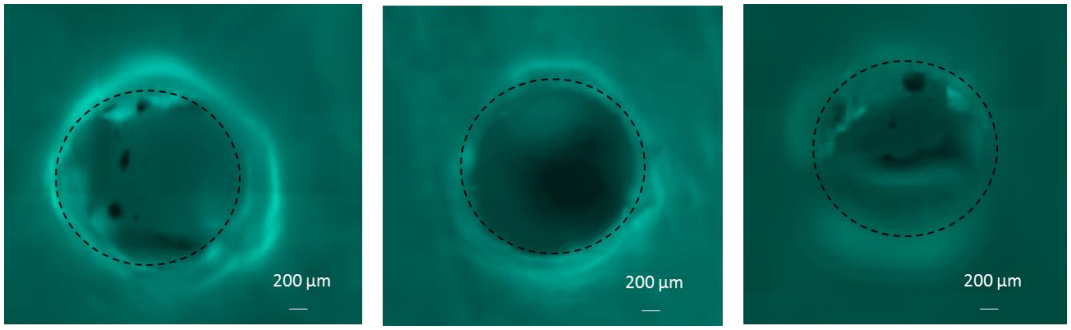

Figure B10- Fluorescence of 3 replicates of FECA condition for static environment day 5

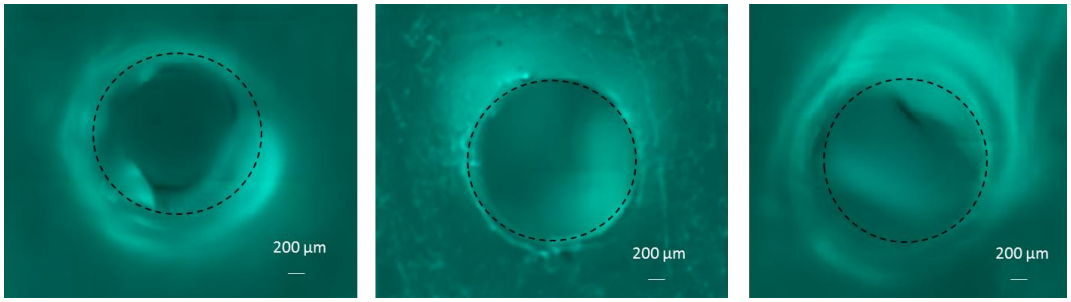

Figure B11- Fluorescence of 3 replicates of FVC condition for static environment day 5

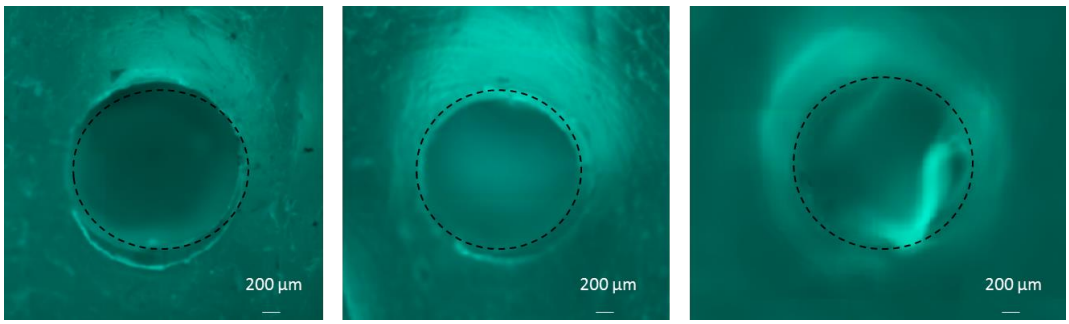

Figure B12- Fluorescence of 3 replicates of EC condition for static environment day 5

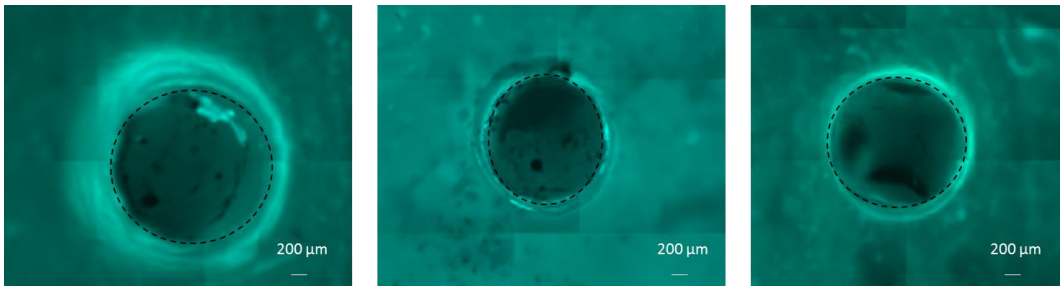

Figure B13- Fluorescence of 3 replicates of ECA condition for dynamic environment day 1

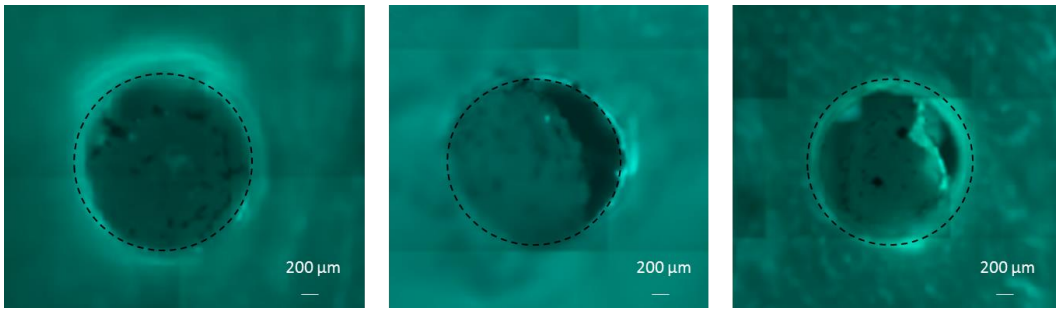

Figure B14- Fluorescence of 3 replicates of FECA condition for dynamic environment day 1

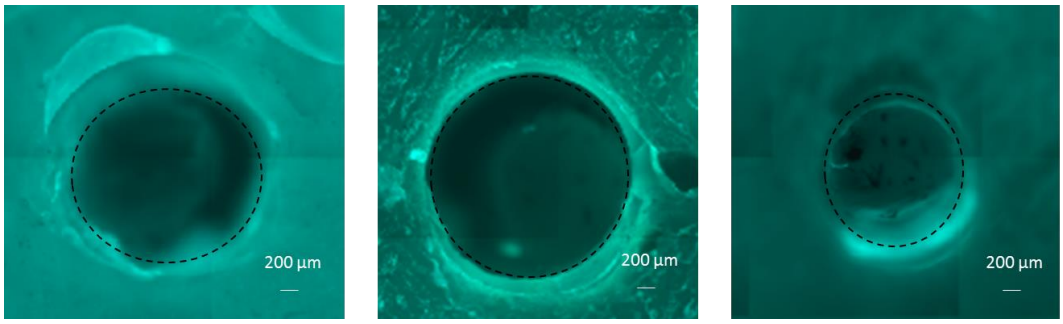

Figure B15- Fluorescence of 3 replicates of A condition for dynamic environment day 1

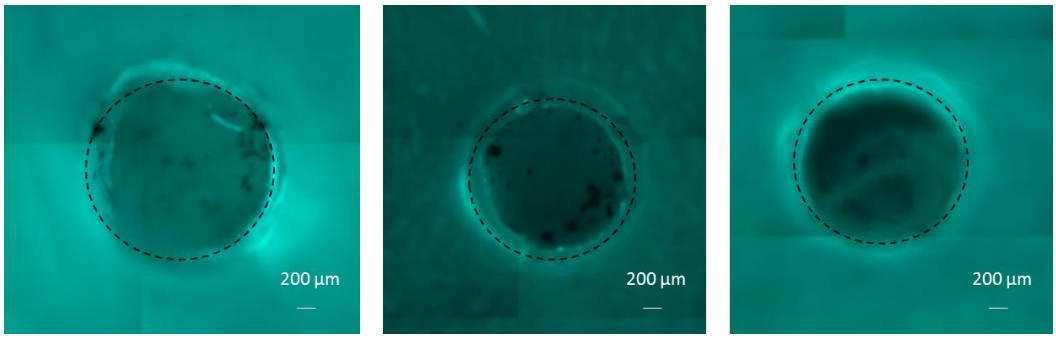

Figure B16- Fluorescence of 3 replicates of FA condition for dynamic environment day 1

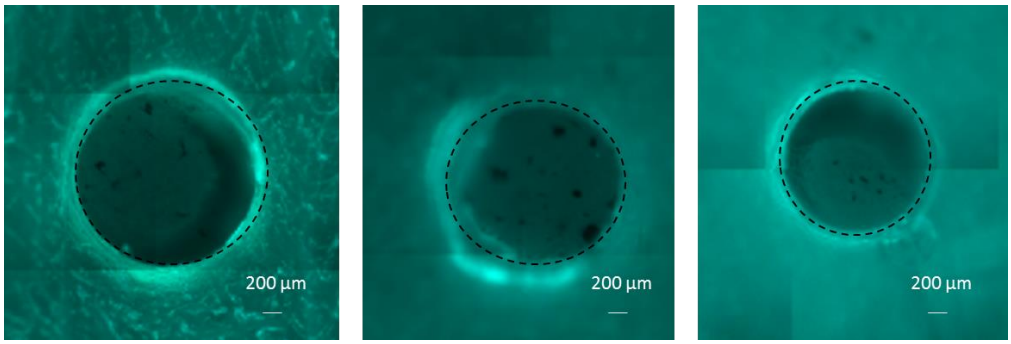

Figure B17- Fluorescence of 3 replicates of FC condition for dynamic environment day 1

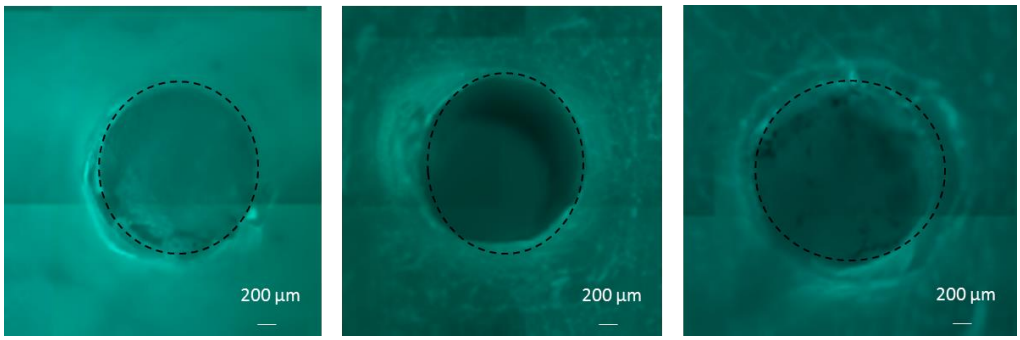

Figure B18- Fluorescence of 3 replicates of EC condition for dynamic environment day 1

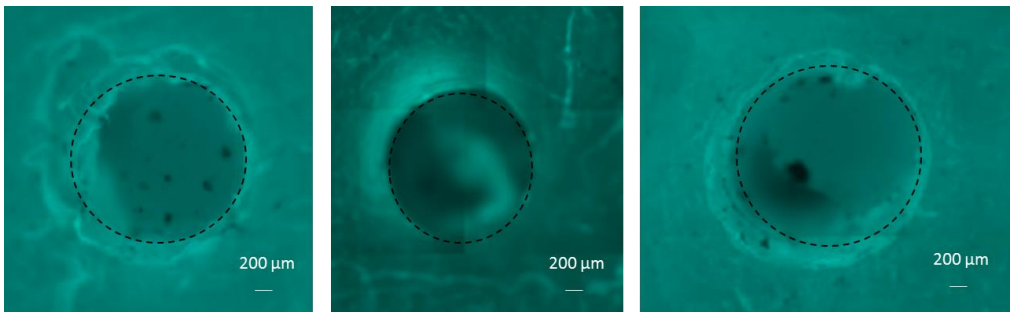

Figure B19- Fluorescence of 3 replicates of FA condition for dynamic environment day 5

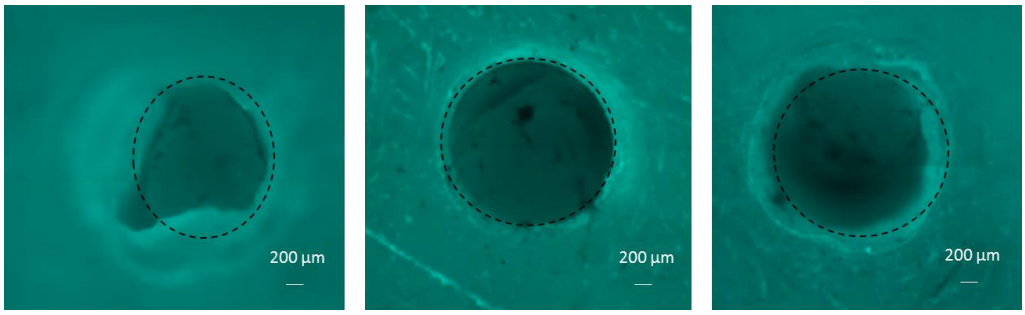

Figure B20- Fluorescence of 3 replicates of ECA condition for dynamic environment day 5

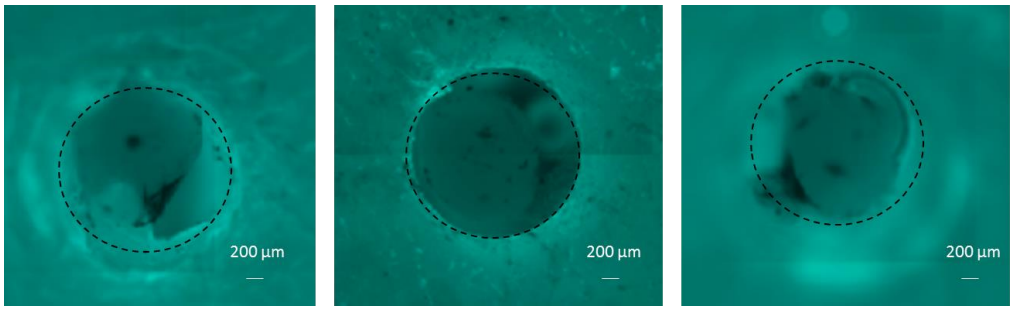

Figure B21- Fluorescence of 3 replicates of FVA condition for dynamic environment day 5

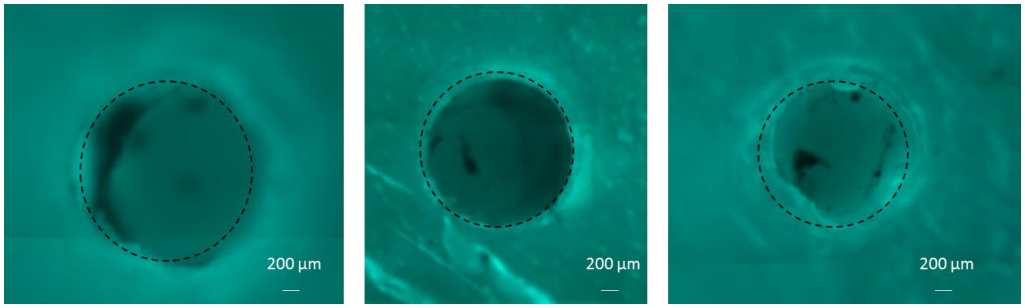

Figure B22- Fluorescence of 3 replicates of FECA condition for dynamic environment day 5

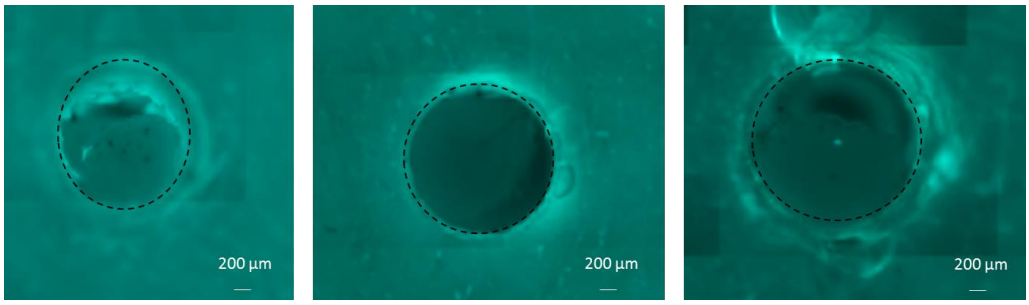

Figure B23- Fluorescence of 3 replicates of FVEC condition for dynamic environment day 5

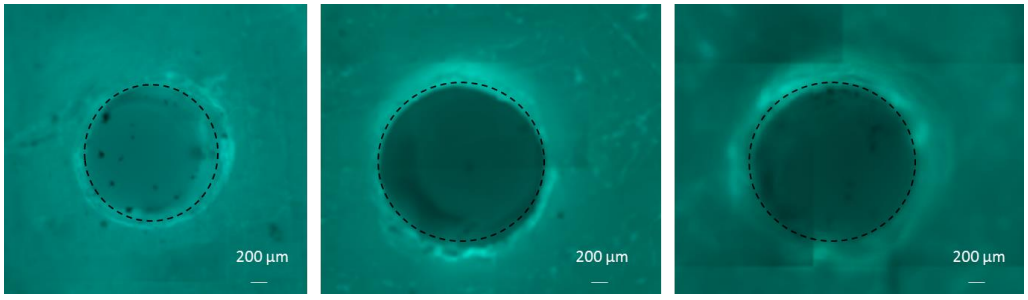

Figure B24- Fluorescence of 3 replicates of FE condition for dynamic environment day 5

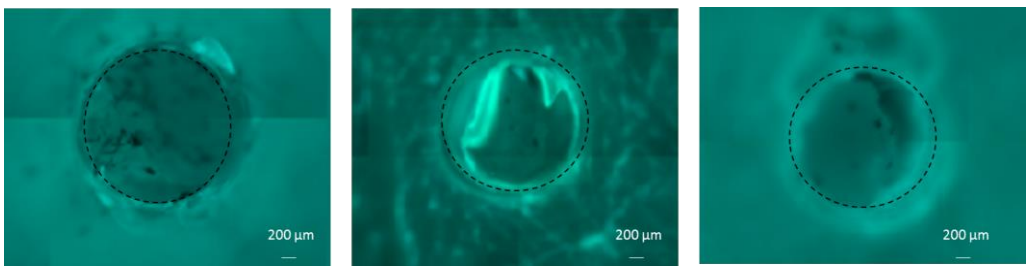

Figure B25- Fluorescence of 3 replicates of the condition with no proteins (control)

C- Plot box for the calcein and ALP data

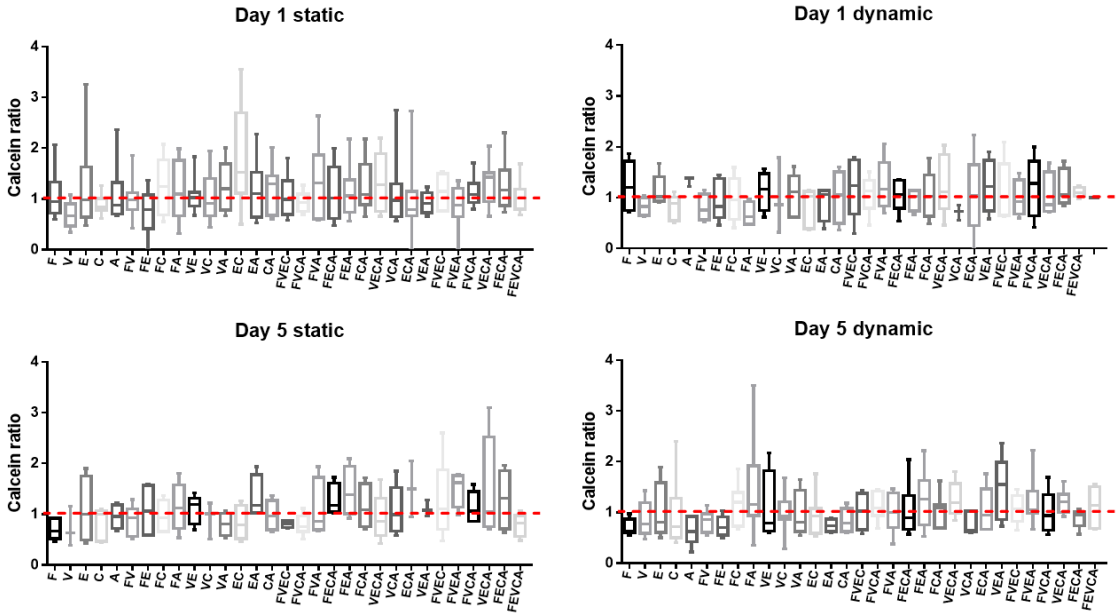

Figure C1- Box plot for calcein data, for the several timepoints and environments

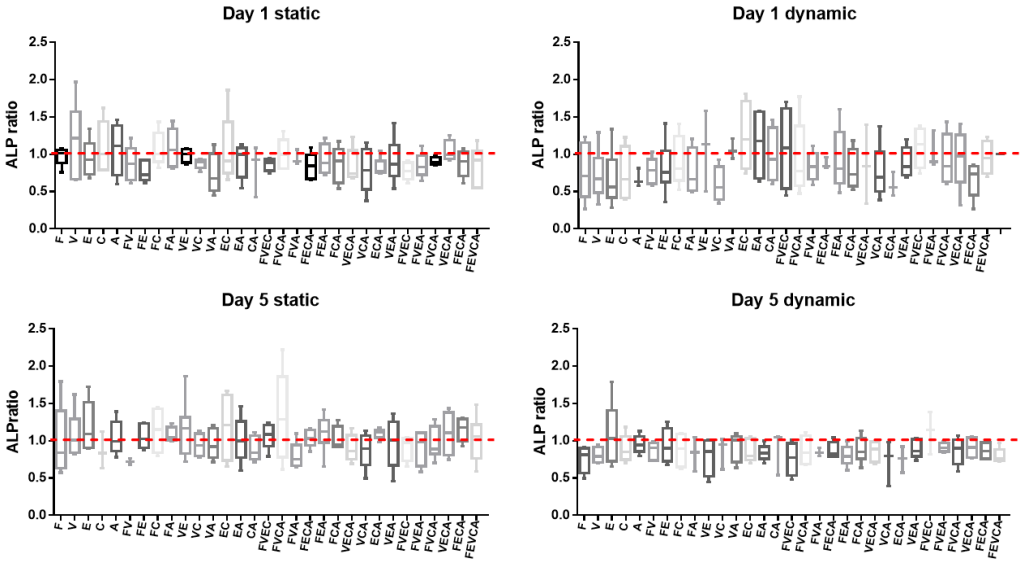

Figure C2- Boxplot for ALP, for the several conditions and timepoints

D- Cluster graphics

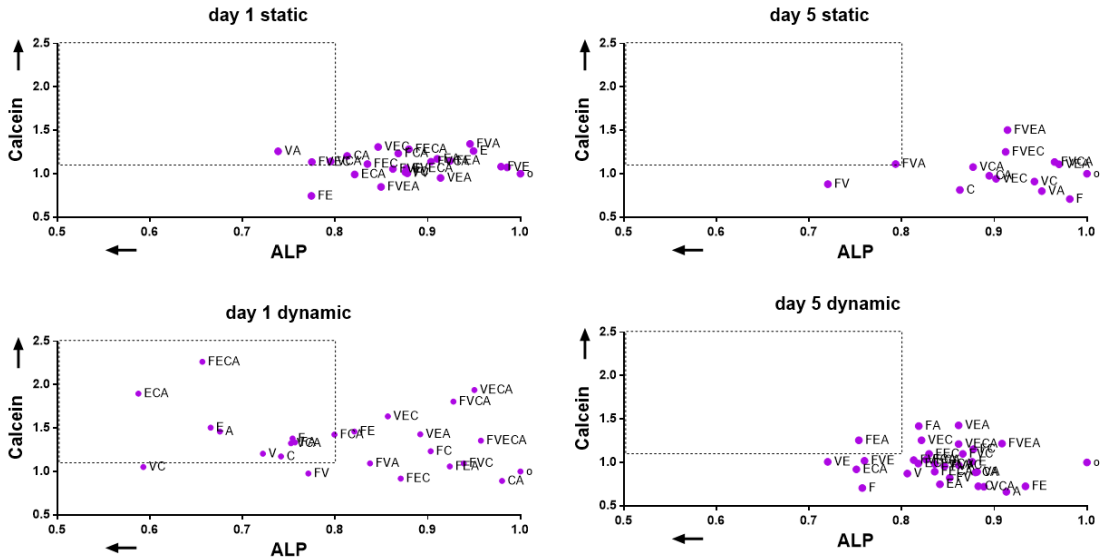

Figure D1- Cluster graphics for the evaluation of calcein/ALP. Relevant conditions are the ones that fall on an area which ALP value is under 0,8 and calcein over 1,1.

E- Effects of the several conditions

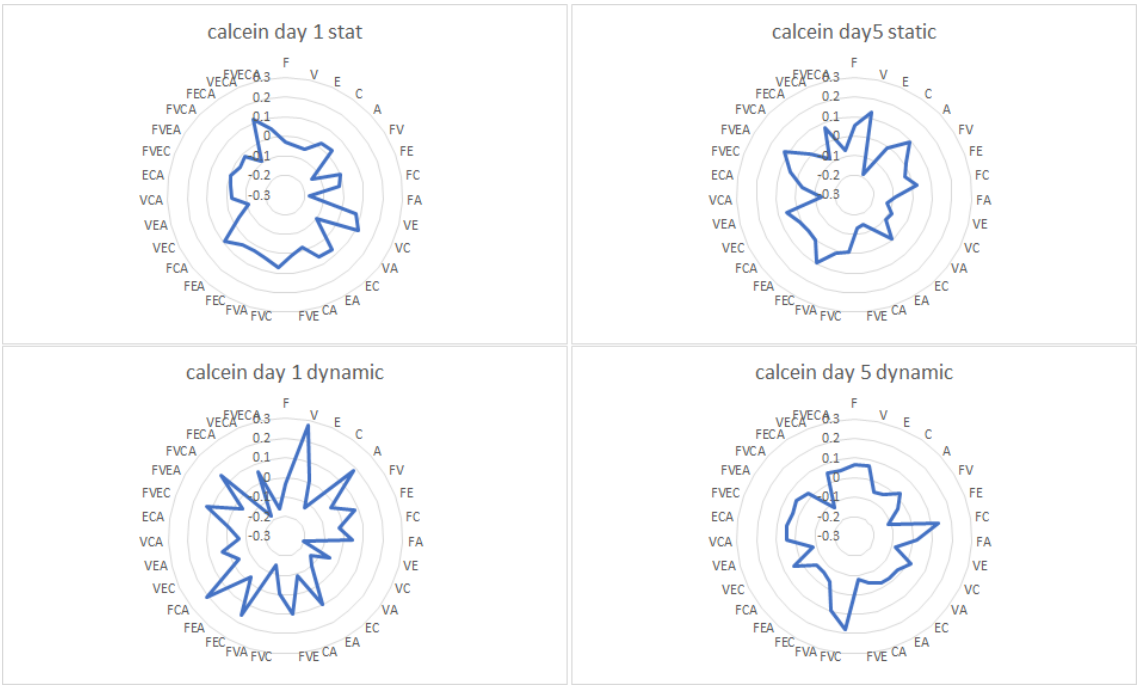

Figure E1- Calcein effects of the several conditions for all the timepoints. In here we can see which conditions induce a better response for cell adhesion.

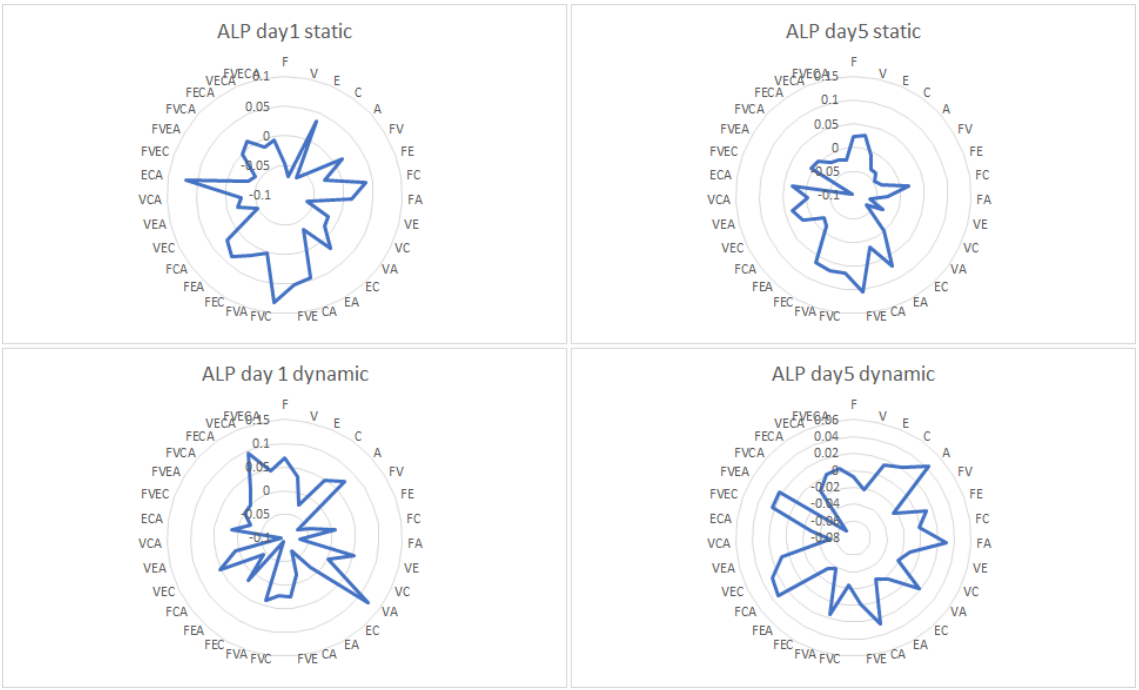

Figure E2- ALP effects of the several conditions for all the timepoints. In here we can see which conditions induce a better response for osteogenic pathway induction.